INTERNATIONAL SCIENTIFIC JOURNAL

MECHANIZATION IN AGRICULTURE & CONSERVING OF THE RESOURCES



Issue 1
2021

Year LXVII, ISSN print2603-3704, ISSN web 2603-3712

SCIENTIFIC TECHNICAL UNION OF MECHANICAL ENGINEERING
BULGARIAN ASSOCIATION OF MECHANIZATION IN AGRICULTURE

PUBLISHERS

SCIENTIFIC-TECHNICAL UNION OF MECHANICAL ENGINEERING "INDUSTRY-4.0"
BUGLARINA ASSOTIOATION OF AGRICULTURAL MACHINERY

ISSN (PRINT) 2603-3704, ISSN (ONLINE) 2603-3712

YEAR LXVII ISSUE 1 / 2021

EDITORIAL BOARD

Chief Editor: Prof. Dr. eng Miho Mihov
Responsible secretary: Corresp. Memb. Prof. D.Sc. Hristo Beloev

MEMBERS:
Acad. D.Sc. Jemal Katsitadze – Georgia
Acad. D.Sc. Sayakhat Nukeshev - Kazakhstan
Acad. D.Sc. Volodymyr Bulgakov – Ukraine
Acad. D.Sc.Valeriy Adamchuk – Ukraine
Prof. Abdullah Sessiz - Turkey
Prof. Abdulrahman Al-soqeer - Saudi Arabia
Prof. Alexander Tokarev - Russia
Prof. Alexey Vassilev - Russia
Assoc.Prof. Angel Trifonov - Bulgaria
Prof. Anupam Kumar Nema - India
Prof. Ayrat Valiev - Russia
Prof. Barbro Ulén - Sweden
Prof. Carmen Puia - Romania
Prof. Cheslav Vashkievich - Poland
Prof.Cumhur Aydinalp - Turkey
Prof. Daisuke Higaki - Japan
Prof. Davor Romic - Croatia
Prof. Domenico Pessina - Italy
Dr. Finn Plauborg - Denmark
Assoc.Prof. Ganka Baeva - Bulgaria
Assoc.Prof. Georgi Mitev - Bulgaria
Prof. Georgi Tassev - Bulgaria
Prof. Haiyan Huang - China
Prof. Hoang Thai Dai - Vietnam

MEMBERS:
Prof. Iliya Malinov - Bulgaria
Prof. PhD Iurie Melnic - Moldova
Assoc.Prof. Ivan Ivanov - Bulgaria
Prof. Jan Szczepaniak - Poland
Prof. Komil Muminov - Uzbekistan
Prof. Krassimira Georgieva - Bulgaria
Prof. Maja Manojlović - Serbia
Prof. Mihail Iliev - Bulgaria
Prof. Mohammad Salem Al-Hwaiti - Jordan
Prof. Papamichail Dimitris - Greece
Prof. Pavel Tlustos - Czech Republic
Prof. Plamen Kangalov - Bulgaria
Prof. Ralph Meissner - Germany
Prof. Rossen Ivanov - Bulgaria
Prof. Svetla Rousseva - Bulgaria
Prof. Tadeusz Pawłowski - Poland
Prof. Tamara Persikova - Belarus
Prof. Valentina Kundius - Russia
Prof. Wojciech Tanaś - Poland
Prof. Yerbol Sarkynov - Kazakhstan
Prof. Zdenko Tkach - Slovakia
Prof. Zinta Gaile - Latvia
Prof. Zivko Davchev - Macedonia

The journal "MECHANIZATION IN AGRICULTURE & CONSERVING OF THE RESOURCES " is continuer of the journals "Mechanized farming" (1948-1957), "Mechanization and electrification of agriculture" (1959-1980) and "Mechanization of agriculture " (1981-1991)

108, Rakovski Str., 1000 Sofia, Bulgaria
tel. (+359 2) 987 72 90, tel./fax (+359 2) 986 22 40,
office@stumejournals.com
WWW.STUMEJOURNALS.COM

C O N T E N T S

MECHANIZATION IN AGRICULTURE

Mathematical model of root head cleaning machine with vertical drive shaft
Volodymyr Bulgakov, Ivan Holovach, Yevhen Ihnatiev, VasilMitkov, Vitaliy Movchan, Viktor Karapetrov 3

Reliability of foreign agricultural machinery operating in Georgia and methods of its improvement
Jemal Katsitadze, Zaur Phutkaradze, Giorgi Kutelia 7

Evaluation of chosen indicators of intermittent seeder´s work quality
Maksym Stankevych, Jozef Rédl, Miroslav Prístavka, Agnieszka Szparaga, Slawomir Kocira, Pavol Findura, Ingrida Košičiarová 10

Selection of the information parameter for the thermography method of diagnostics of dairy cows mastitis
Ivan I. Hirutski, Yuri A. Rakevich, Andrey G. Stankov 14

Kinematics, working parameters and modes of swing-type digging share of elevator-type po-tato combine
Wojciech Tanaś, Mariusz Szymanek 19

Features of calculation of agricultural machines trailed devices in pedagogical technologies of training agricultural engineers for innovative design activities
Viktor Pryshliak 23

CONSERVING OF THE RESOURCES

Study of the influence of irrigation norms on the productivity of raspberry plantations
Rumiana. Kireva, Miho Mihov 26

Utilisation of sustainable Ethanol in a Dual-Fuel Diesel Engine
Aleksandar Damyanov, Peter Hofmann 28

Fem model for the study of agricultural soil compaction under the action of two-wheel tractor
Mădălina Popa (Ivanciu), Sorin-Ștefan Biriș, Nicoleta Ungureanu, George Ipate 38

Mathematical model of root head cleaning machine with vertical drive shaft

Volodymyr Bulgakov[1], Ivan Holovach[1], Yevhen Ihnatiev[2], Vasil Mitkov[2], Vitaliy Movchan[2], Viktor Karapetrov[2]

[1]National University of Life and Environmental Sciences of Ukraine, 15, Heroyiv Oborony Str., Kyiv, 03041, Ukraine;
[2]Dmytro Motornyi Tavria State Agrotechnological University, 18, Khmelnytsky av., Melitopol, 72312, Zaporizhia region, Ukraine;
E-mail:vbugakov@meta.ua, yevhen.ihnatiev@tsatu.edu.ua

Abstract: *The operation of the machine attached to the back of the tractor to clean the heads of root crops from residues in the case of using copying pneumatic wheels causes oscillations of the tops harvester in the vertical plane, which significantly affects the quality of the process. Accordingly, the movement of the horizontal working body will depend on many structural and kinematic factors. Therefore, the development of a mathematical model that will describe the movement of the working body of such a unit is an important task. To solve which the method of construction of calculated mathematical models of functioning of agricultural machines and machine units, on the basis of theoretical mechanics and higher mathematics was used in the work.. Using which the equivalent scheme of movement of the unit is developed and the system of two nonlinear differential equations for detailed research of oscillations of the cleaner of heads of root crops in the longitudinal-vertical plane at movement of its pneumatic copying wheels on roughnesses of a surface of soil is received. The mathematical model of movement of the cleaner with a horizontal cleaning shaft developed on the basis of initial equations of dynamics in the form of Lagrange of the 2nd kind allowed to establish depedencies between constructive and kinematic parameters of the car and its oscillatory characteristics. The found dependences created preconditions for the further mathematical modeling of parameters of the rear-mounted cleaner of heads of root crops, with a horizontal clearing shaft. Using the developed calculation model it is possible to optimize the values of angle β and coordinates y that characterize the oscillations of the machine in the longitudinal-vertical plane.*

KEY WORDS: *HEAD CLEANER, TRACTOR, HITCH, OSCILLATIONS, REACTION, DIFFERENTIAL EQUATIONS.*

.

1. Introduction

In the operation process of the machine for cleaning the heads of roots from the bud remnants wich attached to the rear of the tractor, it performs movements in space, which are determined by the translational speed of the tractor, the field surface, placement of copying pneumatic wheels relative to the hitch system.

The use of copying pneumatic wheels causes oscillations of the cleaning machine in the vertical plane, which will have the greatest impact on the quality of the process. Therefore, we consider the motion of the cleaning machine only in the longitudinal-vertical plane, ie we build a mathematical model of the oscillation of the experimental machine when moving along the irregularities of the soil surface.

The use of a sugar beet cleaner of advanced design, which is hung behind the tractor, leads to its free movements in space, which are determined by the translational speed of the tractor, the relief of the field surface, placement of wheels relative to the hitch system, etc.

2. Preconditions and means for resolving the problem

Аналіз останніх публікацій. An important issue for the field of mechanization of beet growing is the cleaning of the remnants from sugar beet roots heads after its main cutting at the root by cutting devices of beet harvesters. The importance of this issue is confirmed by a number of scientific papers devoted to the study of designs of root crop cleaners [4-7]. They present the results of theoretical and experimental studies of cleaners of sugar beet root heads of different designs: blade, ring, sector, drum types, as well as a cleaner made in the form of a paraboloid. Concerns is the insufficient study of the question of blades oscillation of machines with horizontal drive shafts on moving their working bodies, which have not yet been reflected in the literature. Therefore, studies that would assess the impact of oscillations perturbed by the movement of the cleaner with a horizontal working shaft on the irregularities of the field surface on the quality of roots heads cleaning from buds remnants are relevant.

For example, using the method described in [9], it is possible to build a calculated mathematical model of this machine, which will allow to study the influence of its design parameters on the movement along rows of sugar beet roots and soil surface irregularities.

Thus, the study of the movement of the root crop cleaner and the impact of its oscillations in the longitudinal-vertical plane on the quality of the process requires more in-depth study and justification of structural and kinematic parameters that will ensure high cleaning efficiency of root heads.

The aim of the study. Development of a mathematical model for the theoretical study of the oscillatory motion of the rear-mounted on a wheeled tractor cleaner heads of roots from buds remnants in longitudinal-vertical plane.

Research methods. To achieve the goal of the study, methods of construction of computational mathematical models of functioning of agricultural machines and machine units, based on theoretical mechanics and higher mathematics, were used.

3. Results and discussion

Let's make the equivalent scheme of movement of the clearing machine in the longitudinal-vertical plane which rear-mounted to the aggregating tractor (fig. 1).

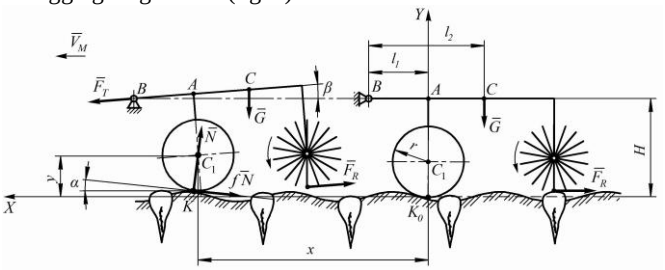


Fig. 1*. Equivalent scheme of movement of the cleaning machineon the unevenness of soil surface*

In this case, we consider the motion of one of the copy wheels with a radius r, given that the second is in the same state as the first. Suppose that in the process of copying wheel, moving in the rows of beet crops on the soil surface of the sinusoidal transverse profile [1], moved from one position to another. In the plane of rotation on the copying wheel are: the force of gravity $\bar{G}$ of the machine and traction force $\bar{P}$. From the side of heads cleaner of root crops there is a resistance force $\bar{F}_R$ equal in magnitude and opposite in direction to the force $\bar{Q}$ of tops crumpling from the root crop head. Under the action of these forces at the point K_1 of contact of the copying wheel with the unevenness of the soil surface there are normal $\bar{N}$ and tangential $f\bar{N}$ reactions (where f is the coefficient of rolling resistance) [2]. The directions of action of normal $\bar{N}$ and tangential $f\bar{N}$ reactions are determined by the angle α. The angle between the traction force $\bar{P}$ and the direction of movement is denoted by β, which determines the nature of the

vertical oscillations of the cleaning machine in the longitudinal-vertical plane. The center of the suspension of the frame of the machine to the tractor is denoted by B, the height of the suspension of the frame – by H. Assume that the hinge B does not move in the vertical plane, and copying process occurs only due to the copying wheels of the cleaner. The speed of translational motion of the machine will be considered constant. We attribute this system to fixed Cartesian coordinates xKy [3], assuming that all its points move only in this plane. The center of the coordinate axes is located at the point K of contact of the copy wheel with the ground. Then, as can be seen from Fig. 1, the location of the center of the copy wheel is determined by the coordinates x and y. We consider in the first approximation the motion of the point of suspension of the cleaner to the tractor (point B) is rectilinear and uniform [8]. The center of gravity of the machine (point C) is at a distance l_2 from the point of suspension. The distance between the axis of the suspension of the cleaning machine (point B) and the axis of attachment of the copying wheels (point A) is denoted by l_1. The mass of the whole cleaning machine is denoted by M, the mass of the copying wheels by m, and $m = m_1 + m_2$ (m_1 - the mass of the first wheel, m_2 - the mass of the second wheel). The force of gravity $\bar{G}$ of the cleaning machine will be considered applied in its center of mass (point C). The mass of the copying wheels is concentrated at a point C_1.

Pneumatic copying wheels will be presented in the form of elastic damping models, which have a stiffness factor c and a damping factor μ. Since there are two copying wheels, these coefficients will be doubled. We believe that copying the wheels in the General case when moving crumple the upper layer of the soil surface, move along the irregularities of the soil surface of the sinusoidal profile, which varies according to the following law [1]:

$$y = h\left(1 + \sin\left(kx - \frac{\pi}{2}\right)\right), \tag{1}$$

where y is the ordinate of the height of the unevenness of the soil surface, m; h - half the height of the unevenness of the soil surface, m; k - frequency of unevenness of the soil surface, m^{-1}; $x = V_M \cdot t$ – value of the current coordinate, m; V_M - speed of the cleaner, $m \cdot s^{-1}$.

In the first approximation, we assume that the copying wheel is in contact with the roughness of the field surface at a point, the position of which belongs to the sine (1).

Since the center of mass of pneumatic copying wheels, due to their elastic properties, performs independent oscillating motions (point C_1) and the ordinates y of the heights of the unevenness of the soil surface are much smaller than the machine displacement x, we can assume that these oscillations can be determined by an independent coordinate y.

In addition, the position of the center of mass of the machine (point C) in the longitudinal-vertical plane is completely determined by the independent coordinate β, which is angle of the machine frame to the horizon, thus, the oscillatory system has two degrees of freedom and its motion is completely determined by two independent generalized coordinates $q_1 = \beta$ and $q_2 = y$. These generalized coordinates will be used in compiling the differential equations of motion of the cleaning machine in the longitudinal-vertical plane.

The speed V of movement of the center of mass of the copying wheels in this case will be equal to:

$$V = \sqrt{\dot{x}^2 + \dot{y}^2}. \tag{2}$$

Given that $x = V_M \cdot t$, we obtain the following expression:

$$V = \sqrt{V_M^2 + \dot{y}^2}, \tag{3}$$

where V_M is the speed of translational motion of the machine, $m \cdot s^{-1}$.

To determine the kinetic energy of a given dynamic system, it is also necessary to determine the angular velocity of the copying wheel and express it through known parameters. It is defined by the following expression:

$$\omega = \frac{dS}{dt} \cdot \frac{1}{r}, \tag{4}$$

where ω is the angular velocity of the copying wheel, rad/s; S - the magnitude of the circular displacement of the copying wheel on the sinusoidal profile of the soil surface, m; r - wheel radius, m

In this case, the differential of the arc of movement of the copying wheel will be equal to:

$$dS = \sqrt{dx^2 + dy^2} = \sqrt{1 + h^2 k^2 \cos^2\left(kx - \frac{\pi}{2}\right)}dx, \tag{5}$$

or:

$$dS = \sqrt{1 + h^2 k^2 \cos^2\left(kV_M \cdot t - \frac{\pi}{2}\right)} \cdot V_M dt. \tag{6}$$

Substituting the value of (6) in (4), we obtain the value of the desired angular velocity:

$$\omega = \frac{\sqrt{1 + h^2 k^2 \cos^2\left(kV_M \cdot t - \frac{\pi}{2}\right)} \cdot V_M}{r}. \tag{7}$$

To compile the differential equations of motion of the considered oscillatory system, we use the initial equations in the form of Lagrange of the second kind of the following type [1]:

$$\frac{d}{dt}\left(\frac{\partial T}{\partial \dot{q}_i}\right) - \frac{\partial T}{\partial q_i} = Q_i - \frac{\partial P}{\partial q_i} - \frac{\partial R}{\partial \dot{q}_i}, \tag{8}$$

where T is the kinetic energy of the system; Q_i - generalized force; P - potential energy of the system; R - dissipative function

Define the components included in expression (8). The kinetic energy of the system is equal to:

$$T = T_1 + T_2 + T_3, \tag{9}$$

where T_1 is the kinetic energy of the translational motion of the cleaning machine (its center of mass); T_2 - kinetic energy of the oscillating motion of the machine frame around the point B; T_3 - kinetic energy of rotational motion copying the wheels around their axes.

The components of kinetic energy will be equal to:

$$T_1 = \frac{MV^2}{2} = \frac{M}{2}\left(V_M^2 + \dot{y}^2\right), \tag{10}$$

where M is the weight of the cleaning machine, kg; V is the speed of the center of mass of the machine, $m \cdot s^{-1}$.

$$T_2 = \frac{I_B \dot{\beta}^2}{2}, \tag{11}$$

where I_B - the moment of inertia of the frame of the cleaning machine relative to the axis that is perpendicular to the longitudinal-vertical plane and passes through a point B, $kg \cdot m^2$; $\dot{\beta}$ - angular speed of rotation of a frame of the car, s^{-1}.

$$T_3 = \frac{I_k \omega^2}{2} = \frac{1}{2r^2} I_k V_M^2 \left[1 + h^2 k^2 \sin^2(kx)\right], \tag{12}$$

where I_k is the moment of inertia of the copying wheels relative to their axes of rotation, $kg \cdot m^2$; ω - angular speed of rotation of the copying wheel, s^{-1}.

Then expression (9) will take the following form:

$$T = \frac{MV^2}{2} + \frac{I_B \dot{\beta}^2}{2} + \frac{I_k \omega^2}{2}. \tag{13}$$

The potential energy P of the system is determined by the following expression:

$$P = c\left(l_1 \beta - y\right)^2, \tag{14}$$

where c is the stiffness coefficient of the tires of the wheels of

the running system, N/m; l_1 - distance from the axis of suspension of the machine to the axis of the copying wheels, m

The dissipative function of this dynamic system is as follows:

$$R = \mu\left(l_1\dot{\beta} - \dot{y}\right)^2, \tag{15}$$

where μ is the damping factor of the copying wheels, N·s/m.

We now find generalized forces Q in generalized coordinates β and y, which are included in the right-hand side of the Lagrange equation of the second kind (8). To determine the generalized force Q_y on the independent coordinate y, we use the expression of the elementary work of forces on a possible displacement δy:

$$\delta W_y = \sum_{i=1}^{n} Q_y \cdot \delta q_y = -G \cdot \delta y - f\,N \sin\alpha \cdot \delta y + \\ + F_R \sin\beta \cdot \delta y + N\cos\alpha \cdot \delta y - P\sin\beta \cdot \delta y. \tag{16}$$

It should be noted that the normal and tangential reactions of the soil on the copying wheel perform elementary work, respectively, on the deformation of the soil and overcoming friction, ie are active forces.

How do we have that the generalized force Q_y is equal to:

$$Q_y = \frac{\delta W_y}{\delta y} = -G - f\,N\sin\alpha + F_R\sin\beta + N\cos\alpha - P\sin\beta. \tag{17}$$

To determine the generalized force Q_β on the independent coordinate β, we use the expression for the elementary work of forces on a possible displacement $\delta\beta$. We will have:

$$\delta W_\beta = N \cdot BB'' \cdot \delta\beta + fN \cdot BB' \cdot \delta\beta + F_R \cdot H \cdot \delta\beta - G \cdot BC' \cdot \delta\beta \tag{18}$$

where BB'', BB', BC' – shoulders of forces $\bar{N}$, $f\bar{N}$, $\bar{G}$ concerning a point B accordingly (fig. 2).

From expression (18) we find the value of the generalized force on the angular coordinate β, which will be equal to:

$$Q_\beta = \frac{\delta W_\beta}{\delta\beta} = N \cdot BB'' + fN \cdot BB' + F_{on} \cdot H - G \cdot BC'. \tag{19}$$

Thus, the generalized force Q_β in this case is the algebraic sum of the moments of all forces acting on a given dynamic system with respect to a point B.

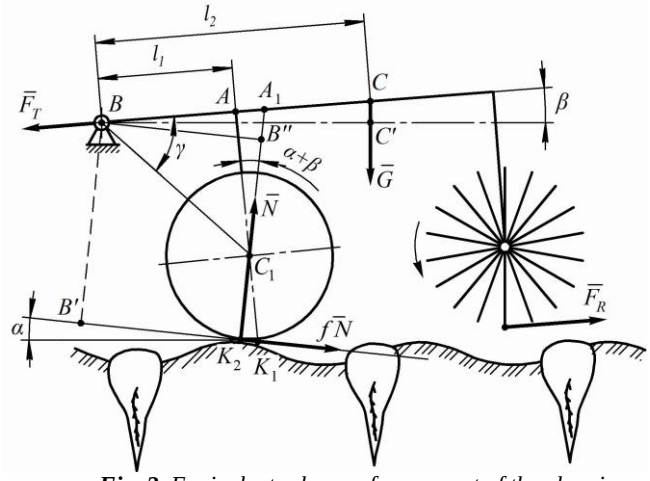


Fig. 2. *Equivalent scheme of movement of the cleaning machine at the time of impact on the unevenness of the soil surface*

Determine the shoulders of the forces included in expression (19), using Fig. 2. As you can see from the figure:

$$BB'' = l_1\cos(\alpha+\beta) + (H-r)\cdot\sin(\alpha+\beta) \tag{20}$$

where α is the angle of tangent inclination to sine (1).

As is known, the tangent of the angle of inclination tangent to the curve $y = f(x)$ at a given point is equal to the derivative of the equation of this curve on the variable x at this point, ie: $tg\alpha = y'_x$. Taking into account expression (1), we obtain:

$$y'_x = hk\cos\left(kx - \frac{\pi}{2}\right). \tag{21}$$

So:

$$\alpha = arctg\left[hk\cos\left(kx - \frac{\pi}{2}\right)\right]. \tag{22}$$

Next, from Fig. 2 we get:

$$BB' = r + \cos\left(90^o + \alpha + \beta - \gamma\right)\sqrt{(H-r)^2 + l_1^2}. \tag{23}$$

With:

$$\mathrm{tg}\gamma = \frac{AC_1}{AB} = \frac{H-r}{l_1}, \tag{24}$$

then

$$\gamma = \mathrm{arctg}\frac{H-r}{l_1}. \tag{25}$$

Next, from the triangle BCC' we obtain:

$$BC' = l_2\cos\beta. \tag{26}$$

Using the obtained expressions (20), (23), and (26) and substituting them in expression (19) we obtain the value of the generalized force Q_β in the coordinate β:

$$Q_\beta = N\left[l_1\cos(\alpha+\beta) + (H-r)\cdot\sin(\alpha+\beta)\right] + \\ + fN\left[r + \cos\left(90^o + \alpha + \beta - \gamma\right)\sqrt{(H-r)^2 + l_1^2}\right] + \\ + F_R \cdot H - Gl_2\cos\beta. \tag{27}$$

Having further determined the necessary partial derivatives of the kinetic energy T of a given dynamic system, potential energy P, dissipative function R and substituting the obtained values of generalized forces Q_y and Q_β the original Lagrange equations of the second kind (8), we finally obtain a system of differential equations of the following form:

$$\left.\begin{aligned} &I_B\ddot{\beta} = N\left[l_1\cos(\alpha+\beta) + (H-r)\cdot\sin(\alpha+\beta)\right] + \\ &+ fN\left[r + \cos\left(90^o + \alpha + \beta - \gamma\right)\sqrt{(H-r)^2 + l_1^2}\right] + F_R \cdot H - \\ &- Gl_2\cos\beta - 2cl_1\left(l_1\beta - y\right) - 2\mu l_1\left(l_1\dot{\beta} - \dot{y}\right), \\ &M\ddot{y} = -G - fN\sin\alpha + F_R\sin\beta + N\cos\alpha - P\sin\beta + \\ &+ 2c\left(l_1\beta - y\right) + 2\mu\left(l_1\dot{\beta} - \dot{y}\right). \end{aligned}\right\} \tag{28}$$

Where do we have:

$$\left.\begin{aligned} &\ddot{\beta} = \frac{N\left[l_1\cos(\alpha+\beta) + (H-r)\cdot\sin(\alpha+\beta)\right]}{I_B} + \\ &+ \frac{fN\left[r + \cos\left(90^o + \alpha + \beta - \gamma\right)\sqrt{(H-r)^2 + l_1^2}\right]}{I_B} + \\ &+ \frac{F_R \cdot H - Gl_2\cos\beta - 2cl_1\left(l_1\beta - y\right) - 2\mu l_1\left(l_1\dot{\beta} - \dot{y}\right)}{I_B}, \\ &\ddot{y} = \frac{-G - fN\sin\alpha + F_R\sin\beta + N\cos\alpha - P\sin\beta}{M} + \\ &+ \frac{2c\left(l_1\beta - y\right) + 2\mu\left(l_1\dot{\beta} - \dot{y}\right)}{M}. \end{aligned}\right\} \tag{29}$$

The obtained system (29) of two differential equations is a calculated mathematical model of the movement of machine for cleaning root heads installed behind the aggregating tractor.

4. Conclusions

1. On the basis of the developed equivalent scheme of movement of the unit the is received system of two nonlinear differential equations that allows to investigate in detail oscilations of root crops heads cleaner in the longitudinal-vertical plane at

movement of its pneumatic copying wheels on roughnesses of a soil surface.

2. The calculated mathematical model of movement of the cleaner with a horizontal cleaning shaft is developed on the basis of initial equations of dynamics in the form of Lagrange of the 2nd kind allows to establish dependecies between constructive and kinematic parameters of this machine and its oscillatory characteristics.

3. The purpose of further mathematical numerical modeling of the parameters of the rear-mounted root heads cleaner with horizontal cleaning shaft, using the developed model is to optimize the values of angle β and coordinates y that characterize the oscillations of the machine in the longitudinal-vertical plane.

5. References

1. Kolychev E.I., Pereltsvaig I.M.On the choice of the calculated case of impact in the study of the smooth running of tractors and agricultural machines. Tractors and agricultural machinery. – 1976. – №3. – pp. 9.–11. (in Russian)

2. Chudakov D.A. Osnovy teorii i rascheta traktor i avtomobilya [Fundamentals of the theory and calculation of a tractor and an automobile]. - 2nd ed., Rev. and add. - M .: Kolos, 1972. – 384 p. (in Russian)

3. Vasilenko P.M. On equations of the dynamics of systems with nonholonomic constraints. - In the book: Agricultural mechanics - a collection of works. - M .: Mashinostroyeniye, 1968. – Vol. II. – pp. 26–34. (in Russian)

4. Khvostov V.A., Reingart E.S. Machines for harvesting root crops and onions (theory, design, calculation). - Moscow: VISKHOM, 1995. - 391 s. (in Russian)

5. Pogorelij L.V., Tatjanko, N.V., Brej V.V. et al. Svekloubo rochniej mashiny: (konstruktirovanie i raschot).. Pod obshchej redakciej L.V. Pogorelogo. Kiev, Tekhnika, 1983, pp.168. (In Russian)

6. Adamchuk V., Bulgakov V., Korenko M., Boris A., Boris M. Laboratory and field equipment workingout and the results of experimental studies of pre-harvesting sugar beet field conditions. Mechanization in agriculture. – Sofia, Bulgaria, 2016. – Issue 1. – pp. 3 – 5.

7. Bulgakov V., Adamchuk V., Nozdrovicky L., Ihnatiev Ye.Theory of vibrations of sugar beet leaf harvester front-mounted on universal tractor. Acta Technologica Agriculturae. – 2017. – Issue 4. – pp. 96 – 103.

8. Butenin N.V., Lunc Ja.L., Merkin D.R. Kurs teoreticheskoj mekhaniky. Tom II. Dynamika. – Moskva: Nauka, 1985. – 496 p. (in Russian)

9. Vasilenko P.M. Vvedenie v zemledelcheskuju mekhaniku. – Kiev: Selkhozobrazovanie, 1996. – 252 p. (in Russian)

10. Bulgakov V., Pascuzzi S., Arak M., Santoro F., Anifantis A.S., Ihnatiev Y., Olt J. An experimental investigation of performance levels in a new root crown cleaner. Agronomy Research. 2019. Vol. 17. No 2. p.p. 358–370.

11. Ihnatiev Y. Theoretical substantiation of topping parameters without sugar beet head copying. IV International scientific Congress "Agricultural machinery". – Varna. – Issue 18 (181). Vol. 1, 22-25 june 2016. – P. 55 – 58.

12. Bosoj E.S. et al. Theory, design and calculation of agricultural machinery. Moscow, Mashinostroenie, 1978, pp. 567. (In Russian)

13. Morozov B.I., Gringauz N.M. Calculation of the movement of a wheeled vehicle on an uneven road. - Mechanization and electrification of socialist agriculture. – 1969. – № 7. – C. 11-14. (In Russian)

14. Reznik N.E. The theory of cutting with a blade and the basics of calculating cutting devices. - Moscow: Mechanical Engineering, 1975. – 311 p. (In Russian)

Reliability of foreign agricultural machinery operating in Georgia and methods of its improvement

Jemal Katsitadze, Zaur Phutkaradze, Giorgi Kutelia
chokhadari@yahoo.com, zpn1962@gmail.com, qutelia.giorgi@mail.ru

Abstract: *The article examines the single and complex indicators of the operational reliability of agricultural machinery (tractors and combines) operating in the special soil-climatic and dynamic conditions of Georgia, highlights the least reliable units and parts that require constructive improvement.*

As a result of research, according to the methodology of probabilistic and statistical modeling developed by us, integral and differential distribution functions of reliability indicators were obtained, their general characteristics were determined, as well as mathematical models and the values of reliability indicators were determined taking into account the distribution law. The adequacy of the probabilistic-statistical models was tested using the Pearson and Kolmogorov goodness-of-fit tests.

As a result of theoretical and experimental studies, characteristic malfunctions and failures of the main units of foreign agricultural equipment operating in Georgia have been established, and constructive and technological measures to improve reliability have been developed.

KEYWORDS: *FOREIGN AGRICULTURAL MACHINERY, TRACTORS, COMBINES, RELIABILITY, PROBABILISTIC-STATISTICAL MODEL, FAILURE.*

1. Introduction:

The agricultural sector of Georgia annually receives foreign agricultural machinery produced in the USA, EU countries and Japan. This process is facilitated by the fact that the country has liquidated the economic borders between Georgia and the West, Georgia has become a member of the European Council and the World Trade Organization. These factors make it possible for farmers and private entrepreneurs in the world market to buy modern agricultural machinery, which ensures the mechanization of labor-intensive agricultural processes using high technologies.

Currently, the main problem is the choice of foreign agricultural machinery that meets the special soil and climatic conditions of Georgia. To do this, it is necessary to have sufficient scientific information about the technical, economic and environmental performance of machines. We believe that before purchasing this equipment, it is necessary to study the indicators of operational reliability and efficiency when working in the special conditions of Georgia.

Soil, climatic and dynamic conditions have a significant impact on the operational reliability of foreign agricultural equipment and cause various typical failures.

2. Main part

Similar studies were carried out in the main regions of Georgia according to a previously developed methodology [1]. All refusals were recorded in special journals and then the results were processed by the method of probabilistic-statistical modeling [2,3,4].

Analysis of failures of foreign agricultural machines operating in Georgia shows that their main reasons are: untimely change of filters of the power supply and lubrication system, use of substandard oils and fuels, elimination of the system supply system or its replacement, untimely, and sometimes incorrect, periodic maintenance by machine operators. It was also found that in most cases the reason for the failures is also the fact that the machine operators and tenants do not have sufficient knowledge of the operation of the machines.Table 1 shows the distribution of failures of units and systems of the NEWHOLLAND tractor in%.

Table.1: *Distribution of failures of units and systems of the NEWHOLLAND tractor,%.*

Tractor systems and units	Failures by complexity group I, II, III, (I, II, III)			
	I	II	III	I, II, III
Total on tractor	54	19	16	11
Engine	62	21	17	20
Transmission	24	28	17	39
Undercarriage	_	_	16	_
Hydraulic system	14	37	50	41
Controls	_	14	_	_

The table shows that the failures of the first group are 62%, the second group is 21%, the third group is 17%, and at the same time for all groups 20% are accounted for by the engine. In total, on a tractor, these indicators are 54%, 19%, 16%, and eleven % . The largest share of failures of the third group, 50%, is distributed to the hydraulic system. More than 120 tractors of the above brand operate in the farms of Georgia.

The analysis of failures of the lubrication system shows that 26% of failures go to the hydraulic pump, 14% to the filter and 5% to the mechanisms of the attachment system.

By the nature of tractor failures, 12% are structural failures, 14 are technological failures, and 24% are operational failures. The failure rates of KLAAS tractors were also investigated (table 2).

Table.2: *Distribution of failures among implements and systems of the CLAAS tractor -is (%).*

Aggregates and systems	Failures by complexity group I, II, III, (I, II, III)			
	I	II	III	I, II, III
Total	59	19	8	14
Engine	79	20	5	6
Transmission	4	_	_	_
Undercarriage	3	_	_	_
Hydraulic system	10	_	_	_
Controls	4	1	_	_

Based on the data obtained, it can be concluded that most of the tractor failures go to the engine, including failures of the first group of complexity -79%, the second group -20%, the third group-5% and all groups together-14%. Of the hydraulic system failures, the most common -10% were linkage failures.

Of the total engine failures, 79% go to the organs of the power supply system -73%, 18% to the lubrication system, 5% to the cooling system and 4% to the crank mechanism. Hence, we can conclude that the most unreliable elements of the engine are the organs of the power supply system. Our research has also shown that when operating in Georgia, CLAAS tractors often fail the finger for transmitting the signal of the hydraulic system mechanism. The reason for this failure is that the machine operators do not carry out a timely oil change, as a result of which the signal transmission finger loses its function - it bends, breaks and the system turns off. We also recorded intensive wear of the shaft under the reverse gear bearing due to oil contamination.

Analysis of the power supply system shows that 29% of the total failures go to the turbo condenser, 22% to the pumps and coarse filters, 14% to the electric pump and 9% to the fine filter.

It was found that out of the total number of failures, -5% are structural failures due to the fault of the manufacturer, 6% are

technological failures and 15% are operational failures. The latter are caused by the fact that machine operators grossly violate the rules of operation and maintenance of tractors, use substandard and non-standard fuels and lubricants. The cause of technological failures is the wrong choice of materials for parts and violation of the modes of mechanical and chemical-thermal treatments.

The results of the study of the reliability of some foreign and agricultural machines produced in the former Soviet Union are given in (table.3).

Table.3: *Data on failures of the main components of some agricultural machines. %.*

Machine type	Brand	Engine	Gearbox	Control system	Electr. Devices	Hydraulics	Coupling Clutch Variator	Variator	Header	Grilles	Belts	Others
tractors	GOLDONI	60,8	9,3	2,7	9,4	4,4	7,7	_	_	_	_	5,7
	MESSEY FERGUSON	26,9	10,1	26,7	9,4	9,6	10,0	_	_	_	_	7,3
	MTZ	14,5	17,4	29,4	10,0	8,5	15,0	_	_	_	_	5,2
	DT-75	35,0	11,0	32,2	4,0	7,8	6,4	_	_	_	_	3,6
	NEW HOLLAND	55,3	9,5	5,3	5,2	9,9	10,0	_	_	_	_	4,8
Combine harvesters	MESSEY FERGUSON	24,5	7,0	2,0	9,3	13,8	_	19,1	7,7	2,0	8,9	5,7
	SAMPO	24,0	6,8	_	5,0	23,0	_	18,0	10,2	2,0	6,0	5,0
	NIVA	22,5	_	3,0	13,6	14,0	_	_	20,0	5,2	7,1	5,6
	KLAAS	25,0	_	_	13,5	22,0	_	_	14,9	2,3	14,0	8,3

Machine type Brand Engine Gearbox Control system Electr. Devices Hydraulics Coupling Clutch Variator Header Grilles Belts Others.

The analysis of the studies obtained shows that most of the tractors produced in the former Soviet Union have failures of parts and components of the control system, which significantly reduces their operational reliability and worsens the working conditions of the operator, and foreign machines have much higher reliability indicators. The only drawback that we recorded for this technique was a large proportion of engine failures in tractors and combines, which was caused by the use of low quality fuel and lubricants and violation of maintenance rules by machine operators. We believe that in order to improve the reliability of this agricultural machinery, structural changes to the power supply and lubrication systems are necessary in order to use double cleaning filters.

With the help of probabilistic-statistical modeling and the methodology developed by us [5, 6], for NEWHOLLAND tractors, we have determined such reliability indicators as mean time between failures -, probability of no-failure operation -, failure rate -, availability and technical use factors - K1i K2. The research results are presented in table. 4 and in the (figure.4).

In these graphs, P (H) is the probability of failure-free operation, f (H) is the probability density of failures, F (H) is the integral distribution function, and they are determined by our method [6]. The dashed lines show their empirical values.

The analysis of the research results showed that foreign agricultural machinery in terms of reliability significantly exceeds that of the machines of the former Soviet Union. So, for example, for a NEW HOLLAND tractor, the probability of failure-free operation when operating motorcycle hours is, for a DT-75 tractor, and the mean time between failures is, respectively, equal to motorcycle hours and motorcycle hours.

Table.4: *Tractor reliability indicators, NEW HOLLAND.*

Operating time interval $a...b$	Middle of the interval H_i	Empirical failure rate m_i	Empirical probability W_i
0.0...300	150	42	0.30
300...600	450	29	0.20
600...900	750	24	0.17
900...1200	1050	17	0.12
1200...1500	1350	12	0.09
1500...1800	1650	8	0.06
1800...2100	1950	5	0.04
2100...2400	2250	3	0.02

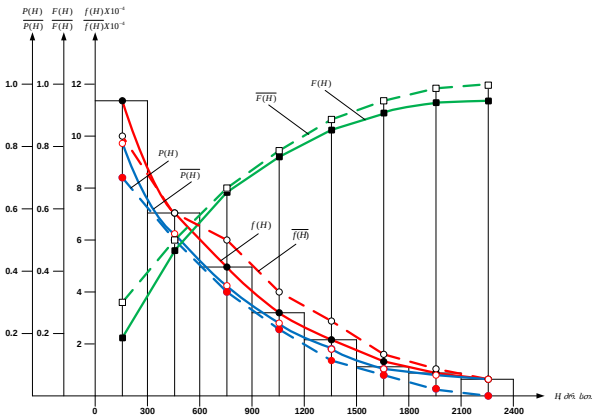


Fig 1*. Tractor reliability charts NEW HOLLAND.*

3. Conclusions:

1. On the basis of theoretical and statistical studies, the main indicators of the operational reliability of foreign agricultural machinery and typical failures when working in the special soil and climatic conditions of Georgia have been established

2. Developed general and specific methods of theoretical and statistical research.

3. Constructive and technological measures to improve reliability have been proposed.

4. References:

1. J. Katsitadze - Reliability and repair of machines, Tbilisi, 2001.-192 p.

2. Pronikov A. S. - Reliability of machines, Moscow ,Mechanical engineering, 1988. - 592 p .

3. Kugel RV - Tests for the reliability of machines, Moscow, 1982 - 230s;

4. Archard T. F., - Hirst W The wear of metals under unlubricated conditions, Proc. R. Soc, 1986, No. 1206, vol. 236, p. 397 ... 410;

5. Brook, R. H. Rellability Concepts in Engineering Manufacture, London, Butterworths, 1982. P. 132.

6. Jemal Katsitadze, Zaur Phutkaradze ,Application of modern mathematical methods for optimizing technological processes to increase machine reliability, Lambert, 2020, 138 p.

Evaluation of chosen indicators of intermittent seeder´s work quality

Maksym Stankevych[1], Jozef Rédl[1], Miroslav Prístavka[1*], Agnieszka Szparaga[2], Slawomir Kocira[3], Pavol Findura[1], Ingrida Košičiarová[1]
Slovak University of Agriculture in Nitra, Slovakia[1]
Koszalin University of Technology, Koszalin, Poland[2]
University of Life Sciences in Lublin, Lublin, Poland[3]
miroslav.pristavka@uniag.sk

Abstract: *As crop and animal production are interconnected, they together form the basic branch of agriculture. A great sense in the process of replacing cultivated crops is the cultivation of sugar beet, which can act as a breaker in planting of narrow row crops, livestock feed or green manure. In addition to seed development, cultivation technology has also been improved, and by that the technique has been modified. During cultivation, it is difficult to prepare the soil before sowing together with a good settlement of seeds in the soil, which creates suitable conditions for germination and subsequent emergence of plants. In the submitted article, we have focused on the evaluation of chosen indicators of intermittent speeder's work quality. The measurements have been performed in accordance with the ISO 7256/1 standard for the evaluation of sowing equipment with intermittent sowing. The vertical distribution of the seed in the soil for field emergence at the seed base of the seeder Kverneland Accord Monopill S, at different working speeds, has been observed. The experiment was performed on aluminous-sandy soil with a soil moisture of 18.2%. In measuring the sowing depth, there were used two measuring systems, the so-called contact (inductive) sensor and non-contact (ultrasonic) sensor in connection with A / D converter with storage in IM memory card. Based on the obtained results, we can state that by increasing the travel speed from 1.11 m.s^{-1} to 3.33 m.s^{-1}, the depth of the sowing foot was reduced on average by 19.61 mm.*

Key words: *SEEDING, WORKING SPEED, ISO STANDARD*

1. Introduction

Sowing represents an important work operation, where for its correct execution, correct setting of the seeder and the control of its operation, it is crucial the technical discipline of operation. The quality of the sowing is than given by the required surface (horizontal) and deep vertical placement of the seed in the soil with minimal damage (Findura & Košičiarová, 2020).

The vertical distribution of seeds is given by its deep placement, the so-called sowing depth. According to the Slovak standard (STN) 46 54 51, the term sowing depth means the distance from the lower edge of the seed to the soil surface above the seed after it has been deposited in the soil. In sowing beets, that definition needs to be clarified. It is true that the sowing depth (h) is given not only by the depth of seed placement in the soil (which is the distance between the lower edge of the seed and the original soil surface), but also by the height of soil loading above the seed. The depth of the seed coulter can vary depending on the soil conditions (Turan et al., 2019). Soil compaction caused by frequent passes of the technique, especially in the spring, has a secondary effect on the resistance of the soil to the deepening of the seed coulter (Findura et al, 2018). A certain solution is the use of soil bio stimulation, which improves the physical and mechanical properties of the soil, i.e. higher porosity, soil structure, better infiltration and consequently lower tensile resistance in tillage (Kocira et al, 2018).

The main factor in choosing the optimal depth is the contact of the seed with the water-conducting layer of the soil (Kretschmar, 1983; Brunotte, 1986; Kästner, 1992).

The aim of the paper is to evaluate the vertical distribution of seeds in chosen seed bases forming a row seed at different working speeds and also to evaluate the conditions under which experimental measurements were performed in accordance with ISO 7256/2 at a chosen seed KVERNELAND Monopill S. The paper was solved within the project VEGA 0102/21 Reducing chemical loads and degradation of agricultural and forestry soils by selecting appropriate agri-technology with regard to climate change.

2. Material and methods

For the methodology of the work, we have used the laboratory technology which is a part of the measurement technology of the Department of Machines and Production Biosystems of the Faculty of Engineering SUA in Nitra. We could divide this methodological part into laboratory measurements and field experiments.

Within the laboratory measurements, we have:

- monitored the properties of the used seeds,
- analysed the soil samples taken in the experimental field.

Within the field measurements, we have:

- monitored the soil condition, this is characterized by several indicators such as soil type, soil structure, soil specific gravity, soil bulk density, soil porosity, soil moisture and penetrometric soil resistance.

In evaluation of soil properties, we have started from the ISO 7256/1 standard for testing the seed drills for precision sowing resp. seeders with intermittent sowing in field conditions and we have used the usual methods of determining the soil properties using Kopecký rollers with sampling after loosening and rows after sowing at depths of 0-30 (15), 30-60 (45), 60-90 (75) with three repetitions.

The structure of the soil as a grouping of individual soil particles and aggregates was monitored by taking samples from a depth of 0-30 mm and processing them by a standard sieve method with gradation of soil fractions from <0.125 mm; 0.125 - 0.063 etc. up to 8 - 16 mm; 16 - 32 mm and over 32 mm after the pre-sowing loosening of the soil.



Figure 1 Apparatus for measuring the soil penetrometric resistance

Description and technology of the machine´s work

The seeder is made as a mounted machine, as the entire weight of the machine during transport rests on the tractor's hydraulic arms. The basic parts of the machine are a frame with a three-point

attachment, seeding units, support and drive wheels, gears, markers and accessories.

When the seeder moves, the individual sowing units connected to the frame by means of a parallelogram are adjusted in height to the unevenness of the soil surface. The front depth wheel evens out the soil surface. The seeds are pushed through a narrow middle wheel and covered with soil wrappers. The rear push wheel closes the sowing process.

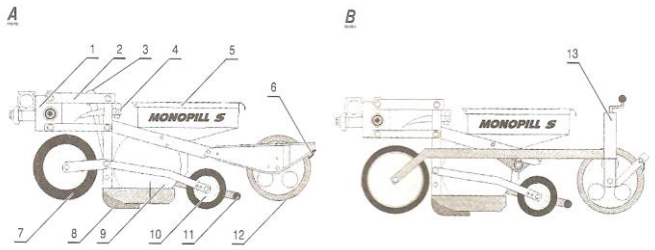


*Figure 2 The sowing unit of Monopill S seeder: **A** - with front depth wheel, 1 - mounting the seeding unit on the frame, 2 - parallelogram, 3 - sowing depth adjustment, 4 - lifting device, 5 - hopper, 6 - squeegee, 7 - front wheel, 8 - heel, 9 - sowing device, 10 - middle push wheel, 11 - wrapper, 12 - rear push wheel; **B** - with tandem wheel arrangement, 13 - sowing depth adjustment*

Depending on the accessories, precise sowing of the seed can be combined with the application of granular pesticides or with belt spraying. The machine is designed for sowing within the conventional technology with pre-sowing soil preparation, but after the adjustment of the sowing feet it is also able to sow into mulch. In the "S" version it is a mechanical version with mechanical gears, and in the "SE" version it is a version with electric drive of sowing units.

***Table 1** Technical parameters of the tested seeder Monopill S*

number of rows		curb weight in kg		sowing depth	optimum working speed	optimum working speed in sowing into mulch	seed spacing in a row	required power of the tractor engine
P - fixed frame	S- folding frame	P- fixes frame	S- folding frame	mm	km/h	km/h	v mm	v kW
6, 12, 18	12, 18	400 (6)	2 180 (18S)	0 - 65	5 - 7,5	5 - 5,5	118 - 278	35 - 120

Methodology for measuring the depth of the seedbed in the soil

Soil is an important natural and economic resource in agriculture (Rovný et al., 2017). It is a crucial natural resource in Slovakia with commodity and non-commodity potential for economic and eco-social development of our society. It defines the territory – it is the principle of statehood, mostly in private ownership and is important for all inhabitants of the state (Findura & košičiarová, 2020). While in the past, soil was considered to be the basic means of production in agriculture, nowadays it is rather understood as a crucial component of the environment, which conditions the agricultural development (Bujnovský et al., 2009).

The quality of seed storage in the soil is given by its vertical distribution, which is the depth and uniformity respectively the variability of its horizontal distribution in the sown rows. We have monitored the seeder at four working speeds of 8, 10, 12, 14 km. h^{-1} and three repetitions (Figure 3). We have performed the measurements in accordance with the ISO 7256/1 standard for the evaluation of sowing equipment with intermittent sowing.

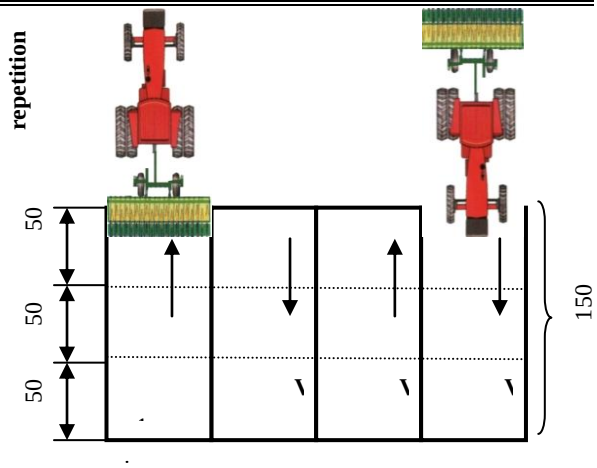


Figure 3 Display of the movement of seeder along defined measuring sections

The term sowing depth in the sense of standard STN 46 5451 means the distance from the lower edge of the seed to the soil surface above the seed after its deposition in the soil. We have used two measurement systems, the so-called contact (inductive) sensor and non-contact (ultrasonic, optical) sensor in connection with A / D converter with storage in IM memory card. The aim was to design a measuring device that allows mounting on various sowing units of monitored seeders. The sowing depth measurement was performed by the continuous measuring of the distance between the seed coulter position and the soil surface.

3. Results and discussion

Results of soil properties

The measurements were performed in temperate conditions in the region of western Slovakia in the district of Nitra on the plots of the university farm VPP Oponice. The experiment was performed on aluminous-sandy soil. The standard for sowing quality evaluation shows to characterize the conditions under which the experiment was performed. Soil is an important indicator and therefore we have evaluated its condition.

From these properties we have monitored the soil type, soil structure, soil bulk density at depths of 0-105 mm, soil penetrometric resistance at depths of 0-200 mm and soil surface balance, etc.

All measurements were performed on aluminous-sandy soil with a percentage of grains smaller than 0.01 mm in the range of 22-33%.

As part of the measurement, we have compared two variants on the soil. Variant A, which is the soil unaffected by the passage of equipment and variant B, where the soil is affected by the wheel of the tractor.

Based on the obtained results, we can state that by increasing the depth of moisture measurement, the humidity has gradually increased. Even for the variant affected by the wheel of the tractor (variant B), a higher average humidity was measured, which can be caused by the rising of water into the soil.

***Table2** Results of evaluation the soil properties*

Plot I mm (ø)	Mass moisture of the soil, %		Porosity, %		Specific weight of soil, t.m-3	
	A	B	A	B	A	B
0-30 (15)	18,04	18,47	58,33	54,33	2,628	2,643
15-45 (30)	19,99	21,31	55,34	50,01	2,638	2,627
30-60 (45)	21,03	22,06	51,48	49,01	2,643	2,637
45-75 (60)	22,35	26,20	50,21	47,96	2,645	2,680
60-90 (75)	23,41	24,18	48,73	46,54	2,653	2,680
75-105 (90)	24,30	24,57	46,87	43,49	2,628	2,663

Another evaluation criterion of soil condition was the measurement of soil porosity. There was a positive trend of higher porosity with a higher content of capillary and non-capillary pores. This has a positive effect on soil infiltration, especially in irregular excessive precipitation. All results listed in Table 2 were evaluated

in the laboratory and were collected at predetermined sampling points.

From the Figure 4, it can be seen the compaction of the soil in the individual soil horizons. At the depth of 30-50 mm, there can be seen the effect of soil compaction by the push system of the seeder, which has to support the soil uptake. At the same time, there can be seen the subsequent decrease of the penetrometric resistance, which can be observed up to the place of compacted so-called "dead soil" located below the depth of tillage.

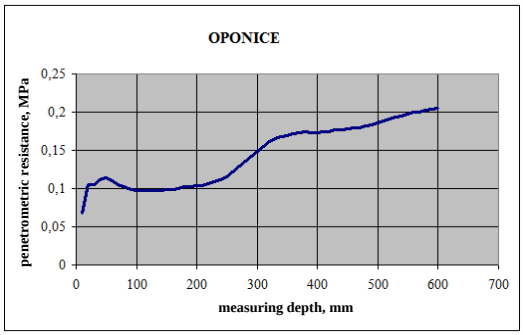


Figure 4 Process of soil penetrometric resistance

Results of dimensional and shape properties of used seeds

Since the 1990s, genetically single-germinal sugar beet seeds have been supplied to the Slovak market (Horská et al., 2010). We require an approximately spherical to lenticular shape. The individual dimensions of the seeds affect the quality of the sowing, depending on the choice of a suitable sowing device.

Table 3 Properties of used seeds

Seed (calibratio)	Germination	Seed dimensions			Shape coefficients				Weight of 1000 seeds
		Length $\bar{d}$	Width $\bar{s}$	Thickness $\bar{h}$	$k_1=\frac{l+s}{2}/h$	$k_2=\frac{s}{h}$	$k_3=\frac{l}{h}$	$k_4=\frac{l}{s}$	
mm	%	mm	mm	mm	-	-	-	-	g
Continental (3,5-4,75)	98	3,92	3,71	3,56	1,072	1,042	1,101	1,057	28,60

$\bar{d}, \bar{s}, \bar{h}$ - average length, width and thickness of seeds, k_1,k_2,k_3,k_4- shape coefficients of seeds

We have expressed the shape properties using the shape coefficients k_1-k_4, the more balanced the mutual values of the coefficients, the more ideal (round) shape the seed will have. Table 3 shows the average values of length, thickness, width and shape coefficients of the seed used for both seeders.

Based on the measured results, we can state that Continental seed was used for the experiment, in the germination test in the laboratory we have achieved 98% germination. Regarding the values of the average length, we have achieved an average value of 3.92 mm, an average width of 3.71 mm and the smallest dimension thickness of 3.56 mm.

The shape coefficient tells us how the shape of the seed approaches the ideal spherical shape. Its determination is based on the basic dimensions, namely length, width and thickness. Based on these coefficients, we can state that there are minimal differences between the shape coefficients and the largest difference is between the coefficient k_2 and k_3.

Results of the evaluation of sowing depth

In the evaluation of the the seedbed depth, for the credibility of the results, there were used two systems. The non-contact system was secured by means of an ultrasonic sensor and a contact system, which was connected to the frame of the seeder by means of a reptile, where each change in the recess was manifested by a change in induction when the core was inserted into the inductive sensor housing.

The task of sowing is to ensure the area and depth distribution of seeds in the soil so as there will be created the most favorable conditions for germination, emergence, development and harvesting of beets. The parameters that affect the distribution of seeds in the soil are mainly the properties of the soil, the parameters of the seeder and its working speed.

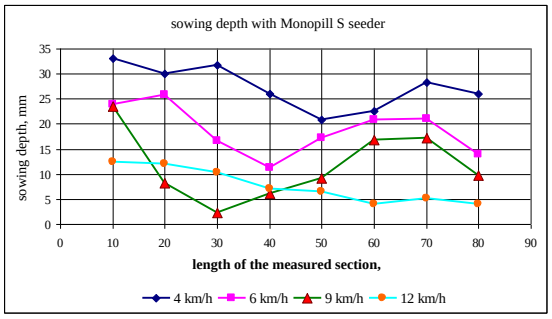


Figure 5 Sequence change of the seed coulter depending on the travel speed

Table 4 Statistical indicators for the evaluation of sowing depth

	1,11m/s	1,6 m/s	2,5 m/s	3,3 m/s
Average	27,33	18,85	11,66	7,69
Mistake of the Mean value	1,51	1,76	2,46	1,21
Median	27,22	19,01	9,48	6,79
Standard deviation	4,27	4,98	6,96	3,43
Selection variance	18,20	24,81	48,47	11,77
Spiky	-1,05	-0,97	-0,44	-1,70
Sloppiness	-0,23	-0,13	0,54	0,43
Difference max - min	12,14	14,57	21,23	8,40
Minimum	20,86	11,23	2,35	4,07
Maximum	33,00	25,80	23,58	12,47
Sum	218,63	150,79	93,28	61,50
Largest (1)	33,00	25,80	23,58	12,47
Smallest (1)	20,86	11,23	2,35	4,07
Reliability level (95.0%)	3,57	4,16	5,82	2,87

Based on the measured and evaluated results, we can state that the working speed of the seeder has a significant effect on maintaining the depth of sowing. The set sowing depth was 30 mm, which is the ideal sowing depth for the given humidity conditions. At a speed of 1.11 m.s^{-1}, the deviation was minimal, with increasing working speed, the sowing depth gradually decreased. Such non-compliance with the sowing depth may, in the case of adverse climatic conditions, affect the germination and emergence of the plants. The largest deviation from the set sowing depth was recorded at a speed of 1.11 m.s^{-1}, only 7.69 mm.

4. Conclusion

Farmers often attribute the failures in sugar beet cultivation to unfavourable climatic conditions, or low-quality seed, but the true is, that the technical parameters of the seeder can be also perceived as a significant factor. They affect both, the horizontal distribution of the seed and its vertical placement to the required depth. We tried to prove the above mentioned with our own measurements in the given field. Based on the obtained results, we can state that:

- All measurements were performed on aluminous-sandy soil with a percentage of grains smaller than 0.01 mm in the range of 22-33%.
- Another evaluation criterion of soil condition was the measurement of soil porosity. There was a positive trend of higher porosity with a higher content of capillary and non-capillary pores. This has a positive effect on soil infiltration, especially in irregular excessive precipitation.
- In the depth of 30-50 mm, the effect of soil compaction can be seen with the push system of the seeder, which is intended to support the soil uptake. At the same time, we can see that subsequently the penetrometric resistance decreases to the place of compacted so-called "dead soil" located below the depth of tillage.
- Based on the measured results, we can state that in the case of Continental seed, which was used for our experiment, in the germination test (in the laboratory)

there was achieved 98% germination. Regarding the values of the average length, we have achieved an average value of 3.92 mm, an average width of 3.71 mm and the smallest dimension thickness of 3.56 mm.

- At the speed of 1.11 $m.s^{-1}$, the deviation was minimal, with increasing working speed, the sowing depth gradually decreased. Such non-compliance with the sowing depth may, in the case of adverse climatic conditions, affect the germination and emergence of the plants. The largest deviation from the set sowing depth was recorded at a speed of 1.11 $m.s^{-1}$, only 7.69 mm.

Acknowledgement
The paper was solved within the project VEGA 1/0102/21 Reducing chemical loads and degradation of agricultural and forestry soils by selecting appropriate agri-technology with regard to climate change.

5. References

1.Bujnovský, R. -- Balkovič, J. -- Barančíková, G. -- Makovníková, J. -- Vilček, J. 2009. Hodnotenie a oceňovanie ekologických funkcií poľnohospodárskych pôd. Bratislava : VÚPOP, 2009. 71 s. ISBN 978-80-89128-56-3.
2.Horská, E. -- Nagyová, Ľ. -- Rovný, P. -- Skořepa, L. -- Kádeková, Z. -- Švec, M. -- Golian, J. -- Záboj, M. -- Halier, B. -- Priya, P. -- George, K. -- Drličková, E. -- Kusá, A. -- Kompasová, K. -- Kaputa, V. -- Maťová, H. -- Kaufmann, H. -- Orphanidou, Y. -- Gronau, W. -- Szafrańska, M. -- Matysik-P. Merchandising a event marketing pre produkty pôdohospodárstva. 1. vyd. Nitra : Slovenská poľnohospodárska univerzita v Nitre, 2010. 329 s. ISBN 978-80-552-0469-7.
3.Findura, P. -- Košičiarová, I. Evaluation of the efficiency of surface placement of seeds for innovative sowing method. 1.vyd. Ostrava : Key Publishing, 2020. 150 s. ISBN 978-80-7418-353-9.
4.Findura, P. -- Prístavka, M. -- Korenko, M. -- Bajus, P. The evaluation quality of sowing independence with selected properties of seeds /: Pavol Findura ... [et al.]. In Mechanization in agriculture. 64, 1 (2018), s. 3--7. ISSN 0861-9638.
5.Kocira, S. -- Szparaga, A. -- Kocira, A. -- Czerwińska, E. -- Wójtowicz, A. -- Bronowicka-Mielniczuk, U. -- Koszel, M. -- Findura, P. Modeling biometric traits, yield and nutritional and antioxidant properties of seeds of three soybean cultivars through the application of biostimulant containing seaweed and amino acids. In Frontiers in Plant Science. 9, 388 (2018), s. 2018. ISSN 1664-462X.
6.Rovný, P. - Dobák, D. -- Kádeková, Z. -- Kubicová, Ľ. -- Smutka, L. Minimum land requirements for average family income produced in the Slovak agriculture. In Agrarian perspectives XXVI. 1. vyd. 463 s. ISBN 978-80-213-2787-0. Agrarian perspectives. Praha : Czech University of Life Sciences, 2017, s. 327-334., s. 33 – 49.
7.Turan, J. -- Višacki, V. -- Oparnica, S. -- Sedlar, A. -- Findura, P. -- Burg, P. Varijabilnost normalizovanih vegetativnih indeksa u šećernoj repi = Variability of normalized vegetative indices in sugar beet. In Savremena poljoprivredna tehnika. 45, 3 (2019), s. 119--126. ISSN 0350-2953.

Selection of the information parameter for the thermography method of diagnostics of dairy cows mastitis

Ivan I. Hirutski, Yuri A. Rakevich, Andrey G. Stankov

Belarussian State Agrarian Technical University – Minsk, Belarus
E-mail: gir_50@mail.ru

Abstract: *In the paper are presented experimental results of exploring the thermography method of diagnostics of dairy cows mastitis depending on the basic used information parameter. Prospects for embedding the information on the udder thermography results into the herd management system are discussed.*
KEY WORDS: *DIAGNOSTICS, MASTITIS, THERMOGRAPHY, DAIRY COW, STATISTICS.*

Introduction

In the information support of dairy cattle breeding, an urgent task is to determine the subclinical mastitis of cows in real time. There are different methods of diagnosis of subclinical mastitis, for example, direct measurement of the somatic cells count (SCC) or California mastitis test (CMT). However, both these methods have poor promptness at loose cow housing conditions. So, it is necessary to develop new technologies and improve existing methods and technical means for diagnosing mastitis allowing identification diseases during milking process and providing individual service to animals in order to prevent the mixing of milk from healthy and sick animals and timely start of veterinary treatment. A thermography method of diagnostics of dairy cows mastitis is of great scientific and practical interest as it is contactless and multifunctional [1-15]. But this method is indirect, therefore, it is necessary to make its experimental research under real production conditions of a dairy farm.

Description

Experimental studies were carried out on an operating dairy farm in the Republic of Belarus. In total, 580 black-and-white cows of the dairy herd were examined. The Inter Clean kenotest was used as a reference option for the diagnosis of mastitis [16]. Experimental studies included two stages. At the first stage, the animals were subjected to a comprehensive clinical examination by the veterinarian specialist. Further, according to the kenotest, there were identified 4 groups, of 30 cows in each one, with different levels of disease. The first group consisted of healthy animals with a negative kenotest test (-); in the second group were cows with a questionable kenotest (+); the third group included animals with a subclinical stage of mastitis (++), and the fourth one – with a clinically pronounced stage of mastitis (+++).

At the second stage, single measurements of udder temperature were carried out by analyzing a thermographic image of each of 30 cows belonging to different animal groups (table 1). Thermographic images of a cow's udder were made during milking process by a handheld thermal imager DT 9875 [17]. The thermal imager was installed on a tripod at a predetermined distance of 0.6 meters. The device allows you to create digital images – thermograms, which makes it possible for their subsequent analysis using a computer. The measurements were carried out with an accuracy of 0.02 °C.

As an informational parameter, the where analyzed the following ones: maximum udder temperature, the difference between maximum temperature values of 4 shares of the cow's udder, dynamics of changes in the maximum temperature of the udder during the milking process and temperature distribution along the length of the cow udder nipple.

The analysis of thermographic images of the udder illustrates the distributed nature of the temperature field (fig. 1). Locally the temperature rises in places with inflammatory processes. Therefore, the maximum temperature of individual udder areas was considered as the information parameter for classification.

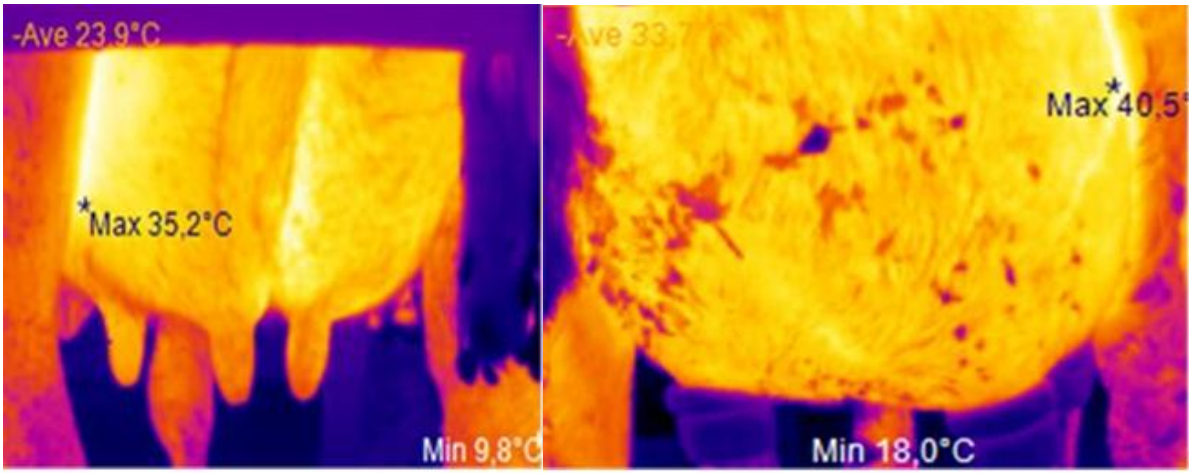


Figure 1 *– Examples of thermographic images of the cow's udder having maximum temperature values of 35,2^{0}C and 40,5^{0}C*

Statistical processing of experimental results shows that with an increase in the incidence of mastitis, an increase of the average temperature of the cow's udder is observed. Analysis of random sample values $Y_1, ..., Y_n$ for their belonging to the normal distribution of probability density according to the criterion of the mean absolute deviation (MAD), shows that they belong to the normal distribution law of random variable (tab. 1).

The experimental value of the MAD criterion is determined by the formulae:

$$\theta_{exp} = \left| \frac{CAO}{S} - 0.7979 \right| = \left| \frac{\sum_{i=1}^{n} |Y_i - \bar{Y}|}{nS} - 0.7979 \right|.$$

The table value of the MAD criterion is:

$$\theta_n = \frac{0.4}{\sqrt{n}}.$$

According to MAD criterion, if $\theta_{exp} < \theta_n$ then the random sample values $Y_1, ..., Y_n$ belong to the normal distribution law; if $\theta_{exp} > \theta_n$ then they don't belong to it. The results of statistical data processing show that the normal distribution law can be used to describe the probability density distribution of the maximum udder temperature of cows for each of the 4 groups of animals (see tab. 1)

Table 1. *The results of experimental data processing on the maximum temperature of the udder for 4 groups of cows, obtained at a confidence level of p = 0,95%*

Experimental data parameters	Negative kenotest (-)	Questionable kenotest (+)	Subclinical kenotest (++)	Clinically pronounced knotest (+++)
Number of cows in a group, *n*	30	30	30	30
Average udder temperature by group of cows, ^{0}C, $\bar{Y}$	36,2	37,3	38,5	39,6
Dispersion, S^2	0,650	0,217	0,198	0,209
Normal distribution test	yes	yes	yes	yes

An important result of statistical processing of the experimental data is the conclusion about the normal nature of the probability density distribution of the maximum temperature of the udder of a cow for all 4 groups of animals. This makes it possible to use in further analysis well developed theoretical methods of statistical data processing for the normal distribution of a random variable. The probability density curves of the maximum udder temperature have overlapping zones (fig. 2). Therefore, the problem arises of finding an algorithm for making a decision on the classification of a particular cow to one of 4 groups of cows based on the results of measuring the maximum udder temperature.

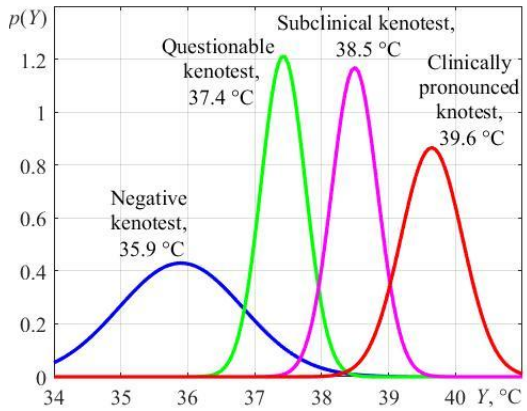


Figure 2 *– Distribution of the probability density of the maximum temperature of the udder for 4 groups of cows according to the stage of mastitis*

When making a decision on the classification of a particular cow based on the results of the analysis of an udder thermographic image, 4 options are possible:

- correct detection of the absence of mastitis;
- correct detection of the stage of mastitis;
- skipping the disease;
- false alarm about the disease.

Mutual overlapping of udder temperature distribution curves for different groups of cows can be explained by the biological nature of the controlled object and the influence of various disturbing factors such as stress, change in ambient temperature, lactation period, etc. Therefore, it is necessary to study the influence of various disturbing factors on the result of the analysis of an udder thermographic image and to explore the possibility of reducing the variance.

Obviously, udder temperature will be influenced by the effects of the milking machine during milking. Therefore, experimental studies were performed on the change in the maximum temperature of the udder in the process of milking for different groups of cows (fig. 3).

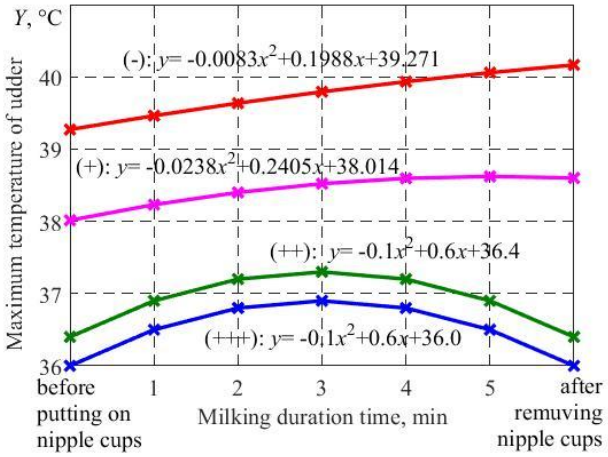


Figure 3 *– The dynamics of changes in the maximum temperature of the udder before putting on the nipple cups of milking machine, then every minute during milking and, finally, after removing the nipple cups*

Thus, as can be seen from Fig. 3, in the process of milking, the temperature of the udder of a cow changes significantly, which must be taken into account when obtaining an udder thermographic image used for the diagnosis of mastitis.

As the next informational parameter, we investigate the relationship between the temperature difference by quarters of the udder and the mastitis test group of cows. The criterion for the early detection of mastitis in cows is the difference in the maximum temperatures of the front and rear lobes of the udder.

$$\Delta T_{max}^{f} = \Delta T_{max}^{a} - \Delta T_{max}^{b}$$

where $\Delta T^{a}_{\max}$ is the maximum temperature of the left anterior lobe of the udder, °C;

$\Delta T^{b}_{\max}$ is the maximum temperature of the right front lobe of the udder, °C.

For the rear lobes the corresponding formulae is the following one:

$$\Delta T^{r}_{\max} = \Delta T^{c}_{\max} - \Delta T^{d}_{\max}$$

where $\Delta T^{c}_{\max}$ is the maximum temperature of the left rear lobe of the udder, °C;

$\Delta T^{d}_{\max}$ is the maximum temperature of the right rear lobe of the udder, °C.

As a result of the experiment, values were obtained for each lobe of the udder during milking (see tab. 2).

Table 2. *Change in the difference between maximum temperatures for each lobe of the udder of cows and the results of the kenotest*

№	Cow ID	Research method	Results of the research of udder lobes					
			front lobes			rear lobes		
			left	right	$\Delta T^{f}_{\max}$	left	right	$\Delta T^{r}_{\max}$
1	132	Kenotest	++	-		-	-	
		Thermal imaging test, ºC	38,6	37,0	1,6	36,8	36,4	0,4
2	736	Kenotest	-	-		-	-	
		Thermal imaging test, ºC	34,5	34,7	0,3	35,1	35,3	0,2
3	656	Kenotest	-	-		-	+++	
		Thermal imaging test, ºC	36,4	36,5	0,2	36.4	40,5	4,1
4	677	Kenotest	+	-		-	-	
		Thermal imaging test, ºC	37,8	36,8	1,0	36,2	35,9	0,3
5	517	Kenotest	-	-		+	-	
		Thermal imaging test, ºC	34,1	34,2	0,1	37,4	36,2	1,2
6	547	Kenotest	+++	-		-	-	
		Thermal imaging test, ºC	39,2	36,7	2,5	36,4	36,4	0
7	786	Kenotest	-	++		-	-	
		Thermal imaging test, ºC	37,0	38,5	1,5	36,5	36,9	0,4
8	862	Kenotest	-	-		-	-	
		Thermal imaging test, ºC	35.6	35,8	0,3	36,2	36,0	0,2
9	211	Kenotest	-	-		-	++	
		Thermal imaging test, ºC	35,1	35,6	0,5	36,6	38,4	1,8
10	314	Kenotest	-	+++		-	-	
		Thermal imaging test, ºC	36,7	39,1	2,4	36,2	36,7	0,5

For calculations, the difference between the maximum temperature values for each lobe of the udder of cows was taken into account. For the case of subclinical mastitis the difference between the maximum temperature values for the anterior lobes of the udder was $\Delta T^{f}_{\max} = 1.6$ ºC, and for the corresponding difference for rear lobes of the udder was $\Delta T^{r}_{\max} = 1.8$ ºC. At more severe stages of mastitis (pronounced inflammatory process), the above difference for the anterior lobes of the udder was $\Delta T^{f}_{\max} = 2.4$ ºC, and for rear lobes of the udder it was $\Delta T^{r}_{\max} = 4.1$ ºC, that indicates an acute form of the disease.

The difference within the range of up to 0.5 ºC between the maximum temperature values for each lobe of the udder corresponds to a healthy udder, the difference in temperature values of 1.0 ºC and more indicates the presence of an inflammatory process. The greater the difference in temperature, the more pronounced the inflammatory process. Thus, the maximum temperature of the afflicted lobes with clinically expressed mastitis (confirmed by kenotest) was 4.1 ºC more high compared to other healthy lobes of udder.

Thus, this parameter - the difference between the maximum temperature values for each lobe of the udder – is informative and can be used in the decision-making algorithm. In this case are required the use of several sensors (thermal imagers) and a rational construction design.

As the next informative parameter in the diagnosis of mastitis, we studied the temperature distribution along the length of the udder nipples for healthy (fig. 4) and sick cows.

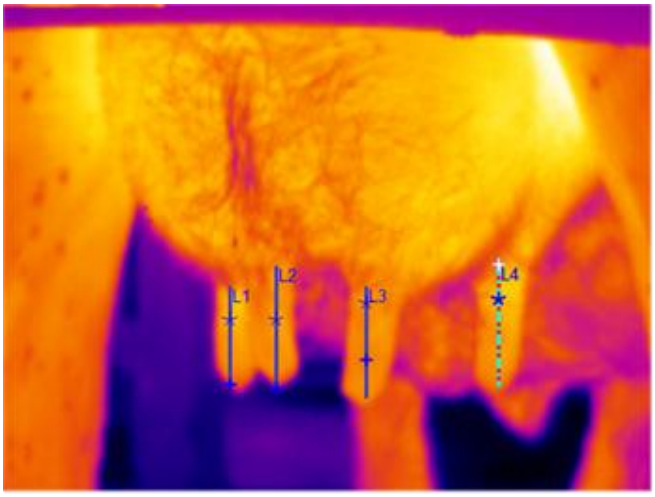


Figure 4 – Infrared image of mastitis-free udder nipples after milking; L1 is left anterior nipple length; L2 is left rear niplle

length; L3 is right rear nipple length;
L4 is anterior right nipple length

It can be seen from the graphs that the temperature distribution along the udder nipple length of a healthy cow is even along the entire nipple length. The maximum temperature was observed at the top of the nipple and it was 34,8 °C (fig. 5).

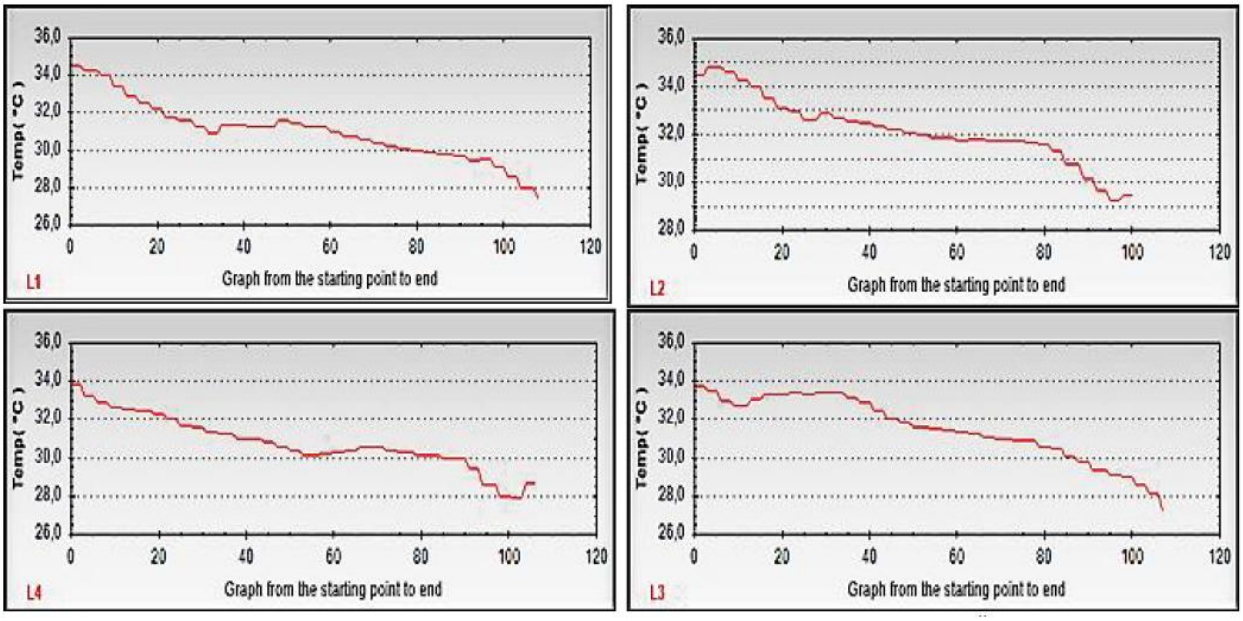


Figure 5 *– Temperature distribution graphs along the length of the mastitis-free udder teats after milking*

At the same time, for a cow with mastitis, it can be seen that the temperature distribution along the length of the udder nipples is uneven at the beginning of the apex of the nipples. The maximum temperature was observed at the top of the nipples and it was 36.2 ° C (fig. 6).

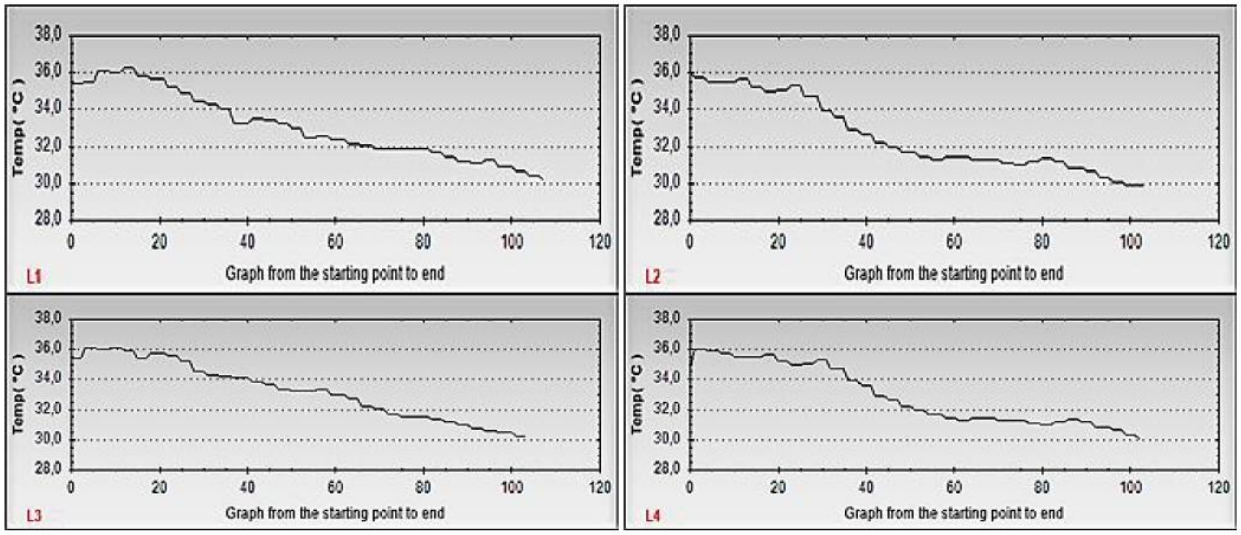


Figure 6 *– Temperature distribution graphs along the length of the mastitis afflicted udder teats after milking*

The use of this informative parameter – the temperature distribution along the length of the udder nipples – can be useful when testing gentle milking modes of various milking machines.

Due to the biological nature of the cow, various disturbing factors can affect the thermometry results, such as stress, ambient temperature, age, feeding time, etc. It is possible to increase the reliability of determining the mastitis disease in dairy cows by repeatedly measuring the maximum udder temperature with subsequent statistical processing of the results using decision theory methods.

The variance of the sample mean is known to be n times less than the variance of one sample. Hence follows the most important property of the result of multiple measurements: its uncertainty is less than the uncertainty of the result of a single measurement.

$$\sigma_{\bar{X}}^2 = \frac{\sigma_X^2}{n} \ .$$

Experimental studies were performed to study the possibility of reducing the data variance by repeatedly monitoring the temperature of the cow udder followed by averaging over a certain time interval. Temperature measurements were carried out for selected 4 cows from different groups according to the degree of mastitis disease. Measurements were taken 2 times a day during morning and evening milking (see tab. 3).

Table 3. *Results of statistical processing of measurement of udder temperature of cows from different sample groups for a 10-day period*

Criteria		Negative kenotest (-)	Questionable kenotest (+)	Subclinical kenotest (++)	Clinically pronounced knotest (+++)
Sample mean	$\overline{Y}$	34,5	37,0	38,4	39,8
Sample variance	S^2	0,154	0,100	0,031	0,176
Experimental value of the MAD criterion	$\mathbf{Q_Э}$	0,0181	0,0246	0,051	0,012
Tabled value of the MAD criterion	$\mathbf{Q_n}$	0,1265	0,1265	0,126	0,126
Normal probability istribution test		positive	positive	positive	positive

Multiple measurements of udder temperature for a particular cow can significantly reduce the data variance and increase the likelihood of making correct decisions on the presence and the degree of mastitis. But, at the same time, it is necessary to find a compromise between the duration the period of collecting data on the cow udder temperature for a particular cow and the promptness of decision-making. At the same time, due to the statistical nature of the depending of cow udder temperature to the stage of mastitis disease, an urgent task is the development of decision-making algorithms based on the statistical theory [18].

Conclusion

Advantages of thermography compared to the other known methods of diagnosing mastitis are contactless, low labor and time costs and the capabilities of integration the information results to an automated herd management system.

At the presented work were performed in an operating dairy farm the experimental measurements of maximum temperature of a cow udder by thermographic method in 4 different groups of animals sampled according to the stage of mastitis determined by kenotest. The probability density function of udder temperature values in all sample groups of cows is described by the normal probability density law. Average maximum udder temperature during milking was 36,2 °C in healthy cows, and 38,5 °C at subclinical stages of mastitis, and 39,6 °C for clinically pronounced stages of mastitis.

It is advisable to accumulate thermographic data about cow udder temperature changes averaged over time over a certain time period. This will reduce the influence of random factors such as ambient temperature variations, lactation phase, stress on the animal, etc. As a result, this will increase the likelihood of correct decisions in identifying subclinical mastitis. In addition, the milking machine also affects the temperature of the cow udder, so it is necessary to take into account the moment of taking a picture during milking.

References

1. Ulrike Passarge. Gesundheitsmonitoring in Milchviehherden mit Hilfe von Infrarot-Thermographie: dissertation doctor rerum agriculturarum / Ulrike Passarge – Berlin, 2013. – P. 1 – 188.
2. Poikalainen, V., Praks, J., Veermae, I. and Kokin, E. Infrared temperature patterns of cow's body as an indicator for health control at precision cattle farming. / Agron. Res. Biosyst. Eng., 2012. – P. 187 – 194.
3. Nikkhah, A., Plaizier, J.C., Einarson, M.S., Berry, R.J., Scott, S.L. and Kennedy, A.D. Infrared thermography and visual examination of hooves of dairy cows in two stages of lactation / J. Dairy Sci., 2005. – P. 2749 – 2753.
4. Montanholi, Y.R., Swanson, K.C., Palme, R., Schenke, F.S., McBride, B.W., Lu, D. and Miller, S.P. Assessing feed efficiency in beef steers through feeding behavior, infrared thermography and glucocorticoids / Animal, 2010. – P. 692 – 701.
5. Alejandro, M., Romero, G., Sabater, J.M. and Diaz, J.R. Infrared thermography as a tool to determine teat tissue changes caused by machine milking in MurcianoGranadina goats / Livest. Sci., 2014. – P. 178 – 185.
6. Polat, B., Colak, A., Cengiz, M., Yanmaz, L.E., Oral, H., Bastan, A., Kaya, S. and Hayirli, A. Sensitivity and specificity of infrared thermography in detection of subclinical mastitis in dairy cows/ J. Dairy Sci., 93, 2010. – P. 3525 – 3532.
7. Berry, R.J., Kennedy, A.D., Scott, S.L., Kyle, B.L. and Schaefer, A.L. Daily variation in the udder surface temperature of dairy cows measured by infrared thermography / Potential for mastitis detection. Can. J. Anim. Sci., 2003. – P. 687-693.
8. Porcionato, M.A., Canata, T.F., De Oliveira, C.E.L. and Santos, M.V.D. Udder thermography of Gir cows for subclinical mastitis detection /Bio. Eng., 3, 2009. – P. 251 – 257.
9. Hovinen, M., Siivonen, J., Taponen, S., Hanninen, L., Pastell, M., Aisla, A.M. and Pyorala, S. Detection of clinical mastitis with the help of a thermal camera / J. Dairy Sci., 91, 2008. – P. 4592 – 4598.
10. Colak, A., Polat, B., Okumus, Z., Kaya, M., Yanmaz, L.E. and Hayirli, A. Short communication: Early detection of mastitis using infrared thermography in dairy cows / J. Dairy Sci., 91(11), 2008. – P. 4244 – 4248.
11. Metzner, M., Sauter-Louis, C., Seemueller, P.W. and Klee, W. Infrared thermography of the udder surface of dairy cattle: Characteristics, methods, and correlation with rectal temperature / Vet. J., 199, 2014. – P. 57 – 62.
12. Berry, R.J., Kennedy, A.D., Scott, S.L., Kyle, B.L. and Schaefer, A.L. Daily variation in the udder surface temperature of dairy cows measured by infrared thermography: Potential for mastitis detection / Can. J. Anim. Sci., 8, 2003. – P. 687 – 693.
13. Chun-He, Y., Xian-hong, G., Zhenghui, C.A.O., Xiaojun, Z., Yue, H., Yunxiang, L., Lei, S. and Yutao, Z. (2015) Study on possibility of left and right quarter skin temperature difference as a detecting indicator for subclinical mastitis in dairy cows /Acta Vet. Zootech. Sin., 46(9), 2015. – P. 1663 – 1670.
14. Schaefer A. L ., Cook N ., Tessaro S. V., Deregt D., Desroches G., Dubeski P. L., Tong A.K. W., Godson D. L. Early detection and prediction of infection using infrared thermography / Can. J. Anim. Sci.Vol. 84, 2004 – P. 73–80.
15. Sathiyabarathi M, Jeyakumar S, Manimaran A, Jayaprakash G, Pushpadass HA, Sivaram M, Ramesha KP, Das DN, Kataktalware MA, Prakash MA, Kumar RD. Infrared thermography: A potential noninvasive tool to monitor udder health status in dairy cows, Veterinary World, 9(10), 2016. – P. 1075 – 1081.
16. Hirutsky, I.I. Analysis of the infrared image of the udder of cows / I.I. Hirutsky, V.I. Perednja, Yu.A. Rakevitch // Agropanorama, 2018. - №6 (130). – pp. 9 -12.
17. Rakevitch, Yu.A. Using infrared thermography to detect bovine mastitis / Yu.A. Rakevitch // Agropanorama, 2020. – №5 (141). – pp.19-22.
18. Detection Theory: A User's Guide/ Neil A. Macmillan, C. Douglas Creelman. – 2nd Edition.

Kinematics, working parameters and modes of swing-type digging share of elevator-type potato combine

Wojciech Tanaś, Mariusz Szymanek
University of Life Sciences in Lublin
ul. Głęboka 28, 20-612 Lublin (Poland)
phone: 0-81 4456123, fax: 0-81 5329463 e-mail: wojciech. tanas@ar.lublin.pl

Abstract: The article presents an analysis of the kinematics, working parameters and modes of operation of swing-type digging share with elliptical profile cutting edge, and opportunities for rational operating regime adjustment of the working body under the conditions of operation. Expressions are derived and an analysis of kinematics, working and regime parameters of the swing-type share with elliptical cutting edge is given.

1. Introduction

The development of means of mechanization in agriculture has resulted in the creation of tractor units realizing new technological and design concepts, overlapping technological operations, provided with multipurpose hook-on machines of modular design for a set of certain regular applications of new active working bodies (AWB) (Furletow 1981, Opiejko 1968, Tanas 2001).

This trend is also realized in the development of a universal elevator-type potato combine, differing from those used so far in the use of the sideways swing design of the digging share. Application of such an AWB permitted improved functionality and reliability of the combine at work (Lisowski 1998a and 1998b, Zaltzman and Schmilovitch 1986).

As tests have shown, the efficiency of a combine depends on the correct choice of design and work regime parameters of the digging share. In connection with this, an analysis of various aspects of the working process of such a share is of interest, with the purpose of determining its laws and developing engineering recommendations for the choice of rational parameters of such an AWB (Abrams et al. 1980, Bujaszow and Tanas 2000, Hyde et al. 1983).

In this work, the features of kinematics of the sideways swing-type digging share have been considered, which allowed the formulation of some recommendations concerning the choice of the design and work regime parameters of such shares and identification of various possibilities of their practical selection and combination for optimum operational setting of the share drive.

2. Kinematics of swing-type share with elliptical cutting edge

Let us define the current coordinates of points on the share edge during combine movement on the working path.

In the $X_1O_1Y_1$ system of coordinates (see Fig. 1) the equation of an ellipse is:

$$\frac{X_1^2}{a^2}+\frac{Y_1^2}{b^2}=1; \tag{1}$$

In the $X_1O_1Y_1$ system of coordinates (parallel axes) we have:

$$\begin{cases} X_2^* = X_1 - C_x; & C_x = 0; \\ Y_2^* = Y_1 + C_y; \end{cases} \tag{2}$$

hence:

$$\begin{cases} X_1 = X_2^* - C_x; \\ Y_1 = Y_2^* - C_y; \end{cases} \tag{3}$$

Substituting (3) in (1)

$$\frac{(X_2^*-C_x)^2}{a^2}+\frac{(Y_2^*-C_y)^2}{b^2}=1 \tag{4}$$

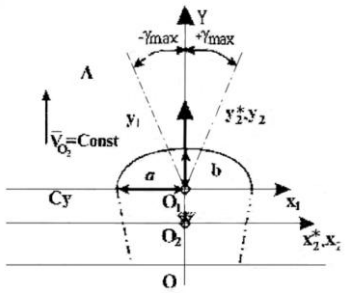


Fig. 1. *Schematic diagram of movement of the swing-type share*

As the share swings within system $X^*_2O_2Y^*_2$ relative to point O_2 (turn of axes) in the system $X_2O_2Y_2$ by an angle γ , we receive:

$$\left.\begin{aligned} X_2 &= X_2^*\cos\gamma_t - Y_2^*\sin\gamma_t; \\ Y_2 &= X_2^*\sin\gamma_t - Y_2^*\cos\gamma_t; \end{aligned}\right\} \quad \left\{\begin{aligned} X_2^* &= X_2\cos\gamma_t + Y_2\sin\gamma_t; \\ Y_2^* &= X_2\sin\gamma_t + Y_2\cos\gamma_t; \end{aligned}\right\} \tag{5}$$

Let us substitute expressions (5) in (4) and we shall receive:

$$\frac{(X_2\cos\gamma_t + Y_2\sin\gamma_t - C_x)^2}{a^2}+\frac{(-X_2\sin\gamma_t + Y_2\cos\gamma_t - C_y)^2}{b^2}=1 \tag{6}$$

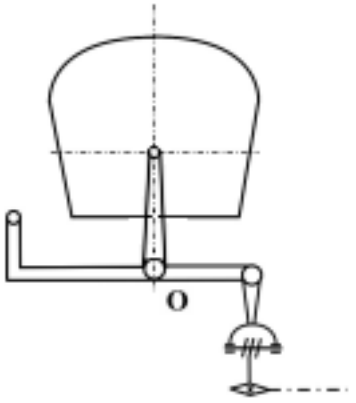
At $V \neq 0$, at the moment of time t, coordinate $X_{2i} = X_i$, and coordinate $Y_i = Y_{2i} + V \cdot t$, then in the motionless system XOY we have:

$$Y_2 = (Y - V{\cdot}t)$$

$$\frac{[X\cos\gamma_t + (Y - V\cdot t)\cdot\sin\gamma_t - C_x]^2}{a^2}+\frac{[-X\sin\gamma_t + (Y - V\cdot t)\sin\gamma_t - C_y]^2}{b^2}=1 \tag{7}$$

$$X_{\max}(t) = a\cdot\cos\gamma_t;$$

a)



b)

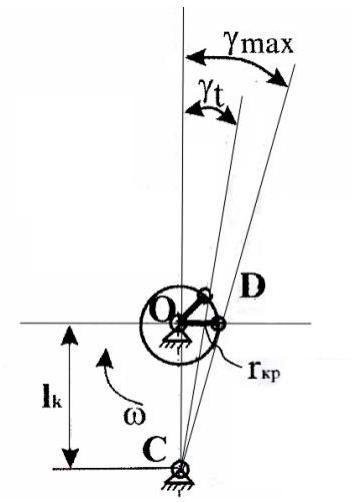


Fig. 2. *Schematic diagram of a variant of the swing-type share drive*

a)

b)

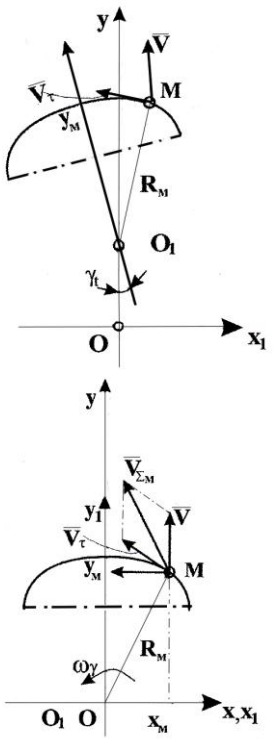


Fig. 3. *Schematic diagrams of swing-type share movement*

Angle γ_t at the moment of time t is defined by the parameters of the share drive and the frequency of swing motions (oscillations) ω of the share (see Fig. 2 b).

In this case of the drive mechanism considered:

$$K_{np} = \frac{r_{kp}}{l_k};\ l_k = \frac{r_{kp}}{K_{np}};\quad \varphi_t = \omega \cdot t;$$

From ΔOBD: OB = $r_{кр.}\cos\varphi_i$; BD = $r_{кр.}\sin\varphi_i$; From ΔCBD:

$$\operatorname{tg}\gamma_t = \gamma_{\max} = arc\sin K_{кр.} = arc\sin\frac{r_{кр.}}{l_{к.}};$$

$$\operatorname{tg}\gamma_t = \frac{BD}{BC} = \frac{BD}{BO+OC} = \frac{r_{kp}\sin\varphi_t}{r_{kp}\cos\varphi_t + k} = \frac{r_{kp}\sin\varpi\cdot t}{r_{kp}\cos\varpi\cdot t + l_k};\quad (8)$$

$$\gamma_t = arc\operatorname{ctg}\left(\frac{r_{kp}\sin\varpi\cdot t}{r_{kp}\cos\varphi_t + l_k}\right) \quad (9)$$

$$\gamma_{\max} = arc\sin K_{кр.} = arc\sin\frac{r_{kp}}{l_k} \quad (10)$$

Let us consider the trajectory of a point M on the contour of the cutting edge. At $t = 0$ and $\gamma_t = 0$ we determine coordinates of point M: X_M and Y_M, fulfilling equation (8). We have point M which participates in two movements: 1) relative, around the centre O_1 of mobile system X_1OY_1 with frequency ω and amplitude γ_{max}; 2) translatable, with centre O_1 in system XOY, with speed V = const along axis OY.

From Fig. 3 a) we have:

$$R_M = \sqrt{X_M^2 + Y_M^2};\quad \omega_\gamma = \frac{d\gamma_t}{dt} = \frac{d}{dt}\left(arc\operatorname{ctg}\frac{r_{kp}\sin\omega t}{r_{kp}\cos\omega t + l_k}\right); \quad (11)$$

In Fig. 3 b) it is visible that $V_\tau = \omega_\gamma \cdot R_M$.
At any moment of time t, $\gamma = \gamma_t$, then

$$\left.\begin{aligned} X &= X_M\cos\gamma_t - Y_M\sin\gamma_t;\\ Y &= (X_M\sin\gamma_t + Y_M\cos\gamma_t) + Vt;\\ \gamma_t &= aarctg\left(\frac{r_{kp}\sin\omega t}{r_{kp}\cos\omega t + l_k}\right); \end{aligned}\right\} \quad (12)$$

Expression (12) is also the required equation of movement of point M during work of the swing-type share. Changing t, it is possible to construct diagrams of change of coordinates $X(t)$, $Y(t)$, $\gamma_t(t)$ of any point of the share cutting edge.

3. Results of calculations of kinematics of the swing-type share

For the start position before the beginning of movement of the digging unit the coordinates of i-points of the share edge are given in Table 1.

Changes of coordinates of some points of the share edge during the movement of the digging unit, obtained with the use of the MathCAD program, are presented in Figs. 4 - 6. At the initial data:

Coordinates of the point (0,26; 0,1) change as follows (see fig. 4):

v:= 1.8; r_k:=0.05; l_k:=0.12; w:= 15.0 x_m:= 0.26; y_m:= 0.1

At a change of frequency of share oscillations we shall receive the following picture of change of the coordinates of the same point on the share.

The qualitative character of the change of kinematic characteristics of movement of points of the swing-type share edge at the change of parities of the work regime parameters of the share (speed of the unit, frequency of oscillation, maximum angle of swing) can be seen in the diagrams in Fig. 6.

From the diagrams it follows that the longitudinal absolute speed of the chosen point of the edge of the swing-type share has periods of movement with negative speed.

With an increase in the speed of movement of the unit at constant frequency of share swing motion, or with constant speed of movement of the harvesting unit at reduced frequency of the share oscillations (see Fig. 6 a) it is possible to change the intensity of undercutting the ridge and weed roots by the share.

Table 1. *Coordinates of points of the initial position of the share edge*

№ i- point	1	2	3	4	5	6	7	8	9	10	11
X,м	0.3	0.29	0.294	0.286	0.275	0.260	0.240	0.214	0.168	0.110	0.0
Y,м	0	0.02	0.04	0.06	0.08	0.10	0.12	0.14	0.16	0.18	0.20

$$x = xm\cdot\cos\left[a\tan\left(\frac{rk\cdot\sin(w\cdot t)}{rk\cdot\cos(w\cdot t)+lk}\right)\right] - ym\cdot\sin\left[a\tan\left(\frac{rk\cdot\sin(w\cdot t)}{rk\cdot\cos(w\cdot t)+lk}\right)\right]$$

$$y = xm\cdot\sin\left[a\tan\left(\frac{rk\cdot\sin(w\cdot t)}{rk\cdot\cos(w\cdot t)+lk}\right)\right] + ym\cdot\cos\left[a\tan\left(\frac{rk\cdot\sin(w\cdot t)}{rk\cdot\cos(w\cdot t)+lk}\right)\right] + v\cdot t$$

$$\gamma = a\tan\frac{rk\cdot\sin(w\cdot t)}{rk\cdot\cos(w\cdot t)+lk}$$

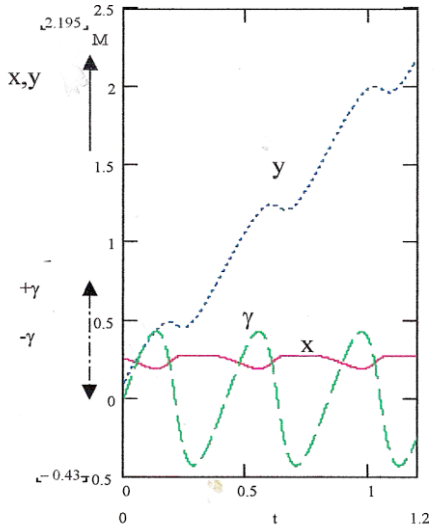


Fig. 4. *Change of coordinates of some points on the share edge during movement of the harvest unit*

$$x = xm\cdot\cos\left[a\tan\left(\frac{rk\cdot\sin(w\cdot t)}{rk\cdot\cos(w\cdot t)+lk}\right)\right] - ym\cdot\sin\left[a\tan\left(\frac{rk\cdot\sin(w\cdot t)}{rk\cdot\cos(w\cdot t)+lk}\right)\right]$$

$$y = xm\cdot\sin\left[a\tan\left(\frac{rk\cdot\sin(w\cdot t)}{rk\cdot\cos(w\cdot t)+lk}\right)\right] + ym\cdot\cos\left[a\tan\left(\frac{rk\cdot\sin(w\cdot t)}{rk\cdot\cos(w\cdot t)+lk}\right)\right] + v\cdot t$$

$$\gamma = a\tan\frac{rk\cdot\sin(w\cdot t)}{rk\cdot\cos(w\cdot t)+lk}$$

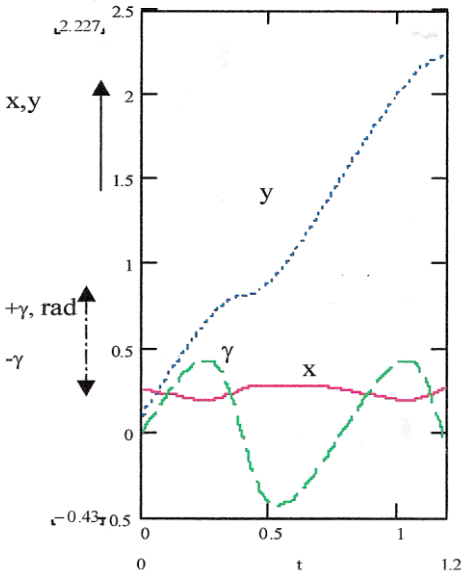


Fig. 5. *Change of coordinates of points on the share edge during movement of the harvest unit*

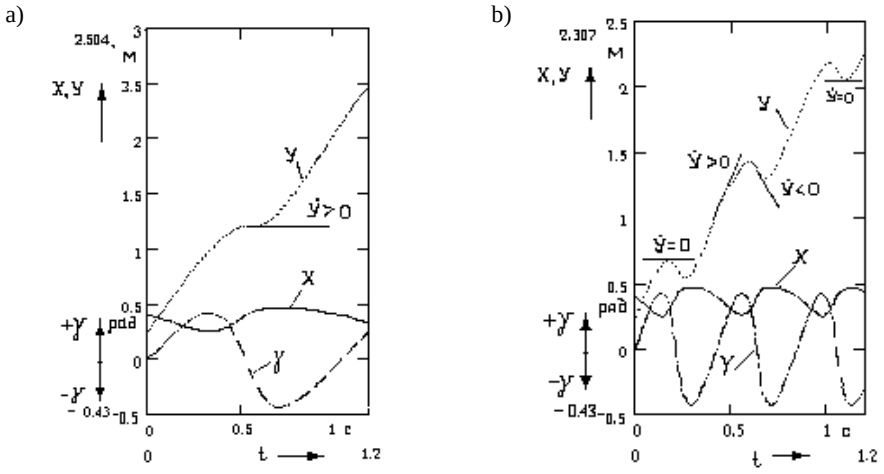


***Fig. 6.** Changes of kinematic characteristics of movement of the points on the share edge*

By differentiating values of X, Y, γ_t in time we shall receive projections to coordinate axes of speeds and acceleration of point M and its angular acceleration in the function of time, which is necessary for the process of dynamic modelling of the swing-type share motion.

Trajectories of endpoints of diameters of the elliptic contour of the share edge have a harmonic character. At $t = 0$: for the median point on the share edge, designated with letter M: $X_M = 0$; $Y_M = b$; for the extreme point T located on the end of the greater diameter of the ellipse of the edge of the share: $X_T = a$; $Y_T = 0$.

From relation (12), the changes of coordinates X of the points are defined by the expressions:

– point M: $x = -b \cdot \sin \gamma_t$ $\pm X_{M\max} = \pm b \cdot r_{кр}/l_k$;
– point T: $x = a \cdot \cos \gamma_t$; $\pm X_{t\max} = \pm a \cdot \cos(\arcsin(r_{кр}/l_k))$;

The character of the movement of points on the contour line in the 1st plane, parallel to the vector of speed V of moving the unit, whose equation is $X_i = \text{const} = d$, shall be defined from the expressions (8) and (9), having substituted for X the value $X_i = d$.
The value of X_i varies from $-a$ to $+a$.

$$\left.\begin{aligned} &\frac{[d\cos\gamma_t + (y - Vt)\sin\gamma_t - C_x]^2}{a^2} + \frac{[(y - Vt)\cos\gamma_t - d\sin\gamma_t - C_y]^2}{b^2} = 1 \\ &\gamma_t = arctg(r_{кр} \cdot \sin wt)/(r_{кр} \cdot \cos wt + l_к) \end{aligned}\right\} \quad (13)$$

The periodic and non-linear dependence follows from the expressions (13) and causes a sign-variable acceleration of points on the share in the direction of the movement of the machine. Thus the amplitudes of this acceleration grow with increasing deflection from axis OY. Similar statement is true and typical for the contour of the share accelerations. It means that the intensity of shock of undercutting the ridge and roots and stalks of weeds by the edge of the share grows with the removal of the contour points from the axis of oscillation and from the plane of its symmetry, and also with increase in the frequency and amplitude $\gamma_{\max}$ of the swing motions.

Rational combinations of the design (a, b, c_x, c_y) and work regime parameters (V, w, $\gamma_{\max}$) of the swing-type share operation are determined by the following conditions: 1 – maintenance of constant width and straightness of the soil strip shifted by the share; 2 – maintenance of swing mode of cutting at all the points of the share; 3 – maintenance of the necessary amplitude and sign of accelerations at any point on the width of strip covered by the share in longitudinal plane for the achievement of cleanliness of cutting and to avoid cut fragments of plants being dragged by the share.

4. Conclusions

The developed approach to the definition of the kinematic characteristics of swing-type share is suitable for any configuration of share edge and coordinates of the poles of its angular swing motion.

On the basis of the received results, drive systems of the developed shares, permitting in-operation adjustments or continuous regulation of the work regime parameters in the function of speed of movement and parameters of conditions of harvest which characterize the condition of the soil, its fertility and contamination with weeds, were developed and tested under natural conditions.

5. References

[1] Abrams, C.F.,L. H. Chen and E. G. Humpries. 1980. Simulation of bulk harvest and handling of sweet potatoes. *Transactions of the ASAE 3*.
[2] Bujaszow, W.P., W. Tanaś. 2000. Usłowija funkcjonirowanija maszin dlia uborki kartofiela i obosnowanije modyfikacji modalnych kombajnow. *Sbornik naucznych trudow NAU, t. VII,* Kijów.
[3] Furletow, W.M. 1981. Optimalizacija parametrow otdielitelja kłubniej kartofelka ot kamniej. *Traktory i Sielchozmasz*. 5.
[4] Hyde, G.M., R.E. Thornton and D. W. Woodruff. 1983. Potato harvester performance with automatic chain-load control. *Transactions of the ASAE* 1.
[5] Lisowski, A. 1998a. Analysis of configuration and technical parameters of digging-screening units of potato combine harvesters (in Polish). *Przegl. Tech. Rol. i Leśn*. 10.
[6] Lisowski, A. 1998b. Effect of technical parameters on chain web length in the potato combine harvester. *Ann. Warsaw Agricult. Univ. – SGGW, Agricult*. 30.
[7] Zaltzman, A., Z. Schmilovitch. 1986. Evolution of potato, fluidized bed medium separator. Transactions *of the ASAE* 5.
[8] Opiejko, F. A. 1968. Torfianyje masziny. Wysszaja Szkoła. Mińsk.
[9] Tanaś, W. 2001. Razrabotka niekotorych riekomendacij po rieszieniju koncepcii powyszenija proizwodstwa kartofielia i owoszczej. Monografia, BG BATU Minsk.
[10] ASAE STANDARDS 1993: Soil Cone Penetrometer. Standard Engineering Practices Data. American Society of Agricultural Engineers, St. Joseph, Mi. 657. 40-th edition.
[11] PN-90/P-04870. Statistical analysis of measurement results (in Polish).
[12] PN-86/R-36500. Agricultural machines. Potato combine harvesters. General requirements and testing (in Polish).
[13] PN-86/R-74456. Root crops. Potato quality testing (in Polish).

Features of calculation of agricultural machines trailed devices in pedagogical technologies of training agricultural engineers for innovative design activities

Viktor Pryshliak
Ukraine, Vinnytsia National Agricultural University
viktor.prishlyak@i.ua

Summary. *The scientific-technical and pedagogical-methodological model of preparation of future specialists in agroengineering for innovative project activity on the basis of studying of agricultural machines on modern technologies of training, deepening of scientific activity of students based on features of calculation of trailers which are used in machine-tractor units has been developed. An equivalent calculation scheme of a technical system consisting of a wheeled tractor as an energy propulsion and a trailer is given. Such theoretical-calculative material is used in institutions of higher education of general and professional competencies of future specialists of agro-industrial production. It is noted that the preparation of future agricultural engineers for innovative project activities is carried out in accordance with industry standards and the Law of Ukraine "On Higher Education". The influence of end-to-end project training on students' readiness to perform scientific and practical tasks has been studied. The condition under which there will be no overloading of front wheels of the machine from its working bodies is substantiated, and ecologically admissible pressure on the ground will remain the same.*

Keywords: *CALCULATION, TRAILERS, MACHINE, TECHNOLOGIES, PREPARATION, PROJECT ACTIVITY*

Introduction.

For agricultural engineering, as for other industries, it is important that the achievements of science are quickly implemented in the educational process and production. Development in a single integrated system of science and educational process provides the best result. The Law of Ukraine on Higher Education [1] states that the educational process is an innovative, intellectual, creative activity of research and teaching staff, students, manufacturers and other groups of people who have concern to the field.

The training of future agricultural engineers is based on the formation of their professional competencies, which provide to solve various problems of production activities. The object of activity of agricultural engineers are the processes associated with the efficient operation of agricultural machinery and mechanized technologies [2]. The educational process of students majoring in "Agroengineering" is aimed at training professionals capable of solving professional specialized tasks and applications related to the use of agricultural machinery in mechanized technologies of production, storage and transportation of agricultural products and etc.

The basic training discipline for future agricultural engineers is "Agricultural Machinery". Studying it, students gain knowledge on the structure and principle of operation of machines, adjusting them to optimal modes of operation. Students also study the theoretical foundations of machines, algorithms for calculating and designing new ones, as well as improving existing machine designs [3]. In addition to classroom classes, the study of the discipline involves independent performance of course work by students. The purpose of the course project is to develop the design of agricultural machinery or its components or to improve existing machinery to ensure the implementation of mechanized production processes for growing crops.

The main scientific directions of student papers of agro-engineering direction are the increase of productivity of units, expansion of their universality, possibilities of combination of power means with other tools and maintenance of effective management, decrease in power indicators of performance of technological processes, improvement of traffic safety, etc.

Practical, scientific and educational activities show that the problematic issues of the calculation of trailers of agricultural machinery in pedagogical technologies for preparing agricultural engineers for innovative design activities are still insufficiently studied and require further fundamental theoretical and experimental research, scientific substantiation and generalizations.

***Prerequisites and means for solving the problem*.**

For a long time, scientific and pedagogical workers were mainly engaged in the study and improvement of the working bodies of agricultural machines, the processes of interaction of the running system with the soil and traction properties of machines. Regarding the design of trailer devices of agricultural machines, as well as in-depth application of algorithms for calculating such trailer technical systems in pedagogical technologies for training agricultural engineers for innovative design activities, these issues are insufficiently studied.

The scientific article [4] presents the main components of the formation of integrated, general and professional competencies of an agricultural engineer as a specialist. In general, an innovative training system is a system combined into physical-mathematical, general technical and special blocks and general and professional competencies, which must have a bachelor's degree in the specialization 208 "Agroengineering".

An innovative system of scientific and methodological developments that influence the formation of special professional competencies of an agricultural engineer is presented in the article [5]. The basic basis of this system are textbooks, manuals, monographs, curricula and other didactic materials. Improved pedagogical technology of teaching, which is based on the thorough, gradual development of the readiness of the future specialist for project activities. This pedagogical learning technology provides a comprehensive, integrated formation of professional competencies of agricultural engineers in accordance with the Laws of Ukraine and educational standards [1, 2]. The scientific activity of students is based on the development and modernization of agricultural machinery which has great importance for the training of agricultural engineers.

Questions of the theory of project preparation were studied by Bryukhanova N.O. [6], Kolesnikova I.A., Gorchakova-Sibirskaya M.P. [7], Nichkalo N.G, Zyazyun I.A., Goncharenko S.U. [8] and others. The theory, methods and practice of project training of agricultural engineers were studied and researched by Bender I.M. [3, 9, 10, 11], Duganets V.I. [12], Pryshliak V.M. [4, 5, 13, 14, 15] and others. Also, the work of O. Kovalenko, D. Chernylevsky, P. Yakovyshyn is devoted to the improvement of methods of training for future engineers, and the method of development of future agricultural engineers is reflected in scientific researches of I. Butsyk, A. Demin, O. Dzhedzhul, P. Luzan, V. Mank, S. Pastushenko, V. Yaroshenko. Transformation of independent educational activity into readiness for professional self-development by means of technologies of personality-oriented learning is reflected in the monograph Bondar M.M., Zhuravskaya L.M., Ostapenko E.O., Pryshliak V.M., Kutsenko A.G. [15].

Solution of the examined problem.

The theory and practice of project training of future agricultural engineers involves large-scale application of the scientific component in the educational process during classes, independent work of students look at the article [5]. Scientifically substantiated thoroughness, consistency and gradual formation of professional competencies involves increasing the quality of training and development of competitive technology. In addition to the fact that students take part in research processes, conferences, project

and model mechanization during their studies, they are engaged in course design in the 3rd year, and in the master's degree (5th - 6th years of studies) - conduct research and design scientific work. During the performance of the above-mentioned types of work, students mainly calculate, design and research the working bodies of agricultural machinery. There are also works in which auxiliary, but at the same time very important units, mechanisms or systems of machines are designed and researched. This also includes the theory, calculation, design and construction of trailers of the agricultural machinery.

The theory and practice of project training of future agricultural engineers involves large-scale application of the scientific component in the educational process during classes, independent work of students, article [5]. Scientifically substantiated thoroughness, consistency and gradual formation of professional competencies involves increasing the quality of training and development of competitive technology. In addition, when operating agricultural units with trailers under certain operating conditions, undesirable phenomena may occur due to the redistribution of loads on the supporting elements of the machine due to changing conditions of traction on the front wheels of the machine through its trailer. Therefore, when designing trailed and semi-trailed agricultural machines, special attention should be paid to the correct choice of parameters of the connecting elements of the machine to the tractor. To solve this problem, it is necessary to solve some specific design problems to determine the optimal parameters of the connecting elements of the trailer [3].

The work must be performed according to the initial data (diagrams of the wheel travel of the machine, its longitudinal base, the coordinate of the center of gravity of the machine, etc.), taken from an individual task for a course work in the discipline "Agricultural Machinery". Calculations must be made on two schemes of the wheel movement.

First, using the original data of only one column of the variant table (Table 1) and one of the schemes of wheel movement, determine the possibility of balancing the additional loads on the front wheels of the machine from the action of its working bodies due to the vertical traction component on the tractor hook. the presence of the angle of the trailer to the horizon. This angle of the trailer is determined by the formula:

$$\psi = arctg\left[\left(gQ_{м}a - n_2 G_2 L + R\sum в\right)/ XP_x\right], \quad (1)$$

where g – acceleration of gravity, m / s^2;

$Q_{м}$ – machine weight, kg;

n_2 – the number of front wheels (according to the scheme);

G_2 – radial load on the front wheel, H;

L – longitudinal base of the machine, m;

R – total load from working bodies, N / cm;

$\sum в$ – the sum of the shoulders of the load R depending on the number of rows of working bodies on the machine, m;

X – horizontal coordinate of the hinge of the car trailer, m;

P_x – tractor traction force, N.

Provided there are two rows of working bodies on the machine $\sum в = \left(в_1 + в_2\right)$,

where $в_1$, $в_2$, – shoulder application of load R, respectively, on one and the second row of working bodies.

$\sum в = в_1$, when only one row of working bodies on the machine is used.

Shoulder load application

$$в_{1,2} = \sqrt{h_0^2 + m^2}\, sin\left(\beta + \alpha\right), \quad (2)$$

where h_0, m – respectively, the vertical and horizontal coordinates of the point of application of the load vector R to the working bodies, m (Fig. 1);

α – the angle of inclination of the vector R, deg:

$$\beta = arctg\left(h_0 / m\right). \quad (3)$$

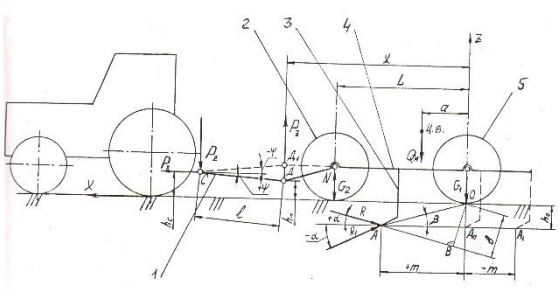


Fig. 1. Calculation scheme of the unit with a trailer:

1 – trailer; 2 – front wheels; 3 – working bodies; 4 – machine frame; 5 – rear wheels of the car; C, $Д$ – trailer hinges

After obtaining the angle ψ by formula (1) it is necessary using the formula

$$\psi_n = \arcsin\left(\left(h_c - h_n\right)/ l\right), \quad (4)$$

pick up the following values h_n and l, in order to $\psi_n = \psi$,

where h_c – height of trailer bracket placement, m (table 1);

h_n – height of placement of the hinge of the trailer of the machine, m. (minimum value h_n = 0,3 m.)

l – railer length, m (l_{min} = 0,8 м).

Table 1

Geometric and power characteristics of the trailer

Indicator	The value of the indicator by options					
Traction force of the tractor P_x, *kH*	1, 2, 3,		4, 5, 6,		7, 8, 9, 0	
	12	25	13,5	26	15,5	28
X, м	2,2	2,4	2,3	2,5	2,4	2,6
h_c, м	0,45	0,5	0,4	0,45	0,5	0,45
R, kH	6	19	7	20	7,5	22
h_0, м	0,05	0,08	0,06	0,1	0,07	0,12
m, м	+0,2	0 та -0,4	0 та +0,3	-0,3	0 та +0,5	-0,2
α, grad	+20	-20	+30	-15	+25	-10

If it is possible to obtain equality when, $\psi_n = \psi$, this means that with the selected l and h_n there will be no overload of the front wheels of the machine from its working bodies, the environmentally friendly pressure on the ground will be maintained. And if this equality cannot be obtained, it is necessary to choose the values of the length l of the trailer and the height h_n of the trailer hinge, which allow to obtain the maximum allowable value of the angle ψ_n of the trailer to the horizon. Then you need to determine what the minimum load can be provided on the front wheels of the machine, using the formula

$$N = \left(gQ_{м}a - P_x X tg\psi_n + R\sum в\right)/ L. \quad (5)$$

Then it is necessary to compare it with environmentally friendly loads on the selected tires of the wheels taking into account the condition

$$N \le z G_{д}, \quad (6)$$

where z – the number of tires on all front wheels of the machine;

$G_{д}$ – permissible load on the tire of the front wheel, which provides environmentally friendly pressure on the ground, N.

If condition (6) is not met, recommendations should be made in the conclusions regarding the need to replace or supplement the number of tires on the front wheels of the machine to meet environmental requirements or to obtain new values for the trailer (l and h_n).

After using the data of one column of the variant table in the calculations, it is necessary to perform calculations according to the data of the second column for the same wheel scheme. Moreover, it should be assumed that the design of the trailer is already calculated, i.e. the values of l and h_n are selected, therefore, the angle ψ_n of the trailer is known, and therefore it is necessary by formulae (5 and 6) only to check changes in load on the front wheels (the second column of table 1) and fulfill the appropriate conclusions.

Thus, as a result of scientific research, an algorithm for calculating the trailer device has been developed, which provides aggregation of agricultural machines in variable production conditions. The use of the developed method of calculating trailers in the educational process will help to improve the quality of formation of design competencies of future agricultural engineers.

***Results and discussion*.**

The developed innovative system of scientific and methodical training of future specialists is based on a thorough, gradual growth of knowledge, skills and abilities of future agricultural engineers. Course design and master's work provide a qualitative growth of project competencies of graduates. The developed method of calculation of trailers is effective both for the design of new machine-tractor units and for the formation of design competencies of future agricultural engineers.

Conclusion.

The results of the research give grounds to conclude that the process of formation of professional competencies of future specialists in agricultural engineering is effective with the use of end-to-end innovative learning technologies. The developed algorithm for calculating trailers is effective both for the development of the latest technical means of agricultural mechanization and for a quality educational process.

References

1. Law of Ukraine "On education" from 01.07.2014, #1556-VII / Newspaper "Voice of Ukraine" dated 08.06.2014. − #148.
2. The standard of higher education of Ukraine is the first (Bachelor) level of education in higher education − bachelor, specialties - 208 Agroengineering // Approved and put into effect by order of the Ministry of Education and Science of Ukraine dated 12/5/2012, #. 1340. - Access mode: https://mon.gov.ua/storage/app/media/vishcha-osvita/zatverdzeni%20standarty/12/21/208-agroinzheneriya-bakalavr.
3. Designing of the agricultural machines. Tutorial / I.M. Bender, A.V. Rud, Y.V.. Koziy and others; ed. by I.M. Bender, A.V. Rud, Y.V. Koziy − Kamyanets-Podilsky: Private Entrepreneur Sysin O.V., 2010. − 640 p.
4. Pryshliak Viktor. Role of project preparation in formation professional competence of future specialists in agroengineering / Viktor Pryshliak // TRANS MOTAUTO WORLD: International scientific journal. – Sofia, Bulgaria: TRANS MOTAUTO WORLD, YEAR II, ISSUE 4/2017. – 162-165, ISSN PRINT 2367-8399, ISSN WEB 2534-8493.
5. Pryshliak Viktor. Theory of project preparation of agroengineers on the basis of scientific work on the development of agricultural machinery / Viktor Pryshliak // SCIENCE. BUSINESS. SOCIETY: International scientific journal. – Sofia, Bulgaria: Scientific-technical union of mechanical engineering “Industry 4,0”, National society «Industrial & national security», YEAR 3, ISSUE 4/2018. – 145-149, ISSN PRINT 2367-8380. ISSN WEB 2534-8485.
6. Brukhanova N.O. Theory and methods of system design teacher training for future engineers-teachers: Dissertation Dr. ped. sciences: 13.00.04 – Kharkiv, 2011. – 594p.
7. Kolesnikova I.A., Gorchakova-Sibirskaya M.P. Pedagogical designing. − Moscow: Academy, 2007. – 288p.
8. Designing the process of professional training in vocational education institutions: monograph / [N.G. Nichkalo, I.A. Zazyun, S.U. Goncharenko and others.]: Ed. N.G. Nichkalo. – K. – Khmelnytsky: KhNU, 2010. – 335 p.
9. Bendera I.N. Full-time course and diploma designing – a way to enhance the independent work of students of agrarian-engineering specialties / Ivan Bender, Wojciech Tanas / Problemy inzynierss rolnitsz w aspekcie rolnictwa zrownowazonego. –- Lublin, 2005. – pp. 180-192.
10. Graduate design in higher educational institutions of the Ministry of Agrarian Policy of Ukraine: teaching method. manual / [I.M. Bendera, O.V. Datsishin, O.V. Korolchuk and others.]; Ed. T.D. Ishchenko, I.M. Bendera. − K.: Agrarian Education, 2006. − 256 p.
11. Bendera I.M. The theory and method of independent work of future specialists in agricultural mechanization in higher education: Dissertation by Dr. ped. sciences: 13.00.04 − K., 2008. – 579 p.
12. Duganets V.I. Theory and practice of production training of future specialists in agrarian-engineering direction: dissertation by Doc. ped. sciences: 13.00.04 / Duganets Viktor Ivanovich. - Kamenets-Podilsky, 2015 - 501 p.
13. Pryshliak Viktor. Method of projects in the theory learning of a future agricultural engineer / Viktor Pryshliak // TRANS MOTAUTO WORLD: International scientific journal. – Sofia, Bulgaria: TRANS & MOTAUTO WORLD, YEAR I, ISSUE 4/2016. – 39-41, ISSN 2367.
14. Pryshliak Viktor. The research peculiarities of parameters and choice of agricultural machines in pedagogical technologies for innovative project activity in training agroengineers / Viktor Pryshliak // TRANS & MOTAUTO’19 PROCEEDINGS: Section “TRANSPORT. SAFETY AND ECOLOGY. LOGISTICS AND MANAGEMENT. EDUCATION THEORY”. – Sofia, Bulgaria: TRANS & MOTAUTO WORLD, YEAR III, ISSUE 1(6) / 2019. – 58-61, ISSN 1313-5031 (Print), ISSN 2535-0307(Online).
15. Transformation independent learning activities in readiness for professional self-development by means of personal technology based learning: Monograph / M.M. Bondar, L.M. Zhuravska, E.A. Ostapenko, V.M. Pryshliak, A.G. Kutsenko. – Nizhin: LLC "Publishing" Aspect-Polygraph", 2016. – 760p.

Study of the influence of irrigation norms on the productivity of raspberry plantations

Rumiana. Kireva, Miho Mihov
Institute of Soil Science, AgroTechnology and Plant Protection "Nikola Pushkarov", Sofia, Bulgaria
Email: R.Kireva@abv.bg ; M.Mihov@abv.bg

Summary: *To establish the effect of irrigation of raspberries grown in soil and meteorological conditions in the area of the village of Chelopechene - Sofia, studies were conducted in drip irrigation of plantations with remontant variety "Lyulin", testing different regimes - from full satisfaction of daily needs of the culture from water to irrigation with reduced by 20% and 40% irrigation rates. A variant under non-irrigated conditions has also been tested.*

When determining the effect of irrigation of raspberries by changing the yield compared to the non-irrigated variant, it was found that in the variant with 100% irrigation rate (optimal) the increase in raspberry yield reaches 59%, and in variants irrigated with reduced irrigation rates, the size yields increased by 54% and 47% respectively. It has been proven that the optimization of the moisture in the active soil layer contributes to a significant increase and stabilization of yields, which for the experimental conditions are from 835 to 1074 kg / dka and the additional yield varies from 404 to 627, kg / dka or from 47 up to 59% on average for the study period.

The established productivity of the irrigation water is the highest in the variants with 40% reduction of the optimal norm and changes during the years of the experiment from 13.0 kg.ha-1.mm-1 to 24.0 kg.ha-1 .mm-1. It is the lowest in the variants irrigated with 100% realization of the irrigation norm.

Introduction

A number of studies have been conducted on the limiting factor - water for the implementation of optimal irrigation regime in our country. Their main goal is to establish the effectiveness of the application of different irrigation regimes for irrigation in case of insufficient water supply. The effect of irrigation in most cases is determined on the basis of the obtained additional yield from irrigation and the productivity of irrigation water (Eneva, 1993; Muhova, R., 2005, Kirkova J.2003.)

Studies conducted so far in the irrigation of raspberries show that to increase yields it is very important to water before the fruit ripens and during the entire period of harvest (Kuiesza, W., 1973, Oosten, A., 1976). According to the same authors, the greatest negative impact of drought has on the yield two weeks before harvest and during ripening. While maintaining a limited water deficit in the soil, the yield increases by more than 9.6%, and in dry years by more than 27.6% compared to non-irrigated variants (Mackenrron, 1982).

The aim of the present study is to establish the effect of irrigation of raspberries grown under conditions of optimal irrigation and water deficit for Sofia region.

In irrigated agriculture, water shortages can occur not only due to physical shortage of water, but also due to its unavailability due to high cost, energy and organizational problems, limited capacity of the sewerage network during the dry and hot summer months, emergencies and etc.

Material and method

The field studies were conducted in the experimental field of ISSAPP "N. Pushkarov" - Sofia. The following irrigation variants have been tested:

1. option 1 - without irrigation;
2. option 2 - irrigation with 100% irrigation rate;
3. option 3 - irrigation with 80% irrigation rate;
4. option 4 - irrigation with 60% irrigation rate;

The amount of irrigation rate was calculated according to the methodology proposed by (Frecman and Garzoli, 1980).

To monitor the dynamics of soil moisture, soil samples were taken with option 2 (100% irrigation rate) at a depth of 0–60 cm every 10 cm, which were processed by the weight-thermostatic method. .

The installation is made with irrigation wings double-walled pipelines for drip irrigation type "Agrodrip" with a diameter of 20 mm and a hole for water supply every 30 cm.

During the experiment, the developed technology for the creation of the raspberry plantation was used, as well as the agricultural techniques for its cultivation by the Experimental Station for Berry Crops - Kostinborod. Irrigation was performed through a drip installation type "Drozbach".

Results and discussions

The productivity of each agricultural crop depends on a complex of factors, the main ones being: the type of crop, its varietal characteristics, the applied agrotechnics, the number of realized irrigations, the way in which they are submitted and last but not least the meteorological conditions.

Table 1. *Rainfall during raspberry vegetation period (1999–2001)*

Periods	Total rainfall,mm			Rainfall factor security, %		
	1999	2000	2001	1999	2000	2001
m. IV - IX	398	182	358	19,2	98,6	33,1
average multi-annual	365	363	362	-	-	-
m. VII - VIII	152	28	75	7,3	96,6	70,8
average multi-annual	108	107	117	-	-	-

The amount of precipitation during the vegetation period of the crop (398 mm) for 1999 is 33 mm higher than the average long-term values, and for the period July - August by 44 mm and characterizes the year as wet (19.2%), and the July-August period is moderately dry. In 2001, which is characterized as moderately humid (33.1%), the amount of precipitation in April - September is almost the same as that of the average long-term series - 358 mm, and in July - August it is 75 mm)

Extremely dry with the provision of precipitation and temperatures - 98.6% and 3.4% is the year 2000, where the amount of precipitation for the period April - September is 182 mm, which is 50% less than the average long-term values.

The months of July and August are particularly dry this year, with the amount of precipitation being 28 mm, much lower than the average long-term values for the same period of 107 mm. These rains were extremely insufficient for the development of raspberries, which predetermined the implementation of a large number of waterings.

The results obtained from the three-year research show that the number of irrigations and the amount of irrigation norms are

determined by the meteorological conditions (precipitation) in the individual years. The number of irrigations varies from 12 to 17, and the size of the irrigation rate from 216 to 450 m3 / dka, with the largest number of irrigations being realized in a very dry year (2000), where the number of irrigations reaches 25 and the size of irrigation norm 450 m^3 / dka

When determining the effect of irrigation of raspberries by changing the yield compared to the non-irrigated variant, it was found that in the variant with 100% irrigation rate (optimal) the increase in raspberry yield reaches 60%, and in variants irrigated with reduced irrigation rates, the size yields increased by 54% and 46% respectively. (Table 2) compared to the non-irrigated variant on average for the research period.

The obtained results for the yield of raspberries during the different years in terms of humidity show the influence of drip irrigation on its size. The largest increase in the yield of raspberries was obtained in the dry year 2000, which is about three times higher than in the non-irrigated variant, and the smallest increase by 247 kg / dka was obtained in the wet year 1999.

When comparing the yields obtained in the irrigation variants with the yield obtained with optimal irrigation, it was found that with the reduction of the irrigation rate by 20% the yield decreases by 11%, and with the greater reduction of the irrigation norm (by 40%) the yield decreases with 23%. On average for the research period, the highest productivity of irrigation water amounting to 4.1 kg of raspberries per 1 m^3 of water was obtained in the variant in which 60% of the irrigation norm is realized. (Table 2)

Table 2. *Efficiency and productivity of irrigation water on raspberry average for the period (1999-2001)*

variant	M	Y	+Y	compared to variant 1 in %	compared to variant 2 in %	P
non irrigated	-	447	100	100	42	-
100% M	324	1074	627	240	100	3,3
80%M	259	963	516	215	89	3,7
60%M	195	835	388	186	77	4,3

Designations in the table: M - irrigation rate, m^3dka, Y - total yield, kg / dka; + Y-Extra. Yield kg / dka; P - productivity of 1m^3 of water.

Another important indicator characterizing the efficiency of irrigation is the productivity of the irrigation norm, showing the additional yield for 1mm of the irrigation norm and with a unit of measurement kg.ha-1.mm-1. The data by variants for all experimental years and on average for the experimental period are presented in Table 3.

Table 3. *Productivity of the irrigation norm, additional yield by variants and years*

variants	1999			2000			2001			average		
	+Y	M	PR	+Y	M	PR	+Y	M	PR	+Y	M	PR
100%M	2470	216	11,4	10090	450	22,4	6230	306	20,3	6263	324	19,3
80%M	1830	173	12,7	8410	360	23,4	5210	245	21,2	5160	259	19,8
60%M	1700	139	13,0	5990	250	24,0	4410	197	22,3	4033	195	20,7

Designations in the table: + Y - additional yield, kg / ha; M - irrigation rate, mm; PR - productivity of the irrigation rate kg.ha^{-1}.mm^{-1}

The effect of irrigation is expressed through the additional yield and productivity of the irrigation rate, as the data by years are presented in (Table 3). It has been proved that in the conditions of regulated water deficit the yield does not change in proportion to the change in the size of the irrigation norm. Therefore, the productivity of the lower irrigation rate is often higher. For the experimental conditions the values vary from 11.4 to 24.0 kg.ha^{-1}.mm^{-1}, with the highest values being reached in the dry year 2000.

The obtained results for the productivity of irrigation norm show (Table 3) that it is the highest in the variants irrigated with 40% reduction of the optimal norm and varies from 13.0 kg.ha^{-1}.mm^{-1} to 24.0 kg.ha^{-1}.mm^{-1}. It is the lowest in the variants irrigated with 100% realization of the irrigation norm. The constant water deficit during the vegetation of the crop leads to yield losses that are not proportional to the percentage reduction of the irrigation rate. In all cases, the reduction in yield is less than the reduction in the irrigation rate. On average for the period of the research with correction of the irrigation norm by 20%, the yield decreases by 11%, and with 40% reduction of the irrigation norm the yield decreases by 23%. In all cases, the reduction in yield is less than the reduction in the irrigation rate

Conclusions

The optimization of the moisture in the active soil layer contributes to a significant increase and stabilization of the yields, which for the experimental conditions are from 835 to 1074 kg / dka and the additional yield varies from 404 to 627, kg / dka or from 47 to 50% on average. for the study period.

Reduced irrigation rates during the growing season of raspberries lead to yield losses that do not correspond to the percentage reduction of irrigation water. At 20% correction of the irrigation rate the yield decreases by 11% compared to the optimal variant, and at 40% reduction of the irrigation rate the losses of raspberry yields reach 22%.

The productivity of the irrigation water is the highest in the variants irrigated with a 40% reduction of the optimal norm and varies from 13.0 kg.ha^{-1}.mm^{-1} to 24.0 kg.ha^{-1}.mm^{-1} . It is the lowest in the variants irrigated with 100% realization of the irrigation norm, as the highest values are during the year with the least precipitation - 2000.

References

1.Eneva St. 1993; Yields and efficient use of water from field crops. Dissertation., P.90

2. Kirkova J.2003. Water use efficiency in different crop regimes. Habilitation work, NCAS, Sofia, p.86

3. Muhova, R., R. Petkova, A. Stoyanova, D. Pavlov.2005. Efficiency in irrigation of soybeans grown in conditions of water deficit. – In: Sb. reports of the Union of Scientists. Scientific Conference - Stara Zagora, Volume II Plant Breeding, 352-355

4.Kuiesza, W., 1973, Zeszyty naukowe, Academi rolniczo - technicznei wolsztynie, Rolnisctwo - Olsztyn. (4), p.32

5.Mackenrron, D. K.L., 1982 Journal of Hoticultural Science, 57 (3) p.45 Oosten, A., 1976, Fruittel, p.69

6.Frecman, B., Carzoli, 1980, Localized Irrigation FAO, Irrigation and Drainage Paper, №36

Utilisation of sustainable Ethanol in a Dual-Fuel Diesel Engine

Aleksandar Damyanov, Peter Hofmann
Vienna University of Technology
Aleksandar.Damyanov@ifa.tuwien.ac.at

Abstract: *The dual-fuel combustion of ethanol and two different mixtures of ethanol and gasoline (E85 and E65) in a modified Diesel engine was investigated. With rising alcohol amount, a significant reduction of soot mass and particle count was observed at all operating points. At some load conditions, substituting diesel with ethanol, E65 or E85 led to a reduction of the NO_x emissions, however, the real benefit concerning the nitrogen oxides was introduced by the mitigation of the soot-NO_x trade-off, allowing higher EGR rates. With regard to the engine efficiency aspect, the results showed a bidirectional behaviour: at low load regimes engine efficiency degraded, whereas combustion became remarkably more efficient at higher engine loads. The measurements showed a high reduction of engine CO_2 emissions in all cases, with the reduction being proportional to the alcoholic fuel energy share at the combustion. Ethanol sustainability is discussed based on the case study of an Austrian bio-ethanol producer.*
Keywords*: DUAL FUEL ENGINE, DIESEL, SUSTAINABLE ETHANOL, EMISSIONS, EFFICIENCY ANALYSIS*

1. Introduction

The transport sector is a major contributor to the greenhouse gas emissions in the European Union with a share of about 23 % in 2019 (excl. international aviation and international maritime transport) [1]. Reducing CO_2 from traffic is crucial for achieving the desired climate stabilizing objectives and lowering the dependence on fossil fuels. The efforts in this field should be supported by rational as well as technically and economically feasible sustainable solutions. Increasing the usage of biofuels is one of these solutions. Ethanol, in particular, is a very well-known fuel produced from different sources and by various methods.

Despite the present alternative powertrain development, the diesel engine is predicted to remain crucial for mobility of people and goods in the long term due to its unmatched efficiency, robustness and operation cost and flexibility. Therefore, the search for diesel substitute fuels that are sustainable and of wide availability is of high priority. The usage of ethanol is normally assumed with spark ignition engines, but not with a compression ignition engine, because of the very low cetane number of this fuel. However, there are several different possibilities to utilise this alcohol in a diesel engine and it is expected to defuse the classical soot-NOx trade-off due to its high oxygen content, advantageous molecule structure and better mixture formation and combustion process. Ethanol can be used as a single fuel in a dedicated ethanol compression ignition engine with a higher compression ratio. Such engines are available on the market. To ensure ethanol ignition, however, fuel additives are necessary [2]. Adding the alcohol to the conventional diesel fuel in the form of a so-called "blend" is another way of using it in a diesel engine. Though it is the simplest method, the ethanol quantity is very limited due to separation issues, poor ignitibility and current diesel norm EN590 violation in terms of cetane number and flash point. Perhaps the most promising technique for ethanol usage in a diesel engine is the unconventional application in the form of a dual-fuel combustion process. In this case, the alcoholic fuel is fed into the engine as a separate fuel and the ignition of the directly injected diesel fuel starts the combustion of the alcohol-air mixture. This approach provides high substitution ratios and flexible operation based on the fuel availability – diesel only or dual-fuel.

The dual-fuel combustion process itself is not a novelty, it has been used in certain applications since the very early age of the internal combustion engine with different fuels, mostly natural gas [3, 4], but also liquefied petroleum gas [3], gasoline [5], hydrogen [3], reformed gases [6, 7] and other alternative fuels [8]. It was in 1901 that Rudolf Diesel obtained a U.S. patent covering the concept of the dual-fuel engine [9]. Similarly, to the other low reactivity fuels mentioned, alcohols like ethanol or methanol [10, 11] can also be very successfully utilised in a dual-fuel designed diesel engine. There are several possibilities to configure the dual-fuel system depending on the mixture formation method – external or internal. On the one hand, the alternative fuel can be added to the intake air upstream via manifold injection [12], carburetor or evaporator – a method widely known as "fumigation". On the other hand, the fuel may be directly injected into the combustion chamber through a dedicated injector or a special dual-fuel injector for diesel and alternative fuel.

This study handles the operation of a diesel engine in a dual-fuel mode with an intake manifold ethanol injection. Several researchers have published articles on investigations of the dual-fuel combustion process with alcohols. The findings, however, are not always consistent and differ at some points, as can be concluded from a comprehensive review of many publications on this topic in [13]. In terms of NOx emissions, most articles report a reduction with increasing ethanol percentage [13, 14] but statements about NOx increase can also be found like in [15] or [16]. Regarding engine efficiency, it is found to increase with higher ethanol percentage in [17], while other authors report that a positive change in engine efficiency occurs only at higher engine loads and the rise of ethanol share at lower loads even degrades engine efficiency [10] [18, 19]. The literature review did not offer satisfactory explanations for the observed efficiency changes with rising amount of intake manifold alcohol injection; therefore, an engine-process model for the test engine was generated and selected operating points from the engine experiments were analysed with it. The conducted efficiency loss analysis supports the understanding of the measured results.

Furthermore, the role of bioethanol as a biogenic energy carrier is introduced. Special attention is given to the production of bioethanol and the greenhouse gas saving potentials of this fuel. A case study of AGRANA's bioethanol plant in Austria is presented.

2. Bioethanol-fuel from socio-economic perspective

Currently, bioethanol is mainly obtained as a so-called first-generation biofuel and blended to fossil gasoline. That includes every conventional fermentation procedure for agricultural raw materials containing sugar and starch in which the fruit of the respective raw material plant is exploited. The key advantage of second-generation biofuel production is that, in future, any kind of biomass such as timber, cellulose or vegetable waste could be utilised. Though being very promising due to the reduced competitiveness to food production, these fuels are still produced only in insignificant amounts. According to the World Bank [20], more than 50 % of food price increases derive from crude oil prices, not from the usage for production of biofuels. In 2008, just 4 % of the world's grain was used for bioethanol production, taking the combined production of animal feed into consideration. Since 2008 EU Biofuels production increased by 68 % [21], while global food prices dropped by 20 % [22]. Moreover, the Food and Agriculture Organization of the United Nations (FAO) and the International Food Policy Research Institute (IFPRI) recognize the chances sustainable and ethically maintainable biofuel production could offer for both food security and modern bioenergy development [23, 24]. Only around 2 % of EU produced grain and only 6 % of EU

sugar substrate are utilised for bioethanol production. The most important byproduct of ethanol production is a high-quality protein animal feed DDGS (Distiller's Dried Grain with Solubles), which helps reduce the soya imports from abroad, meaning that soya-growing areas in export countries can be used to grow foodstuffs.

In Europe, but especially in Austria, a stringent set of rules and environmental regulations apply. All economically useful crops, including those destined for energy production, are cultivated in line with strict environmental criteria. It is illegal to cut down forests to produce bioethanol in Europe. Energy crops to be used for bioethanol production are grown on existing areas of land or on land which had previously been forcibly laid fallow in order to limit exports and which was once again made available for agricultural production by the EU Commission in 2009.

Despite a perceptible trend towards drive train electrification in the road transport, liquid fuels are expected to play a crucial role in defossilising mobility in the next decades, especially in hard-to-electrify sectors. Organizations like the International Renewable Energy Agency (IRENA) and the International Energy Agency (IEA) often call for more biofuels in EU's policy and stress on the importance of bioethanol [25, 26] for achieving the Union's energy and climate targets. The United Nations Framework Convention on Climate Change (UNFCCC) also addresses the strengths of bioethanol in reducing CO2 emissions from transport [27].

The European Union Directive 2009/28/EC on the promotion of the use of energy from renewable sources set the following targets to be achieved by 2020: a 20 % cut in greenhouse gas emissions and 20 % renewable energy, with 10 % share of energy from renewable sources in transport [28]. The new Renewable Energy Directive 2018/2001 (known as RED II) [29] prescribes 14 % renewable energy share in transport by 2030 and confirms the importance of sustainably produced crop-based biofuels such as European ethanol for achieving EU climate goals. However, it still caps at 7 % energy share the contribution these low-carbon fuels can make. So-called "advanced" biofuels (e.g. from straw or non-food cellulosic material) should account for at least 3.5 % energy share and can be double-counted. In accordance to this directive, the greenhouse gas emission savings for biofuels produced in installations starting operation from 1 January 2021 shall be at least 65 % compared to fossil fuels.

3. Bioethanol by AGRANA

Production

In Pischelsdorf (Lower Austria), AGRANA Stärke GmbH operates a bioethanol fuel plant and a starch factory, collectively referred to as "biorefinery". The residual starch slurry produced in the starch factory is processed into bioethanol and animal feed DDGS and wheat gluten feed at the bioethanol plant. Up to 650 000 tons of grain per year can be converted to 260.000 m³ or 210.000 tons of bioethanol. In addition to the fuel, up to 160.0000 DDGS and 110.000 of wheat gluten feed (mixture between bran and syrup) can be produced each year. This high-quality, certified GMO-free protein-rich animal feed helps to make the production of bioethanol commercially viable, with the quantities produced replacing round about a quarter of Austria's soya imports from countries that can no longer guarantee GMO-free production. As a by-product of bioethanol production, up to 90.000 t/a of biogenic carbon dioxide are produced for the food industry and various technical applications.

The raw material sources for the bioethanol production are surplus cereals such as wheat, rye, triticale, barley and maize, all in animal feed quality. Food quality crops are not used. A new additional facility started operation in 2019 and today, the starch-containing residuals from the wheat starch processing at the starch factory (second flour, small grains and residual starch slurry) make approx. 45 % of the bioethanol raw material. Especially the residual slurry from wheat starch production is converted into approx. 80.000 m^3 of bioethanol with this compound plant.

The delivered raw material is fed via a silo intermediate storage to the grinding, suspended by addition of water, then enzymatically and thermally liquefied and introduced into a simultaneous saccharification and fermentation. In the course of the saccharification, the dextrins contained are decomposed by enzymes into monosaccharides. This raw material is then converted by yeast fermentation into an alcoholic mash, which is subsequently processed in a multi-stage distillation to raw alcohol. Via molecular sieves, a further dehydration of the raw alcohol to fuel alcohol is carried out.

The protein-rich distillation residuum (distiller's wash) is centrifuged. The thin slurry (centrate) is concentrated in the evaporation to syrup or occasionally recirculated to the liquefaction process. The thick slurry (wetcake), which are the centrifugalized fiber residuals, is mixed with the syrup and then carefully dried and pelletized to storable DDGS.

The bioethanol plant is equipped with an energy supply system: a thermal waste incineration plant owned by the EVN group supplying high-pressure steam. The carbon-based calorific power plant located nearby was shut down. The supply of steam is coming from the waste incineration plant and a backup steam boiler. The total efficiency of the industrial compound (electricity and steam) is hence higher than for a stand-alone facility. The energy sources for steam generation are 100 % waste, coal is no longer used. For power generation AGRANA purchases green electricity.

Greenhouse gas emissions calculation

In order to assess the sustainability of bioethanol production at the AGRANA facilities, life-cycle analyses are carried out. A life-cycle analysis (as defined by ISO 14040) calculates emission levels and the cumulated primary energy demand which are associated with providing a certain transport service using a bioethanol or petrol-driven car. Each individual material and process involved in both transport services is recorded ("from the cradle to the grave"), ranging from the way in which the raw material is extracted from the environment to how material and energy is discharged. This analysis includes every process related to emissions and energy, both domestically and abroad, which is necessary to run vehicles on bioethanol. Finally, the results are compared with the assessments of the supply and application of petrol. When producing bioethanol and DDGS, for the biogenic carbon used it is assumed that the balance of net carbon fixing during photosynthesis, the amount of carbon stored and the combustion of bioethanol and DDGS use, is zero, as set out in the guidelines for the energy industry produced by the Intergovernmental Panel on Climate Change (IPCC).

As a biofuel producer, AGRANA has to provide the results of the greenhouse gas savings through external certifications in accordance to the International Sustainability and Carbon Certification (ISCC); Fig. 1 and Fig. 2.

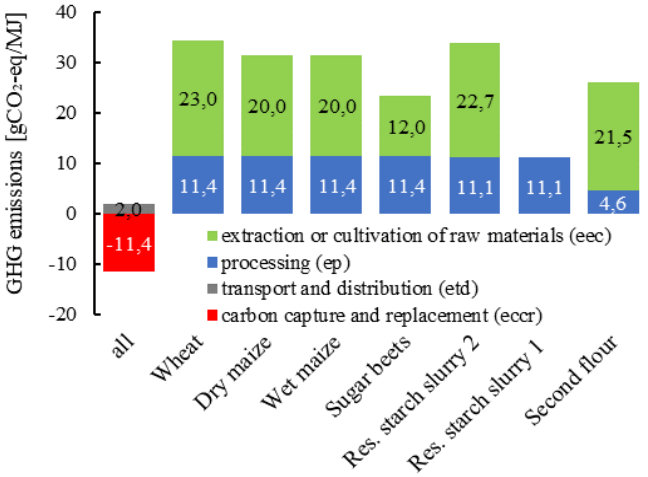


Fig. 1 *GHG shares calculated in accordance to EU Directive 2009/28/EC for bioethanol from different raw materials; starch slurry 1 calculation*

Some countries, like England, accept that no cultivation emissions are to be accounted for the raw material residual starch slurry (calculation method ISCC EU). The greenhouse gas savings from bioethanol produced by AGRANA are at least 68 and are certified by ISCC.

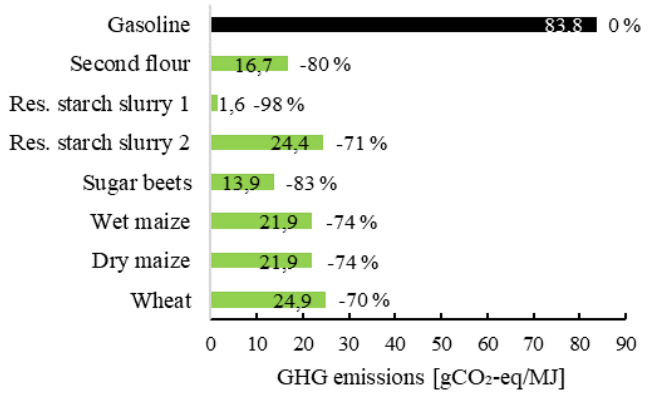


Fig. 2 *GHG emissions and reductions calculated in accordance to EU Directive 2009/28/EC for bioethanol from different raw materials; starch slurry 1 calculation method ISCC EU, starch slurry 2 – ISCC DE*

4. Investigated Fuels

Table 1: *Properties of the investigated fuels*

Fuel notation	Diesel	EtOH	E85	E65
Density [kg/m³]	831	789	782	773
Lower heating value [MJ/kg]	42.68	26.68	29	31.46
Cetane number [-]	54	8	-	-
Research octane number [-]	-	111	105	101
C-fraction [wt %]	85.4	51.5	56.5	62.8
H-fraction [wt %]	14.2	13.7	12.8	13.8
O-fraction [wt %]	0.4	34.1	29.8	23.3
H/C atomic ratio [-]	1.99	3.2	2.72	2.65
O/C atomic ratio [-]	0.004	0.5	0.4	0.28
gCO_2/MJ	73.3	71.22	72.02	73.12
gH_2O/MJ	29.94	46.54	40.08	39.69

Table 1 gives an overview of some of the properties of the tested fuels.

In this study, a certified CEC test diesel fuel was used as a reference for comparison. Technically pure ethanol was the first representative of the investigated oxygenated fuels. However, the intake manifold injected fuel does not necessarily have to be of high purity – a great advantage lies within the possibility of using lower-grade ethanol, since even higher water contents had no harmful impact on the engine. Additionally, E65 and E85 gasoline-ethanol mixtures were supplied, because their availability at filling stations is more presumable. E85 (RF-01-08) was delivered by a supplier and E65 was self-mixed (35 vol% winter quality gasoline RF-04-03).

5. Test engine and test methodology

Test engine and measurement equipment

A modern in-line four-cylinder diesel engine was modified for single cylinder operation and used as a test engine. Only the first cylinder was fired, while the other three were deactivated and their gas exchange was separated from the gas exchange of the fired cylinder. The cylinder had a displacement of 537 cm^3 and a compression ratio of 17.5. Bore and stroke were 88 and 88.34 mm, respectively. The original high-pressure common rail diesel injection system was equipped with seven-hole nozzle solenoid injectors and could handle a pressure of up to 2000 bar. Fig. 3 depicts a schematic layout of the test bench. Charging was performed with an external electrically driven supercharger. An electrically adjustable flap valve was used to adjust a turbocharger comparable exhaust gas back pressure. Cooled high-pressure exhaust gas recirculation (EGR) was applied. The standard exhaust gas aftertreatment system was removed and emission sampling took place in the raw exhaust gas. The temperatures of the charge air and the fuel were conditioned. The alcoholic fuel was injected with a pressure of 4.5 bar (abs.) into the intake air through a conventional gasoline injector, which was installed in a specially designed intake manifold.

The test engine was equipped with high- and low-pressure indication and standard exhaust gas measurement, as well as AVL Micro Soot Sensor 483 and AVL Particle Counter 489.

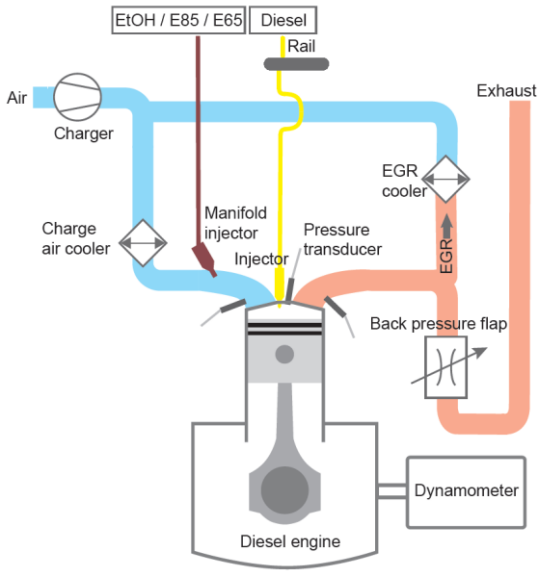


Fig. 3 *Schematic layout of the test bench*

Test methodology

The investigations were conducted at five operating points, which cover a typical commercial vehicle engine operating map. The most important engine operating parameters are depicted in Table 2. Variations of the exhaust gas recirculation (EGR) rate, of the combustion center position MFB50% (by adjusting the start of injection) and of the proportion of diesel fuel to alcoholic fuel (as percent energy share of the alcoholic fuel in relation to the total fuel energy, [%e.]) were carried out. At the dual-fuel investigations, the manifold fuel injection started at 0 °CAaTDC(firing). The pure diesel operation was the reference for the comparison. All specific emission values in this article are with respect to the indicated engine work. The results at OP-1500/5 may be seen as representative for OP-2000/5, therefore OP-2000/5 will not be discussed in further detail in the following sections. The diesel fuel was always injected through a single injection event, multiple injection strategies were not pursued within the scope of the investigations. Given the fact that the combustion calibration of modern diesel engines advances towards multiple injection systems with enhanced pressure, it should be borne in mind that a diesel engine with an optimised injection hardware and strategy would deliver better results regarding combustion shaping, efficiency and emissions [30]. The dual-fuel combustion process shown in this paper, however, also offers significant optimisation potentials, since neither the diesel combustion chamber has been modified, nor has the manifold injection been designed to fulfill an optimum.

Table 2: *Investigated operating points with engine parameters*

Operating point OP-	1500/5	1500/15	2000/5 [a]	2000/20	3000/20
Speed [rpm]	1500	1500	2000	2000	3000
IMEP [bar]	5	15	5	20	20
Power Output [kW]	3.3	10	4.5	17.9	26.8
Rail pressure [bar]	~670	~1040	~800	~1240	~1400
Int. manifold pressure [mbar]	1130	2250	1230	2500	2600
Δp exhaust-intake [mbar]	270	500	330	300	300

[a] Will not be discussed in further detail due to similarity to OP-1500/5

The reproducibility of the measurements was proved by conducting the experiments three times. The results were carefully analysed and the middle value was built for the representations.

Simulation model for efficiency loss analysis

Besides the experimental investigations at the engine test bed, a 0D/1D-simulation model of the combustion process was additionally set up and selected operating points were analysed with it. The software used was GT-POWER. An important feature of the simulation is the optional efficiency loss calculation, which contributes to the understanding of eventual efficiency differences between the discussed operating modes. The approach used for burn rate calculation was three pressure analysis (TPA) and required three measured pressure curves: intake, cylinder and exhaust. The test bed measurements delivered the input and calibration data for the simulation.

6. Results of the investigations

In the course of the investigations, at low load, degrading combustion quality, poor controllability and high cycle variation determined the maximum possible alternative fuel amount. In this project, a maximum substitution rate of 60-70 % energy share was possible with the fuels used. At high loads it was the occurrence of knock and auto-ignition that prohibited further increase of the substitution ratio. Nevertheless, at OP-1500/15 still 50-60 %e. (% energetic) substitution rate was achieved; the corresponding ranges for OP-2000/20 and OP-3000/20 were measured to be approximately 40 %e. and 25 %e., respectively. In accordance with its higher octane number, pure ethanol ensured slightly higher substitution rates at high load testing, whereas at OP-1500/5 it failed to provide stable combustion before E65 and E85 did.

Polluting emissions

NO_x, soot and particle emissions

The results of the NO_x and soot emissions measurements over the substitution rate for the tested operating points are depicted in Fig. 4 and Fig. 5. The soot mass in the exhaust gas was very effectively reduced at all operating points even when a relatively small diesel amount was replaced by ethanol, E85 or E65. Several factors play an important role in minimizing the soot emissions at dual-fuel operation. Ethanol per se is a substance known for its almost soot-free combustion. The molecule contains only two carbon atoms, which are single bonded, the H/C ratio is higher than for many other fuels and the oxygen atom is available for the combustion directly within the reaction zone. Furthermore, the low boiling point of 78°C promotes faster homogenisation. Distinctive for the dual-fuel combustion process with external alcohol supply is the fact that enough time is available for the air-fuel mixture to be premixed and homogenised before the diesel jet induces the ignition. Thus, the local fuel-rich zones are less and the formation of soot is limited. The lower aromatics amount also reduces the tendency to form soot precursors [31].

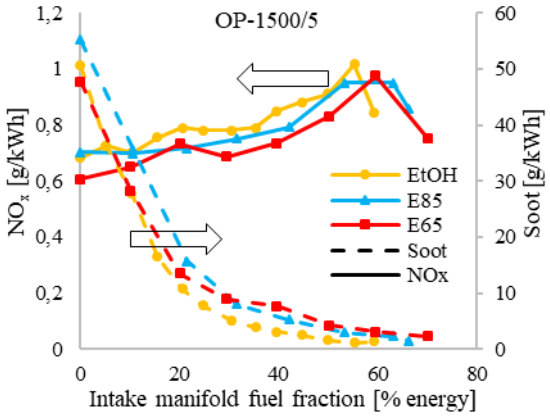


Fig. 4 *NO_x and soot emissions at OP-1500/5, 30 % EGR, MFB50% = 7.5°CAaTDC*

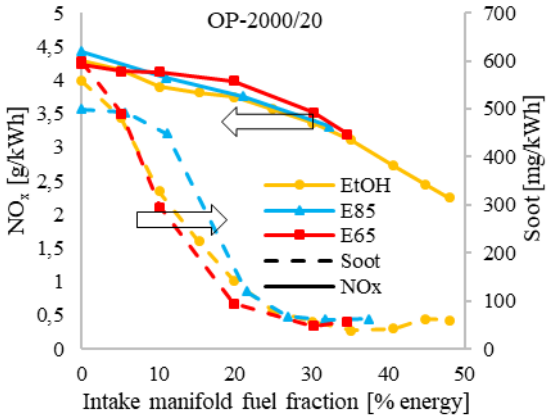


Fig. 5 *NO_x and soot emissions at OP-2000/20, 0 % EGR, MFB50% = 17.5°CAaTDC*

By replacing diesel, the appearance of diffusive diesel combustion is reduced and therefore less soot is produced. Ethanol has also a very high enthalpy of evaporation, which causes a strong cooling effect. With the cylinder charge temperature sinking, the injected diesel fuel needs more time to auto-ignite, its ignition delay is prolonged and more time remains available for diesel spray homogenisation.

The behavior of the NO_x emissions over the substitution rate depends on the load conditions: at OP-1500/5 an increase was measured, while a strong reduction occurred at the tests with 20 bar IMEP. The most important factors for NO_x formation are temperature, reactant availability and time. On the one hand, the extended ignition delay results in a faster and more compact combustion with higher heat release and higher peak temperatures. This aspect and the higher oxygen availability, which ethanol provides, increase the NO_x production. On the other hand, the charge cooling effect of the ethanol evaporation decelerates the pollutant onset. The combustion of the premixed mixture reduces the local peak temperatures because the heat is released in the whole combustion chamber and not only in a small area around the diesel jet. Higher thermodynamic combustion efficiency means that less fuel is burnt and therefore less heat is released, which also may lower the NO_x output. Additionally, ethanol burns with lower flame temperature than diesel due to the composition of the combustion products [2, 32].Whether the NO_x emissions rise or sink when substituting diesel through manifold injected alcoholic fuel depends on the weight and occurrence of the factors listed above.

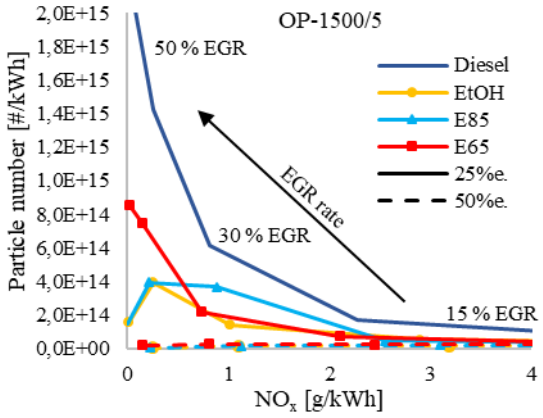


Fig. 6 *Particle number-NO_x trade-off at OP-1500/5, MFB50% = 7.5°CAaTDC*

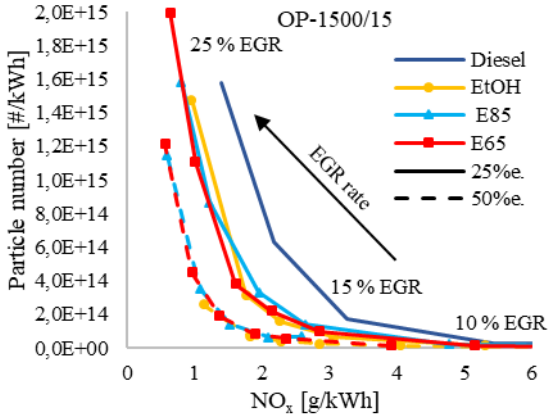


Fig. 7 *Particle number-NO_x trade-off at OP-1500/15, MFB50% = 7.5°CAaTDC*

Together with the soot mass, the particle number also dropped as diesel was replaced by the alternative fuel. By mitigating the smoke problem of the diesel engine, more EGR could be used as an in-cylinder measure for further NO_x emission reduction – the diesel typical soot-NO_x trade-off was weakened, Fig. 6 and Fig. 7. An outstanding advantage is visible for dual-fuel operation mode, in particular for OP-1500/5. In the case of 50 %e. EtOH, at 40 % EGR and a NO_x level of 0.25 g/kWh 3.5 mg/kWh of soot and an FSN of 0.043 was measured.

HC and CO emissions

Compared to the diesel reference operation, the output of unburnt or partly burnt fuel was found to be considerable at dual-fuel mode, especially at low loads. The amount of unburnt hydrocarbons (HC) and carbon monoxide (CO) steeply rose with the substitution rate. At OP-1500/5 the HC emissions increased by approx. 2 g/kWh per additional 10 %e. alcoholic fuel. This severe disadvantage resulted in lower engine efficiency; Fig. 8. The higher load points provided higher in-cylinder temperatures and pressures, hence ignition and combustion of the cylinder charge were much better supported and the incomplete combustion influence on the engine efficiency diminished.

Efficiency and CO_2 emissions

Increasing the substitution rate at OP-1500/5 resulted in a considerable drop of engine efficiency until approximately 30 % energy share and affected no significant further changes up to the maximum possible alcoholic fuel amount; Fig. 8. In contradiction to this case, a very pronounced efficiency gain was measured at the medium and high load operating points, as can be seen in Fig. 8 and Fig. 9. Due to prolonged combustion duration and associated efficiency loss, the highest efficiency at "diesel only" operation was measured at a MFB50% of 17.5°CAaTDC for OP-2000/20 and at a MFB50% of 20°CAaTDC for OP-3000/20. Substituting diesel by an intake manifold injected alcoholic fuel moved the highest efficiency combustion center to more advanced MFB50% but, as could be expected, cylinder peak pressure, pressure rise rate and nitrogen oxide emissions were very high. Fig. 8 and Fig. 9 also include an error analysis of the experiments. In order to just outline the repeatability bandwidth of the experiments regarding the measured efficiency without overloading the diagrams, not all measured points are presented with error indicators. As can be seen, the results at OP-1500/5 show the highest deviations due to the higher uncertainties when measuring very small fuel flow rates at the single-cylinder engine.

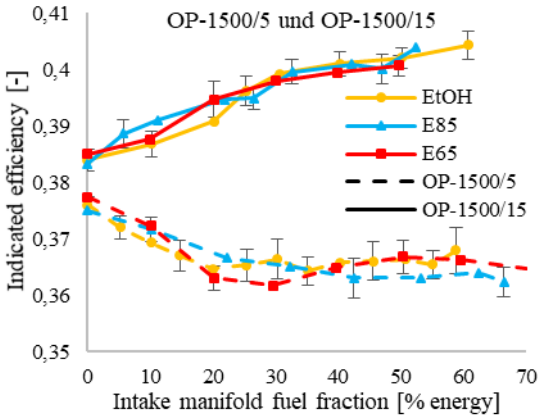


Fig. 8 *Indicated efficiency at OP-1500/5 with 30 % EGR and OP-1500/15 with 15 % EGR, MFB50% = 7.5°CAaTDC*

Operating the engine in dual-fuel mode with high alcoholic fuel energy shares also introduced a much higher tolerance against high EGR rates; Fig. 10 and Fig. 11. This benefit allowed the application of higher EGR rates without degrading the efficiency the same way as in pure diesel operation mode. In Fig. 11, the already mentioned additional engine efficiency enhancement, which results from advancing MFB50% when operating in dual-fuel mode at high loads, is shown together with the measured NO_x values for some interesting points.

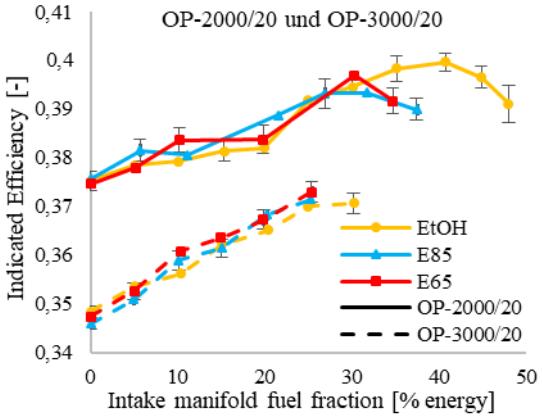


Fig. 9 *Indicated efficiency at OP-2000/20 with MFB50% = 17.5°CAaTDC and OP-3000/20 with MFB50% = 20°CAaTDC, 0 % EGR*

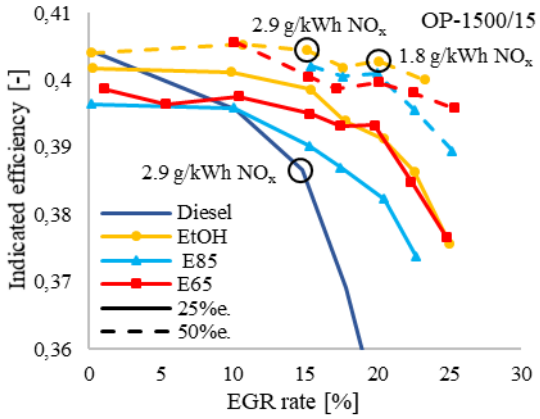


Fig. 10 *Indicated efficiency at OP-1500/15, MFB50% = 7.5°CAaTDC*

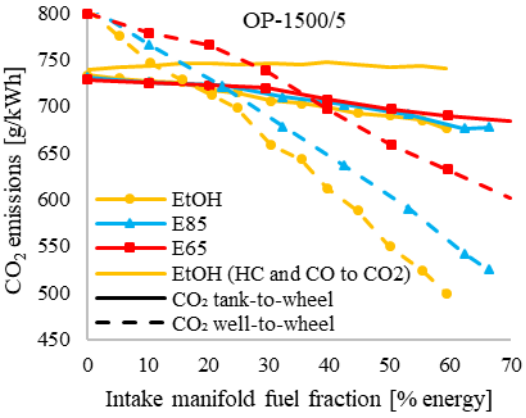


Fig. 12 *CO_2 emissions at OP-1500/5, 30 % EGR, MFB50% = 7.5°CAaTDC*

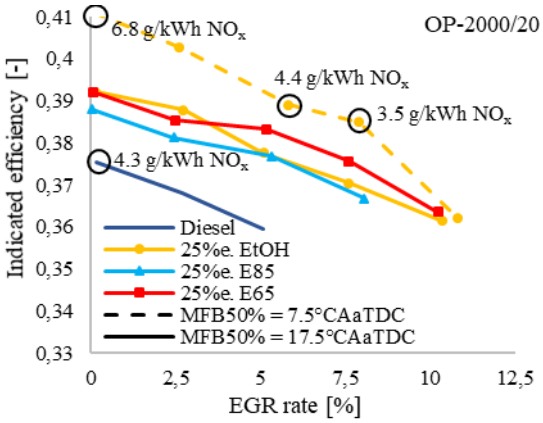


Fig. 11 *Indicated efficiency at OP-2000/20*

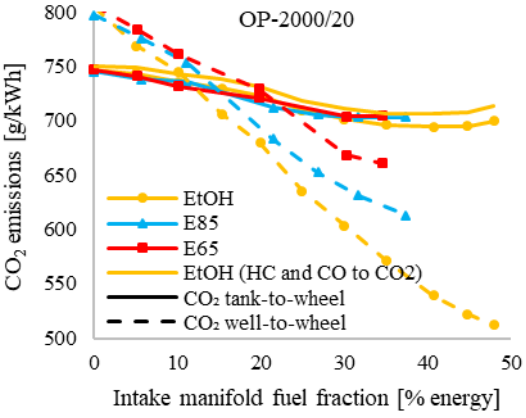


Fig. 13 *CO_2 emissions at OP-2000/20, 0 % EGR, MFB50% = 17.5°CAaTDC*

A significant reduction of the raw exhaust gas carbon dioxide emissions (tank-to-wheel) was measured with increasing substitution rate at all operating points, e.g. Fig. 12 and Fig. 13. Apart from OP-1500/5 (and OP-2000/5), the CO_2 reduction reflects the efficiency increase at dual-fuel operation mode, which is illustrated by a comparison between Fig. 13 and Fig. 9. As will be proved later, the poor dual-fuel efficiency at OP-1500/5 was the consequence of high amounts of unburnt fuel, which do not react to CO_2. At dual-fuel operation mode, the part of the fuel that gets ignited combusts thermodynamically more efficient than diesel at "diesel only" operation; therefore, less energy input (= less fuel that ignites and burns) is needed to deliver the same engine power output and less CO_2 is produced. The part of the fuel, which does not ignite and combust, is emitted as HC emissions and reduces the net engine efficiency. Additionally, the CO emissions increased with higher substitution rate. Unlike unburnt fuel (HC emissions), CO is a (incomplete) combustion product and its formation reduces the amount of the complete combustion product CO_2. However, knowing this, the operation at load points with high HC and CO emissions cannot be rated as CO_2 advantageous, since in a real-world application these pollutants would be converted to CO_2 in an oxidation catalyst. For this reason, within a simplified approach the full conversion of HC and CO to CO_2 was calculated for the case with pure ethanol operation following the presumption that all measured HC emissions in fact are unburnt ethanol molecules. The resulting CO_2 emissions are added to the measured CO_2 emissions in Fig. 12 and Fig. 13. As can be seen, at low load operation with ethanol, the theoretical CO_2 emissions are even slightly higher than in "diesel only". Nevertheless, at medium and high load operation with significantly less HC and CO pollutants, the CO_2 savings are still considerable.

As can be seen in the diagrams, the regenerative nature of the biofuel allowed remarkable well-to-wheel CO_2 savings. For these calculations, the 70 % greenhouse gas saving potential of AGRANA's bioethanol was adopted.

7. Combustion analysis

The analysis of the indicated data generally showed that at dual-fuel mode the combustion process was characterized by a shorter burning duration, Fig. 14 – Fig. 17. At low load in dual-fuel mode, more time was needed for combustion to start and the start of diesel injection had to be advanced from -11.3°CAaTDC to -13.4°CAaTDC in the case of 40 %e. EtOH (Fig. 14). Compared to diesel reference operation, at medium and higher load, the ignition delay in dual-fuel mode was shortened and the same MFB50% was set by a retarded injection timing. The start of diesel injection had to be delayed from -14 in diesel only operation to -7.6°CAaTDC in dual fuel operation with 40 %e. EtOH (OP-1500/15, Fig. 15) and from -10.7 to -2.8°CAaTDC for 30 %e. EtOH at OP-2000/20 (Fig. 16). For achieving the same MFB50% of 7.5°CAaTDC at OP-2000/20 in dual-fuel operation with 25 %e. EtOH, the diesel SOI had to be retarded from -24.1 to -14.4°CAaTDC (Fig. 17). After ignition occurred, the main combustion phase was completed faster than at "diesel only" operation. The post-combustion phase, which is distinctive for the oxidation of the soot formed during the diesel main combustion phase, was in most cases shorter and with a lower heat release. From an efficiency point of view, all these aspects lead to a thermodynamic beneficial cylinder pressure curve shaping.

Besides the above-mentioned, at some conditions a very important combustion phenomenon was detected – a cyclic reproducible auto-ignition of the premixed homogenous charge. Fig. 16 shows the heat release in diesel reference operation and dual-fuel operation mode with 30 % energy share of ethanol or E85 at OP-2000/20, MFB50% was at 17.5°CAaTDC. As can be seen,

the combustion in the case of ethanol clearly begins before the start of the diesel injection. After a rapid and intensive heat release, the main combustion of the injected diesel continues at a moderate rate. With E85 (and E65), the combustion starts even earlier and the heat release of the premixed stage is remarkably higher. According to the octane number of the fuels, E85 is more reactive and ignites easier than ethanol. The described auto-ignition of the premixed charge was not accidental, but permanent and stable in every cycle. It appeared with late MFB50% at medium and high load and was more distinct at low speeds. As could be expected, it emitted more noise, but the cylinder peak pressure was only inconsequentially higher than in the diesel reference operation (approx. 150 bar). The experiments proved that the auto-ignition was existent even after the diesel supply had been completely turned off. Fig. 17 shows the same operating point, but with an advanced MFB50% of 7.5°CAaTDC. This combustion center position was much too advanced for diesel reference operation and resulted in an efficiency decrease due to a disadvantageous heat release timing. As can be seen in the graph, in the case of "diesel only", a lot of energy is released long before the piston reaches the top dead center, thus high blow-by and wall heat losses occur.

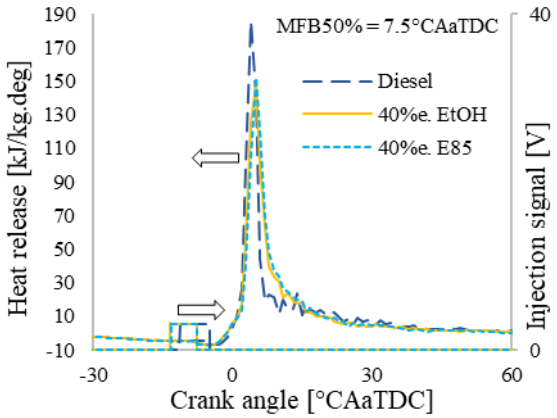


Fig. 14 *Indicated heat release rates OP-1500/5, 30 % EGR, MFB50% = 7.5°CAaTDC*

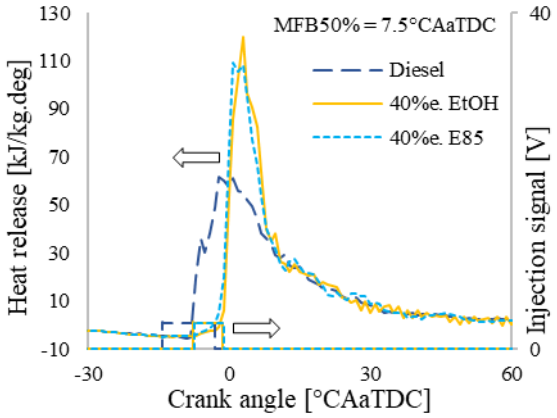


Fig. 15 *Indicated heat release rates OP-1500/15, 15 % EGR, MFB50% = 7.5°CAaTDC*

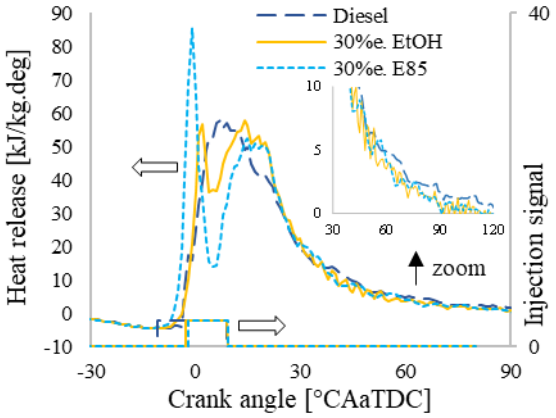


Fig. 16 *Indicated heat release rates OP-2000/20, 0 % EGR, MFB50% = 17.5°CAaTDC*

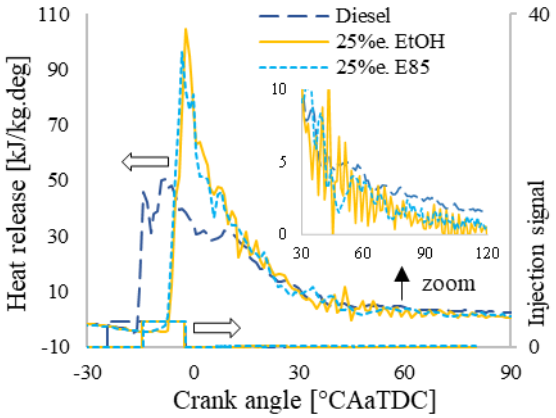


Fig. 17 *Indicated heat release rates OP-2000/20, 0 % EGR, MFB50% = 7.5°CAaTDC*

Since dual-fuel operation provided a much faster combustion, engine efficiency was even impressively increased at an MFB50% of 7.5°CAaTDC, see Fig. 11. Cylinder peak pressure was, however, in the range of 200 bar and the energy fraction of the alcoholic fuel had to be lowered to 25 %e. to prevent mechanical damage. The maximum pressure rise rate with 25 %e. ethanol was 8.5 bar/°CA at an MFB50% of 17.5°CAaTDC and 18 bar/°CA at an MFB50% of 7.5°CAaTDC. Compared to Fig. 16, advancing MFB50% in Fig. 17 demands a much earlier start of injection and the diesel combustion starts before the theoretical start of the ethanol auto-ignition, so no pre-ignition is detected.

It can be seen from the heat release curves in Fig. 14 – Fig. 17 that the combustion in dual-fuel mode is generally faster than in diesel-only operation. It is commonly known that ignition timing and burning duration have close relationship to emission output. In the case of accelerated combustion, the effect on NO_x emissions and noise becomes of particular interest. The ignition timing of the (not auto-igniting) combustion cycles was determined by the ignition of the direct injected diesel jet. Since both the ignition delay and the burning duration were changed with different substitution ratios in dual-fuel mode, for the following discussion, the combustion center position MFB50% is a more appropriate reference parameter than the ignition timing. Table 3 presents numeric values of the operation cases depicted in Fig. 14 – Fig. 17. The burning duration is specified as the difference between MFB90% and MFB05% and it was significantly shorter in dual-fuel mode at any load point. In OP-1500/5, the reduced burning duration in dual fuel mode was the result of a shorter post oxidation phase in comparison to the diesel reference and not of a higher heat release rate. The faster combustion at OP-1500/15 and OP-2000/20 was accompanied by a steep gradient and high peak value of the heat release. As Table 3 shows, this inevitably led to high noise emissions at dual-fuel mode. As could be expected, the first combustion stage of the auto-ignition

at dual-fuel mode with 30 %e. E85 in Fig. 16 produced a higher noise peak than the combustion with 30 %e. EtOH. Advancing the center of combustion MFB50% in OP-2000/20 from 17.5 to 7.5 °CAaTDC increased the noise level for both diesel and 25 %e. EtOH. It can be concluded that the higher noise emissions at middle and high load in dual-fuel mode are a disadvantage compared to the diesel reference operation mode.

Table 3: *Combustion center position, burning duration, specific NO_x and noise emissions for selected points in both operating modes*

	MFB50% °CAaTDC	Burning duration MFB90% - MFB05%	Noise dB	ind. NO_x g/kWh
OP-1500/5				
Diesel	7.5	33.7	95.7	0.68
40%e.EtOH	7.5	27.1	92.1	0.83
40%e.E85	7.5	28.8	92.7	0.78
OP-1500/15				
Diesel	7.5	43.8	87	2.94
40%e.EtOH	7.5	30.5	94.3	2.86
40%e.E85	7.5	31.9	94.4	2.92
OP-2000/20				
Diesel	17.5	49.6	86.6	4.3
30%e.EtOH	17.5	41.1	92.3	3.37
30%e.E85	17.5	45.7	97.8	3.36
Diesel	7.5	73.8	91	4.59
25%e.EtOH	7.5	41.8	97.2	6.84
25%e.E85	7.5	43.5	97.1	6.82

Higher noise emissions are normally associated with increased NO_x output. While this is an expected correlation within observations of different combustion shaping at equal operation points and the same engine and combustion process type, no direct relation between the heat release shape and the NO_x emissions can be sought when comparing two different combustion concepts like conventional diesel and dual-fuel operation. The heat release shape is just one of many parameters that influence the formation of nitrogen oxides in a combustion engine and these parameters widely differ for both observed combustion processes. The comparison between the dual-fuel results measured in OP-2000/20 with late and advanced MFB50% and similar substitution ratio (25 and 30 %e.) reveals an extreme increase of the pollutant generation with earlier combustion center position, Table 3. The noise emissions in operation with E85, however, were barely changed. The reason for this behaviour is the similarity of the heat release gradient at the start of combustion for both MFB50% cases: due to the auto-ignition, the operation with E85 produced high noise levels already at a MFB50% of 17.5°CAaTDC. Advancing the combustion center position in this case did not increase the noise level, but only the NO_x emissions due to higher in-cylinder peak temperature.

8. Efficiency loss analysis

An efficiency loss analysis is shown in Fig. 18 for low, medium and high load operation. In agreement with the engine test bed findings, compared to the diesel reference operation, the indicated efficiency in dual-fuel mode is reduced only at the 5 bar IMEP load point. The bar chart clearly visualizes the source of the major efficiency loss – a high percentage of incomplete combustion. At the other investigated load points, a higher share of incomplete combustion is also encountered in dual-fuel mode, it is however significantly lower than at OP-1500/5 and is being overcompensated by a series of efficiency gains.

Due to the changed fluid composition, the real charge and real fluid properties losses sink at all dual-fuel operating points. Since MFB50% and the pressure difference "exhaust – manifold" are held approximately equal for each pair "diesel only – dual-fuel", the losses due to combustion phasing and gas exchange are also basically identical. The "real burn rate" shares in the diagram prove the accelerated combustion at dual-fuel mode to be one of the main reasons for higher efficiency.

Another loss that is generally reduced when operating with intake manifold alcoholic fuel injection is the wall heat transfer. Surprisingly, the calculated heat transfer loss at OP-2000/20 is equal for both combustion processes. The efficiency loss is calculated by relating the specific particular work loss to the work that would result from the brought-in fuel energy with no losses at all (100 % efficiency). The software calculates 2.6 bar mean effective pressure loss due to heat transfer for the "diesel only" case and 2.5 bar for the dual-fuel case with 30 %e. ethanol, so both cases differ by only 0.1 bar. However, dual-fuel mode operation also requires less fuel energy than diesel reference operation (2.73 vs 2.85 kJ/cycle), so the percentual heat loss share in this case is barely changed.

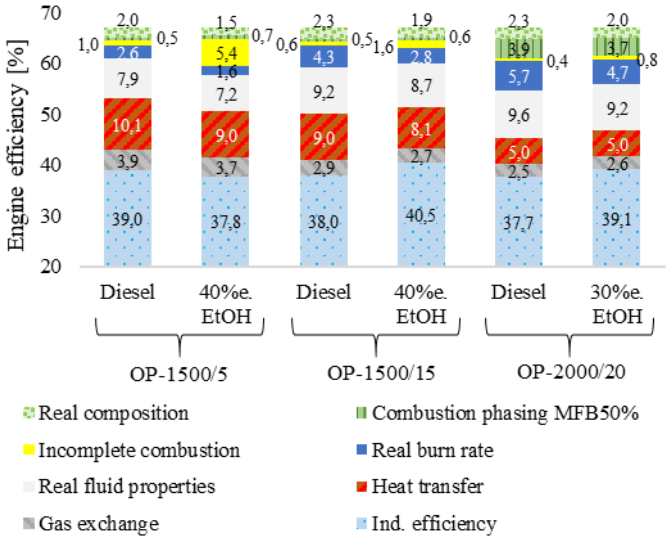


Fig. 18 *Results of the efficiency loss analysis for three operation points. Comparison between "diesel only" operation mode and dual-fuel operation*

It should be noted that the calculated values for wall heat transfer have to be interpreted with care when comparing stratified operation (as in pure diesel mode) and partially premixed operation (as in dual-fuel mode), as the wall heat transfer model used in the 0-dimensional approach (Woschni Classic) does not account for stratification effects. Therefore, wall heat loss for stratified operation tends to be overestimated in comparison to homogenous (or partly homogenous) operation.

9. Summary/Conclusions

The usage of ethanol and two different mixtures of ethanol and gasoline (E85 and E65) was investigated on a modified diesel engine designed to work in a dual-fuel combustion mode with intake manifold alcohol injection. The maximum ratio of alcohol to diesel fuel was limited by irregular combustion phenomena like degrading combustion quality and poor process controllability at low load and knock as well as auto-ignition at high load. At low load testing, up to 70 % of the diesel energy could be substituted by the alcoholic fuels, whereas at high loads the maximum substitution rate declined to approximately 30 %e. With rising alcohol amount, a significant reduction of soot mass and particle number was observed. At some testing points, substituting diesel with ethanol, E65 or E85 led to a reduction of NO_x emissions; however, the real benefit concerning the nitrogen oxides was introduced by the mitigation of the soot-NO_x trade-off. The indicated engine

efficiency was significantly improved with enhanced substitution ratios at high loads (by up to 6 %), whereas it dropped at low loads (by approx. 3 %). The combustion process tolerance against high EGR rates in dual-fuel mode allowed more exhaust gas to be recirculated without affecting engine efficiency the same negative way as in "diesel only" operation. The analysis of the indicated cylinder data revealed that at some high load conditions in dual-fuel mode, a cyclic reproducible auto-ignition of the premixed charge occurred. An engine-process simulation model showed that the high amounts of unburnt fuel at dual-fuel operation were the main reason for efficiency degradation, whereas the reduced losses due to real charge composition, real fluid properties, real burn rate and heat transfer enhanced the efficiency of the engine at dual-fuel mode. Substituting diesel with manifold injected alcoholic fuels reduced the engine CO_2 emissions at medium and high load operating points. The catalytic conversion of the high HC and CO emissions measured at low load testing would eventually lead to higher tailpipe CO_2 emissions at this operating point. A case study of the bioethanol production by AGRANA demonstrated fuel-related greenhouse gas saving potentials of up to 72 %. By using this bioethanol as a second fuel in the dual-fuel designed engine, the well-to-wheel CO_2 emissions could be cut down by almost 40 %. Conventional biofuels have the potential to contribute to the mitigation of the problems surrounding energy supply as well as food and feed production, provided that sustainability and socio-economic criteria are fulfilled and certified.

10. References

1. European Environment Agency, "Approximated estimates for greenhouse gas emissions," https://www.eea.europa.eu/data-and-maps/data/approximated-estimates-for-greenhouse-gas-emissions-2, accessed Mai. 2021.
2. Iverfeldt, E., Stalhammar, P., Sarby, H., Ihrfors, C. et al., "Sustainable Transportation by Using Ethanol in Diesel Engines," *Proceedings of the 36th International Vienna Motor Symposium* (1):290-307, 7-8 May 2015, ISBN 978-3-18-378312-0.
3. Karim, G. A., "Dual-Fuel Diesel Engines," CRC Press Taylor & Francis Group, 2015, ISBN 978-1-4987-0308-6.
4. Sprenger, F., Fasching, P., Eichlseder, H., „Erdgas-Diesel Dual-Direct-Injection – Ein alternatives Brennverfahren zur signifikanten CO2-Reduzierung," H. Tschöke, R. Marohn (eds); *Proceedings of the „10. Tagung Diesel- und Benzindirekteinspritzung 2016"*, 24-25 November 2016, Berlin, https://doi.org/10.1007/978-3-658-15327-4_22.
5. Lee, J., Chu, S., Kang, J.; Min, K. et al., "Operating strategy for gasoline/diesel dual-fuel premixed compression ignition in a light-duty diesel engine," *International Journal of Automotive Technology* 18(6):943-950, December 2017, https://doi.org/10.1007/s12239-017-0092-7.
6. Damyanov, A., Hofmann, P., Derntl, M., Schüßler, M., Pichler, T., Schwaiger, N., Siebenhofer, M., "Regenerative Oxygen-Containing Diesel Substitute Fuels as an Ecological Option for Increasing Efficiency and Minimizing Emissions," Nikolai Schubert (eds); *Proceedings of the 11th International Colloquium Fuels* p. 315-331, Ostfildern, Germany, 27-29 June 2017, ISBN 978-3-943563-32-0.
7. Lau, C. S, "Biogas upgrade through exhaust gas reforming process for use in CI engines," Dissertation, University of Birmingham, 2012.
8. Theinnoi, K., Suksompong, P., Temwutthikun, W., "Engine Performance of Dual Fuel Operation with In-cylinder Injected Diesel Fuels and In-Port Injected DME," *9th International Conference on Applied Energy*, ICAE2017, 21-24 August 2017, Cardiff, UK, https://doi.org/10.1016/j.egypro.2017.12.072.
9. Diesel, R., "Method of Igniting and Regulating Combustion for Internal Combustion Engines," US Patent 673,160, April 1901
10. Zhang, Z. H., Tsang, K. S., Cheung, C. S., Chan, T.L., Yao, C.D., "Effect of fumigation methanol and ethanol on the gaseous and particulate emissions of a direct injection diesel engine," *Atmospheric Environment* 45(11):2001-2008, 2011, https://doi.org/10.1016/j.atmosenv.2010.12.019.
11. Ogawa, H., Shibata, G., Kato, T., Zhao, P., "Dual Fuel Diesel Combustion with Premixed Ethanol as the Main Fuel," SAE Technical Paper 2014-01-2687, 2014, https://doi.org/10.4271/2014-01-2687.
12. Heuser, B., Kremer, F., Pischinger, S., "An Experimental Investigation of Dual-Fuel Combustion in a Light Duty Diesel Engine by In-Cylinder Blending of Ethanol and Diesel," *SAE Int. J. Engines* 9(1):2016, https://doi.org/10.4271/2015-01-1801.
13. Imran, A., Varman, M., Masjuki, H. H., Kalam, M. A., "Review on alcohol fumigation on diesel engine: A viable alternative dual-fuel technology for satisfactory engine performance and reduction of environment concerning emission," *Renewable and Sustainable Energy Reviews* 26:739-751, 2013, http://dx.doi.org/10.1016/j.rser.2013.05.070.
14. Cheung, C. S., Cheng, C., Chan, T. L., Lee, S. C., "Emissions Characteristics of a Diesel Engine Fueled with Biodiesel and Fumigation Methanol," *Energy & Fuels* 22(2):906-914, February 2008, https://doi.org/10.1021/ef7003915.
15. Jiang, Q., Ottikkutti, P., VanGerpen, J., VanMeter, D., "The Effect of Alcohol Fumigation on Diesel Flame Temperature and Emissions," SAE Technical Paper 900386, 1990, https://doi.org/10.4271/900386.
16. Padala, S., Woo, C., Kook, S., Hawkes, E., "Ethanol utilisation in a diesel engine using dual-fuelling technology," *Fuel* 109:597-607, 2013, http://dx.doi.org/10.1016/j.fuel.2013.03.049.
17. Abu-Quadis, M., Haddad, O., Qudaisat, M., "The effect of alcohol fumigation on diesel engine performance and emissions," *Energy Conversion & Management* 41(4):389-399, March 2000; https://doi.org/10.1016/S0196-8904(99)00099-0.
18. Cheng, C. H., Cheung, C. S., Chan, T. L., Lee, S. C., Yao, C. D., "Experimental investigation on the performance, gaseous and particulate emissions of a methanol fumigated diesel engine," *Science of the Total Environment* 389(1):115-124, January 2008, https://doi.org/10.1016/j.scitotenv.2007.08.041.
19. Zhang, Z. H., Cheung, C. S., Chan, T.L., Yao, C. D., "Emission reduction from diesel engine using fumigation methanol and diesel oxidation catalyst," *Science of the Total Environment* 407(15):4497-4505, 2009, https://doi.org/10.1016/j.scitotenv.2009.04.036
20. Baffes, J., Dennis A., "Long-Term Drivers of Food Prices," Policy Research Working Paper 6455, The World Bank, May 2013.
21. Eurostat, "Primary production of renewable energy by type," https://ec.europa.eu/eurostat/web/products-datasets/-/ten00081, accessed Nov. 2018.
22. Food and Agriculture Organization of the United Nations (FAO), "World Food Situation," 2017, http://www.fao.org/worldfoodsituation/foodpricesindex/en/.
23. Food and Agriculture Organization of the United Nations (FAO), "Impacts of Bioenergy on Food Security; Guidance for Assessment and Response at National and Project Levels," Environment and Natural Resources Working Paper No. 52, Rome, 2012, ISBN 978-92-5-107151-9.
24. Kline, K. L., Msangi, S., Dale, V., Woods, J. et al., "Reconciling food security and bioenergy: Priorities for action," *GCB Bioenergy* 9(3):557-576, 2016, http://dx.doi.org/10.1111/gcbb.12366.
25. International Renewable Energy Agency (IRENA), "Global Energy Transformation: A Roadmap to 2050,"Abu Dhabi, 2018, ISBN 978-92-9260-059-4.
26. International Energy Agency (IRENA), "Market Report Series: Renewables 2018. Analysis and Forecasts to 2023," Oct. 2018, ISBN PDF 978-92-64-30684-4.

27. United Nations Climate Change, "Ethanol Producers Work with UN to Accelerate Shift to Low Carbon," UN Climate Press Release, 18 Oct. 2018, https://unfccc.int/news/ethanol-producers-work-with-un-to-accelerate-shift-to-low-carbon.
28. Directive 2009/28/EC of the European parliament and of the council of 23 April 2009 on the promotion of the use of energy from renewable sources and amending and subsequently repealing Directives 2001/77/EC and 2003/30/EC. Available from: http://eur-lex.europa.eu/.
29. Directive (EU) 2018/2001 of the European parliament and of the council of 11 December 2018 on the promotion of the use of energy from renewable sources (recast). Available from: http://eur-lex.europa.eu/.
30. Vassallo, A., Beatrice, C., Di Blasio, G., Belgiorno, G. et al., The Key Role of Advanced, Flexible Fuel Injection Systems to Match the Future CO2 Targets in an Ultra-Light Mid-Size Diesel Engine," SAE Technical Paper 2018-37-0005, 2018, https://doi.org/10.4271/2018-37-0005.
31. Gargiulo, V., Alfe, M., Blasio, G. D., Beatrice, C., "Chemico-physical features of soot emitted from a dual-fuel ethanol-diesel system," *Fuel* 150:154-161, 2015, http://dx.doi.org/10.1016/j.fuel.2015.01.096.
32. Glaude, P. A., Fournet, R., Bounaceur, R., Moliere, M., "Adiabatic flame temperature from biofuels and fossil fuels and derived effect on NOx emissions," *Fuel Processing Technology* 91(2):229-235, 2010, doi:10.1016/j.fuproc.2009.10.002.

11. Definitions/Abbreviations

°CAaTDC	Crank angle degrees after top dead center
CEC	Certified test diesel fuel
DDGS	Distiller's dried grain with solubles
E65	Mixture of 65 vol% ethanol and 35 vol% gasoline
E85	Mixture of 85 vol% ethanol and 15 vol% gasoline
EGR	Exhaust gas recirculation
EtOH	Ethanol
EU	European Union
FSN	Filter Smoke Number
GHG	Greenhouse gas
GMO	Genetically modified organism
IMEP	Indicated mean effective pressure
MFB	Mass fraction burned
OP	Operating point
SOI	Start of injection

Fem model for the study of agricultural soil compaction under the action of two-wheel tractor

Mădălina Popa (Ivanciu) [1] Sorin-Ștefan Biriș[1] Nicoleta Ungureanu[1], George Ipate[1]
1) University "Politehnica" of Bucharest, Romania;

Abstract: *This paper presents a theoretical model that allows estimating the state of tension in agricultural soil under the action of the wheels of a cultivator (two-wheel tractor), using the finite element method. Improper operation of cultivators and their improper use can lead to the degradation of agricultural soil by generating excessive mechanical stresses that favor the occurrence of artificial soil compaction. The finite element analysis models developed in this paper allow a dramatic reduction in the costs of experimental testing as well as the time required to estimate the possibility of artificial compaction of agricultural soil under the action of cultivators.*
KEYWORDS: *COMPACTION, FINITE ELEMENT METHOD (FEM), WHEELS, TWO-WHEEL TRACTOR*

1. Introduction

Artificial soil compaction is perceived as a mechanical pollution, which appeared as an effect of the mechanical loads induced by the passages made during the agricultural works by the two-wheel tractor.

There are factors that influence soil compaction, such as: soil properties (texture, bulk density, structure) [1], soil type, number of passes of agricultural machinery, contact pressure, soil moisture content, speed of agricultural machinery, the size and shape of the footprint between the tire and the ground, the wheel load [7, 5, 6]. Usually, the use of two-wheel tractor involves an increased number of passes on the ground, thus increasing the compaction of agricultural soil [1].

The cultivator is a specialized technical equipment used for preparing agricultural soil through a series of blades that are used to rotate the soil.

It can be adjusted according to the specific requirements of the soil. Tillage machines have become famous all over the world for preparing the germination bed in the field. These equipments are often used for breaking or processing the soil in greenhouses, solariums, landscaping, gardens, etc. [8].

The weight on the wheel (the size of the external load) directly and largely influences the distribution of stresses in the soil facilitating artificial compaction.
The tire pressure shown in Fig. 1 is of particular importance on the shape of the contact surface between the tire and the ground and implicitly on the distribution of stresses in the ground [9].
For different soil conditions (soil type, humidity, etc.), depending on the tire pressure, different stress distributions in the soil can be obtained [9].
The pressure distribution in the contact spot is not uniform, but varies along both the longitudinal and transverse axes. When the tire is running, the pressure distribution tends to be higher at the front of the contact spot [3].

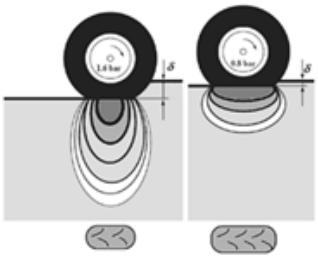


Fig. 1. *Influence of tire air pressure on the shape of the contact surface and on soil stress distribution*

Due to the fact that agricultural soil is not a homogeneous, isotropic and ideally elastic material, the mathematical modeling of the stress distribution phenomenon is quite difficult. The finite element method has proven to be extremely useful for modeling this phenomenon. For agricultural soils, stresses and strains are determined by measurements in laboratory conditions or directly in the field.

The finite element method is one of the numerical methods for obtaining approximate solutions of ordinary and differential equations that describe the phenomenon of stress distribution and deformation in the soil [3].

2. Materials and method

Using two-wheel tractor, primary and secondary processing operations could be combined in a single stage [9]. Therefore, agricultural soil could be prepared in a single pass with this type of tillage tools. This results in a decrease in the number of equipment passing through the field and subsequently results in a decrease in the artificial compaction of the soil that could be obtained due to excessive crossing of equipment in the field. Despite the high energy consumption, because the cultivator has the capacity to perform several types of tillage operations in a single stage, the total power required for this equipment is reduced [5]. Because the power of the cultivator is transmitted directly to the processing blades, the efficiency of power transmission in the two-wheel tractor is high [10].

In order to simulate with the finite element method the behavior of agricultural soil under the action of a two-wheel tractor's tire, shown in Fig. 2, we have a volume of soil with dimensions 1 m x 1m x 1 m

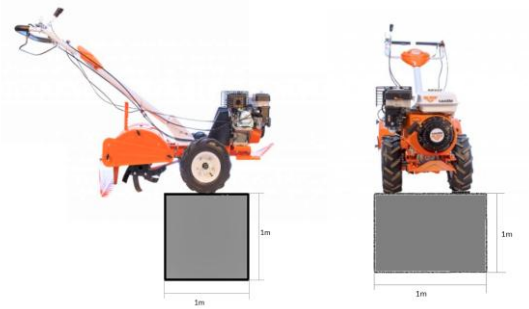


Fig.2 *Ruris 5800R two-wheel tractor*

Features of the Ruris 5800R two-wheel tractor [11]:

- Weight -70 kg
- working width - max 480 mm
- working depth max 150 mm

The simulation was performed for a soil type, having the following characteristics:

Cohesive soil (clay) with the characteristics [2]:
- Young's modulus of elasticity: $E = 3 \cdot 10^6$ Pa;
- Poisson's ratio: $\nu = 0{,}329$;
- cohesion: c = 18,12 kPa;
- angle of internal friction: $\varphi = 30°$;
- density: $\rho = 1270$ kg/m³;
- moisture content w = 24 %

3. Results and discussions

The simulation with the Finite Element Method was performed on a half model, in order to obtain the highest possible accuracy of the results.

Locks (fixings) were applied to the discretized model in two directions, so as to allow the ground to move only in the vertical direction.

For the simulation, the width of the contact spot was first fixed on the surface of the soil volume. It was considered that the force applied to the soil by the agricultural machine (contact pressure) is evenly distributed in the contact spot.

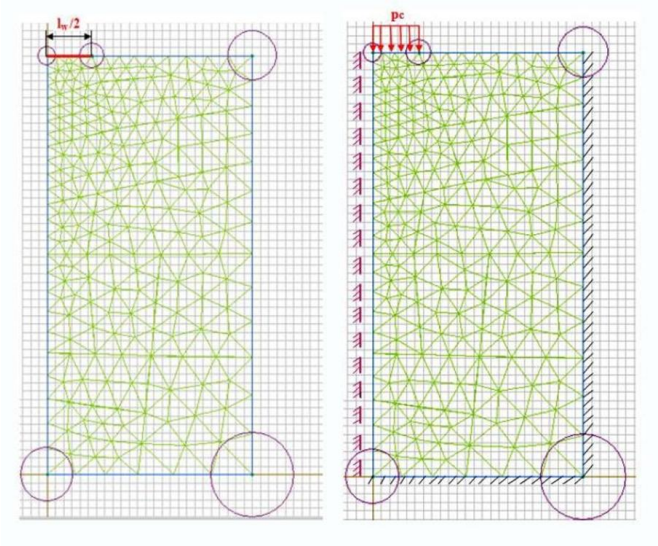


Fig. 3 *Meshed half-model of the analyzed volume of soil*

As a result of the application of the demands on the discretized model of the agricultural soil, different distributions of the equivalent stresses and of the displacements appeared in the soil were obtained, during the process of artificial compaction by the tire of the two-wheel tractor.

In Fig. 4 and Fig. 5 shows the distribution of equivalent stresses according to the von Mises criterion, respectively the distribution of displacements in the cohesive soil, in case the tire pressure of 0.1 MPa was considered. These models correspond to a contact pressure pc = 0.044 MPa, which is uniformly distributed in the contact spot whose area is A = 0.020m²

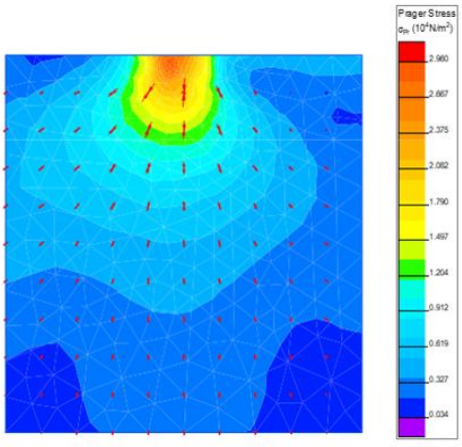


Fig.4 *Distribution of equivalent stresses in the cohesive soil (clay) in the longitudinal plane, for the contact pressure of 0.044 MPa and the width of the contact spot of 0.020m²*

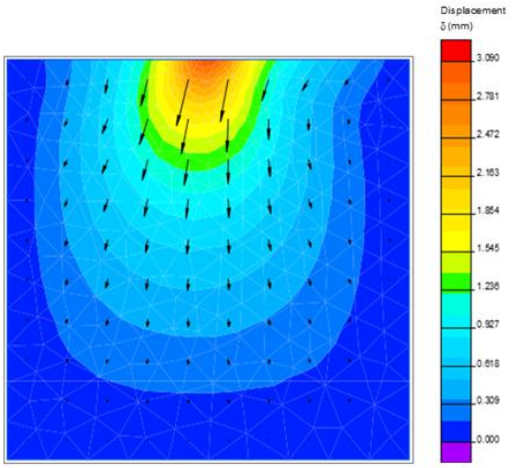


Fig.5 *Distribution of total displacements in the cohesive soil (clay) in longitudinal plane, for the contact pressure of 0.044 MPa and the width of the contact spot of 0.020 m²*

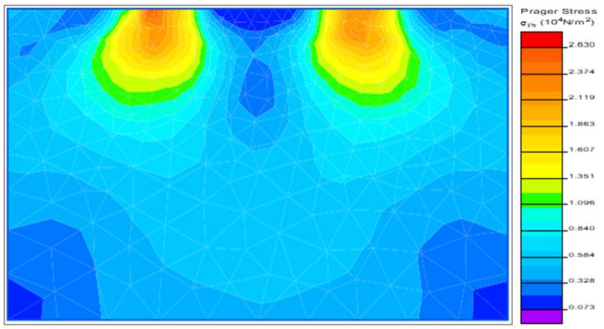


Fig. 6 *Distribution of equivalent stresses in cohesive soil (clay), for the contact pressure of 0.044 MPa and the width of the contact spot of 0.020 m^2*

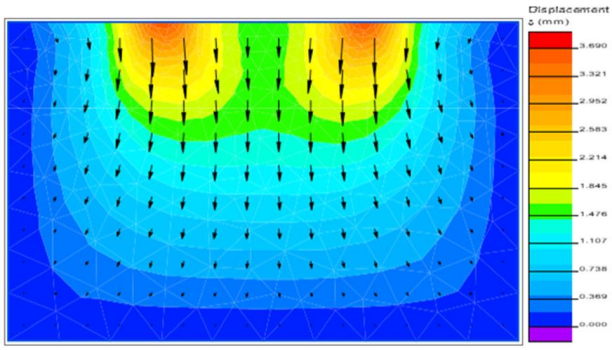


Fig. 7 *Distribution of total displacements in the cohesive soil (clay), for the contact pressure of 0.044 MPa and the width of the contact spot of 0.020m^2*

The obtained results showed that, when applying a contact pressure pc = 0.044 MPa in the contact spot having the area of 0.020 m2 (width of the contact spot L = 0.12 m), in longitudinal plane, in the case of cohesive soil (fig. 4), maximum soil stresses of 2.88 MPa were obtained and they were concentrated in the upper part of the soil, at a depth of 10-12 cm, and the minimum stresses were of the order of 1.2 MPa, the maximum soil displacement clay being 10.8 mm.

In fig. 4 shows the distribution of equivalent voltages according to the von Mises criterion, respectively in Fig. 6 shows the distribution of displacements in the cohesive soil, obtained by

simulation, in case the tire pressure of 0.1 MPa was considered. These correspond to a contact pressure pc = 0.044 MPa, evenly distributed in the contact spot having the area 0.020 m2 (width of the contact spot lw = 0.020m^2).

The obtained results showed that, when applying a contact pressure pc = 0.044 MPa in the contact spot having the area of 0.020 m2 (width of the contact spot L = 0.12 m), in frontal plane, in the case of cohesive soil (Fig. 6 and Fig. 7), maximum soil stresses of 2.64 MPa were obtained and concentrated in the upper part of the soil, at a depth of 10-12 cm, and the minimum stresses were of the order of 0.3 MPa, the maximum displacement of the clay soil being 10.8 mm.

4. Conclusions

Thanks to numerical calculation programs, it is possible to mathematically model the artificial compaction of the soil at the interaction with various working or rolling organs. The finite element method (FEM) is based on the discretization of a domain or a region into subdomains or subregions (finite elements), so on replacing a domain with an infinite degrees of freedom with a system with a finite number of degrees of freedom.

The reduction of the average pressure in the contact surface between the wheels and the ground is generally obtained by increasing the contact surface, a process that can be achieved mainly by the following methods: use of low tire pressures, equipping wheel cultivators with wide width, the use of special low-pressure or twin-wheel tires.

To reduce the pressure on the ground, it is recommended that the cultivator be equipped with large tires and that the tire pressure be adapted to the ground conditions.

The high pressure in the tire causes a small contact surface, the pressures distributed over a larger surface means that the stresses in the soil are concentrated in the upper layer, not in depth and the soil will decompact more easily.

At low pressures in the tire the tensions are transmitted deeper, and up to 1m in the ground sometimes, thus forming the compact layer (hardpan) at depths that do not reach the cultivator's knives.

5. Reference

1. Alakukku L., 1999 - Subsoil compaction due to wheel traffic. Agricultural and Food Science in Finland, vol. 8, pp. 333-351
2. Biriș S.Șt., 2010Mathematical modeling of agricultural soil compaction, Printech Publishing House, Bucharest;
3. Biriș S., Maican E., Ungureanu N., Vlăduț V., Murad E. (2011). Analysis of stress and strain distribution in an agricultural vehicle wheel using finite element method, Proceedings of the 39 International Symposium On Agricultural Engineering "Actual Tasks on Agricultural Engineering", pag 107÷118, Opatija;
4. Culpin C. Farm Machinery. 10th edition. Granada: Granada Technical Books Press, Spain 1981.
5. Dexter A. R., Czyz E. A., Gate O. P., 2007 - A method for prediction of soil penetration resistance. Soil & Tillage Research, vol. 93, pp. 412-419;
6. Donaldson C. H., 1986 - Simple techniques for estimating soil compaction. Grootfontein College of Agriculture. Published Karoo Agric., vol. 3(7), pp. 55-58;
7. Gysi M., 2000 - Soil compaction due to heavy agricultural wheel traffic. Swiss Federal Institute of Technology, Zurich, Switzerland;
8. Hendrick JG, Gill WR. Rotary tiller design parameters, part III-Ratio of peripheral and forward velocities. Transactions of the ASAE 1971c; 14:679-683.
9. Topakci M, Celik HK, Yilmaz D, Stress analysis on transmission gears of a rotary tiller using finite element method. Akendiz Ünivresitesi Ziraat Fakultesi Dergisi, 2008; 21(2): 155-160.
10. Yatsuk, EP, Panov, IM, Efimov, DN, Marchenkoc, OS, Chernenkov AD. Rotary soil working machines (construction, calculation and design). 1st edition. Amerined publishing company. PVT. LTD., New Dehli. 1981.
11. https://www.ruris.ro/msc-content/uploads/products/cat-36/fise_tehnice/fisa-tehnica-motosapa-ruris-5800r-RURIS_5800R-ro.pdf